SURFACE WATER INVESTIGATIONS ON MARS

ELLIOT SAIVE

A THESIS SUBMITTED TO THE FACULTY OF GRADUATE STUDIES
IN PARTIAL FULFILLMENT OF THE REQUIREMENTS FOR THE
DEGREE OF

MASTER OF SCIENCE

GRADUATE PROGRAM IN PHYSICS AND ASTRONOMY

YORK UNIVERSITY

TORONTO, ONTARIO

AUGUST 2023

Abstract

A key discovery of the NASA Phoenix mission of 2008 was of perchlorate salts in the Martian regolith, which are highly deliquescent, meaning they can adsorb water from the atmosphere and form liquid solutions. In addition to deliquescence, these solutions can form from straightforward contact between perchlorate crystals and water ice. Like many saline solutions, perchlorate brine has a depressed freezing point compared to pure water, and has been shown previously to remain liquid at Mars environmental conditions for hours at a time. Study of these phenomena is of importance for characterizing the Martian hydrological cycle, and furthermore, such brine is a potentially habitable environment for living organisms.

Advancements were made in demonstrating the deliquescence of perchlorate salts in a simulated cross-section of the Martian surface and subsurface. First, deliquescence was demonstrated on top of a sample of Mars regolith simulant at Mars-measured surface temperature and pressure, but with higher water vapour content in the air than on Mars. Subsequently, lessons from a series of experiments led to the design of a new experimental apparatus for demonstrating deliquescence in environmental conditions at the surface of Mars, targeting key obstacles like temperature control and frost deposition. The tests described herein represent progress towards the ultimate demonstration of deliquescence on or in regolith and subsequent liquid transport through the subsurface.

Experiments are also presented which explored whether a layer of liquid water forms at the ice table in the shallow subsurface due to contact between perchlorate and water ice on Mars. Samples of regolith simulant were mixed with varying concentrations of magnesium perchlorate and deposited over ice to simulate the ice-regolith interface as was seen on Mars. Over multiple temperature cycles, the temperatures of melting of the ice and full freezing of the resulting brine were recorded using an embedded moisture sensing device. Based on temperatures simulated to constrain the ice table at the Phoenix landing site, a perchlorate concentration of 5% is sufficient for a layer of liquid water to form which can persist for days a time, while no liquid forms for a Mars-measured concentration of 0.6%. Other concentrations in between are also explored.

Acknowledgements

Thank you to my supervisor Dr. James Whiteway, whose constant support and generosity with laboratory resources made this work possible, and whose dedication to science and vast subject matter expertise are an inspiration.

Thank you also to my co-supervisor Dr. Michael Daly, for allowing me access to your laboratory resources, and to Dr. Isaac Smith, for serving on my supervisory committee, and for lending me the odd emergency tank of liquid nitrogen. To Eamonn McKernan, who assisted with every query, and never left the room without checking if there was anything (else) I need help with.

Thank you to my family, and especially my parents and my brother, whose unconditional love and support has allowed me to pursue, and become, anything. To all past mentors, who have taught me so much. And to Callie, my main inspiration, with whom I'm so grateful to share the next adventure with.

Lastly, thank you to Vincent and Sven for the warmest welcomes home.

Contents

List of Figures

Preface

Section 3.3: Example Experiment - Deliquescence of Magnesium Perchlorate has been adapted from previously submitted work: E. Saive, "GS PHYS 6001A: W22 Research Evaluation." Written report, Fac. of Graduate Studies, Physics and Astronomy, York Univ., Toronto, 2022.

1 Introduction

Mars has been the subject of significant study spanning several decades. In particular, there is interest in characterizing the Martian water cycle, since liquid water is essential for our present understanding of life. A full accounting of the water present on Mars aids in advancing knowledge of the planet as a whole, and in particular, its prospects for past or present habitability. While relatively dry and cold compared to Earth, Mars does have a dynamic water cycle, which features familiar hydrological phenomena such as water ice clouds and precipitation [1], water frost deposition and sublimation [2], and polar ice caps [3]. The presence of large quantities of liquid water, however, is constrained to the far geological past, including in the form of ancient lake beds, one of which is currently being explored by the Mars 2020 Perseverance rover [4].

An achievement of the 2008 NASA Phoenix lander mission was the discovery of perchlorate salts in the Martian regolith in relatively high concentrations, which has implications for the stability of liquid water [5]. Perchlorates can take up water vapour from the atmosphere in a process called deliquescence and form liquid solutions with greatly depressed freezing points [6]. These brines can also form from straightforward contact between perchlorate and subsurface water ice [7]. Past work from this laboratory demonstrated that a liquid magnesium perchlorate solution formed through deliquescence would be stable on Mars from -51°C to -67°C over approximately 3 hours in the evening and through -62°C to -51°C over approximately 2 hours in the morning. Once formed, brines such as these may be a suitable environments for microbial life [8]. This MSc thesis reports on work done to advance understanding of the Martian hydrological cycle. The two research goals are:

1. Demonstrate deliquescence of magnesium perchlorate at environmental conditions equivalent to those on Mars at the Phoenix landing site in a sample of simulated Martian regolith with Mars-measured thickness over ice.

2. Determine if a layer of liquid saline water forms at the ice table which was found at the Phoenix landing site on Mars [2] (primary goal).

Chapter 2 gives a brief summary of the current understanding of the Martian water cycle and

discusses why liquid water is generally not thought to be detected on the surface. This is followed by a discussion of some relevant thermodynamics with respect to water exchange between reservoirs or surfaces and the surrounding air. This provides technical background for hydrological phenomena observed on Mars during landed missions such as deposition, sublimation, and precipitation. Perchlorate salts are then introduced, followed by an introduction to the phenomena known as deliquescence (and the associated inverse process called efflorescence), as well as the freezing point depression inherent in salty solutions formed through deliquescence or other means. The implications of this for Mars are then discussed, citing possible evidence for liquid water as a result of this very process based on direct observational evidence on Mars and laboratory experiments.

Chapter 3 builds on previous experiments which demonstrated the deliquescence of magnesium perchlorate hexahydrate at Martian environmental conditions [6, 9, 10]; this pertains to the first goal enumerated above. The ideal demonstration involves the detection of deliquescence on or inside regolith, which itself would be sitting atop a simulated Martian ice table, as was observed by Phoenix [2]. Transport of liquid within the regolith after deliquescence could then be observed. The section opens by introducing relevant experimental equipment and techniques, including the environmental chamber where experiments took place and associated pressure, humidity, and temperature control techniques. These are used to emulate the conditions measured at the Phoenix landing site on northern Mars in 2008. Then, the phenomenon known as Raman scattering is introduced, since the technique known as Raman spectroscopy (using a laser Raman LIDAR apparatus, also discussed) is employed for some experiments to detect phase changes of perchlorate from dry crystals to a salty liquid water solution. An example experiment, which emulates previous work, is then presented to provide an explicit example of the deliquescence of perchlorate crystals at Mars conditions and illustrate key principles of using laser Raman LIDAR to detect phase changes of water. After this, experiments are presented which represent numerous attempts since 2022 to advance the demonstration shown in the example experiment. In the presented experiments, different conditions are altered, including humidity, air flow, and temperature to build up a working demonstration. Ultimately, the key demonstration has not yet been achieved, for reasons which will be discussed; the primary challenge involves cooling the regolith (and perchlorate) while still allowing sufficient moisture to be present in the air, and not depositing moisture onto cold surfaces

while cooling the sample and the air around it. In the discussion for this section, future work is suggested as a result of this progress.

Chapter 4 presents experiments for determining whether a thin layer of liquid brine forms at the interface between ice and regolith at shallow subsurface depths on Mars. This pertains to the second research goal enumerated above, which was considered the primary goal of this MSc research. First, an overview is given on physical moisture sensing technology, with a subsequent introduction to the working principles of the instrument chosen for the presented experiments. In these tests, the same environmental chamber as in Chapter 3 is used, but instead of testing for deliquescence of perchlorate on top of simulated Martian regolith, perchlorate is mixed into the regolith at varying concentrations (including in one trial a Mars-measured concentration) and deposited onto ice. This simulated cross-section of the Martian subsurface is then subjected to temperature cycles which pass through the expected temperatures on Mars. A moisture detection probe is embedded into the ice, and indicates points of freezing and melting of a liquid perchlorate solution at the ice which results from contact between the perchlorate-regolith mixture and the ice. It turns out that at perchlorate concentrations measured on Mars (0.6%, [5]), melting would not occur at the ice table during the mid-summer at regolith depths of the Phoenix landing site. However, at the high concentration of 5%, liquid water would form, and persist for potentially entire seasons at the ice table based on melting and freezing temperatures.

Chapter 5 concludes discussion for this MSc research by revisiting the research goals and summarizing specific progress towards each.

2 Background

2.1 Past and Contemporary Martian Water

There is evidence for large quantities of past liquid water on the surface of Mars in the form of ancient shorelines [11, 12], valley networks and channels [13], and past lakes [4, 14], some of which may have been habitable to primitive life [4, 15]. However, Mars, like all planets, goes through distinct geological eras, and at present day, there are no such basins and flows of liquid water. The Mars atmosphere is 95% CO_2 [16], but unlike Earth, Mars has no significant greenhouse effect, and has an average surface temperature of -60°C [17]. Further, Mars has an atmospheric surface pressure only around 1% that of Earth's, and though some regions can reach pressures up to 700 or 800 Pa [18] (which is above the 600 Pa pressure at the triple point of water), the low temperatures at these regions (below 273 K, even in the summer [18,19]) prevent pure liquid water from forming. Still, there is presently a dynamic hydrological cycle occurring on Mars, and characterizing this cycle not only advances understanding of the evolution of Mars, but has implications for the possibility of present day biological life. A key point is that liquid water can exist in the form of salty brines at conditions unfavourable to pure water, as will be discussed below.

2.2 Water Exchange Principles

The saturation vapour pressure over water (e_s) is the partial pressure[1] of water vapour where the rate of water molecules condensing from the air onto the surface of a flat body of water is equal to the rate of molecules evaporating into the air. It is temperature-dependant; e_s is greater for warmer air than for cooler air. Note that for experiments at Mars environmental conditions, saturation vapour pressure over ice (e_i) is more commonly used than saturation vapour pressure over water. An important related quantity is relative humidity (RH), commonly expressed in percent, which is the percent of water vapour in the air relative to how much it would hold if it were saturated. More explicitly, it is the partial pressure of water over the saturation vapour pressure, converted to percent ($\frac{e}{e_s} \times 100\%$). Below 0°C, which is the freezing point of pure water, relative humidity is often referred to as relative humidity over ice (RHi), and is instead computed as ($\frac{e}{e_i} \times 100\%$). If the air is

[1] *Partial pressure* (of, say, water vapour) is the pressure exerted only by water vapour in a given mixture of gas. Alternatively, it's the pressure that would be exerted if that much water vapour were the only gas in the mixture.

cooled such that $e = e_i$, that is said to be 100% RH, and the air is saturated. If $e > e_i$ above a cool surface of temperature T, the air is supersaturated, and net deposition will be seen on the surface in the form of frost or ice. The temperature at which $e = e_i$, and thus RH = 100% is called the frost point temperature (T_f, or FPT in some figures of this report). In other words, at RH = 100%, $T = T_f$.[2] Then, once the inverse condition is fulfilled ($e < e_i$, now that $T > T_f$, say), the rate of sublimation will surpass the rate of deposition, and net sublimation off the surface will be observed.

Note: In experiments below, despite being denoted as a "temperature," the reporting of frost point temperature (T_f or FPT) is actually a measure of water vapour content in the air. For instance, some experiments occurred at T_f = -35°C, which is more humid than others which occurred at T_f = -55°C, the latter of which having been observed on Mars during the Phoenix mission [20].

2.3 Present-day Mars Water Cycle

Various physical phenomena comprise our current understanding of the present-day Mars water cycle. The 2008 NASA Phoenix lander mission provided direct, ground-based detection of some of these, including daily cycles of water frost deposition and sublimation (Figure 1a) and water-ice clouds and precipitation (Figure 1b). A longer-term cycle is evident with respect to the northern polar ice cap, where water is seasonally sublimated into the air from the ice cap for transport through the atmosphere to lower latitudes during the summer [3]. Water is then re-deposited back onto the ice cap as temperatures cool after summer.

[2] Over liquid water, the frost point is instead called the dew point (T_d), and where $e = e_s$ (or $T = T_d$), condensation of liquid water onto the surface is seen, rather than the deposition of frost.

(a) Image of frost formation on Mars regolith on sol 80 of the Phoenix mission [2].

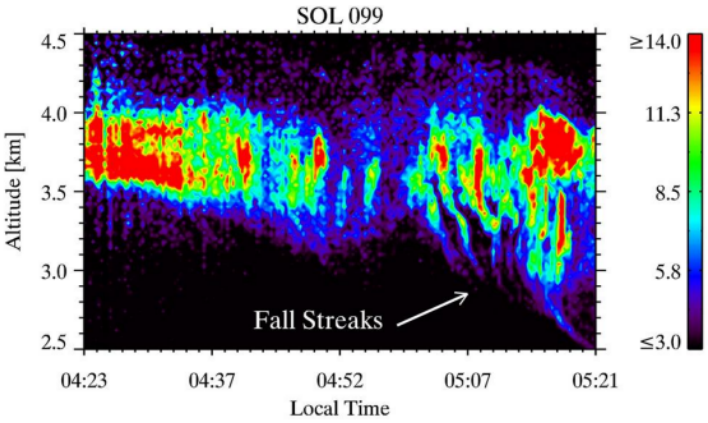

(b) Clouds and fall streaks indicating precipitation from the Phoenix LIDAR instrument [1].

Figure 1: Evidence of a dynamic Martian hydrological cycle from the NASA Phoenix mission.

A similar exchange (sublimation and deposition of water, facilitated by diffusion) has been demonstrated experimentally to occur between the atmosphere and subsurface ground ice, which is not constrained just to the extreme polar regions [21]. This ground ice, the boundary of which (the "ice table") is in contact with ice-free regolith, is a reservoir holding a significant quantity of the total Martian inventory of water. At the Phoenix landing site, evidence for the subsurface water ice table was provided by camera (Figure 2a and 2b) and by the Phoenix Thermal and Evolved-Gas Analyzer; the ice table was found to sit between 5 and 18 cm below the top surface [2].

(a) Image of ice table exposed by Phoenix landing thrusters [2].

(b) Subsurface ice table exposed by Phoenix Robotic Arm [18].

Figure 2: Physical evidence of Mars subsurface ground ice at the Phoenix landing site.

2.4 Perchlorate Salts

In addition to providing ground-based confirmation of various phenomena pertaining to the Martian water cycle, a notable outcome of the Phoenix mission was the detection of perchlorate (ClO_4^-) in the Martian regolith in concentrations of up to 0.6% (wt%) by the Phoenix Wet Chemistry Laboratory (WCL) [5], and potentially in small patches of higher concentrations [22]. Perchlorate has also been detected by the NASA Curiosity rover at Gale Crater in similar concentrations, suggesting perchlorates are globally distributed [23]. One study, which compared data from an engineering model of the WCL with the *in situ* data at the Phoenix landing site, identified the most likely perchlorate parent salts as $Ca(ClO_4^-)_2$ (60%) and $Mg(ClO_4^-)_2$ (40%) [24]. Another study, which used chemical modelling, suggests instead that perchlorate was most abundant in the form of magnesium perchlorate hexahydrate ($Mg(ClO_4^-)_2{\cdot}6H_2O$), followed by sodium perchlorate dihydrate ($NaClO_4^-{\cdot}2H_2O$) and potassium perchlorate ($KClO_4^-$) [25].

2.4.1 Deliquescence and Efflorescence

Perchlorate salts have a high affinity for water vapour, meaning water in the atmosphere will adsorb onto the perchlorate molecule due to polar attraction between the water molecule and the perchlorate ions. The amount of adsorption which occurs depends on the ambient relative humidity (RH). As the local RH increases, so does the amount of adsorbed water, until the ionic bonds of the salt are broken and the salt dissolves [26]. This process, which results in a salty liquid solution or brine, is called deliquescence. The critical relative humidity as which the dissolving occurs is called the deliquescence relative humidity (DRH) and is characteristic to the salt in question, that is, different perchlorates have different DRHs. Figure 3 shows camera images of this process occurring in room air at York University (23°C and 60% relative RH) over the course of one hour as a large sample of dry magnesium perchlorate hexahydrate crystals form a liquid solution.

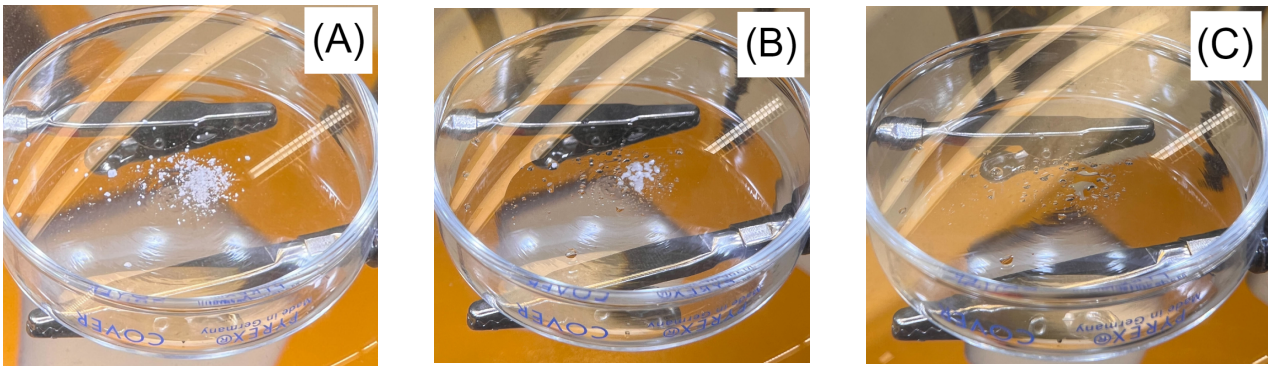

Figure 3: Deliquescence of magnesium perchlorate hexahydrate in room air over one hour at York University. (A) The perchlorate begins in crystalline form. (B) As moisture is taken up from the atmosphere, liquid droplets form around the edges of sample. (C) Full deliquescence has occurred and the sample is completely liquid. The sample container is approximately 1 inch across for scale.

The DRH over ice of magnesium perchlorate hexahydrate, which is a top candidate for the perchlorate in highest relative abundance on Mars [25], is 60% [9]. For instance, in a previous study, the onset of deliquescence of a sample of magnesium perchlorate mixed with quartz sand occurred when the temperature of the sample reached -51°C at an ambient humidity of -55°C frost point temperature; here, RHi = 60% [9]. This is shown in Figure 4, where deliquescence is evident in the darkening of the sample as the RH increases past the DRH. In this study, laser Raman LIDAR was used as the primary means of detection of deliquescence; more on laser Raman LIDAR below. The reverse process to deliquescence, called efflorescence, is the re-crystallization of the salt and the associated return of the water to the atmosphere as water vapour once the RH decreases to the critical value called the efflorescence relative humidity (ERH).

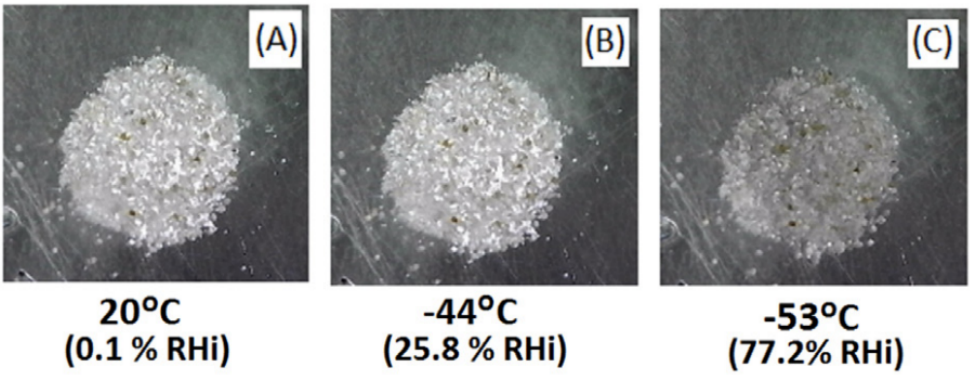

Figure 4: Deliquescence of magnesium perchlorate mixed with quartz sand in a previous study [9]. (A) White specs of perchlorate can be seen atop grey sand. (B) Just prior to reaching the DRH, the sample remains dry. (C) After passing through RH = 60%, the perchlorate deliquesced and formed a liquid solution, as indicated by darkening of sample. The sample is about 10 mm in diameter.

On Mars, deliquescence of perchlorates is thought to be a possible mechanism for the formation of liquid water during summer seasons [5, 6, 27]. Indeed, the study shown above [9] demonstrated perchlorate deliquescence during temperature and humidity conditions which matched those seen at the Phoenix landing site in 2008 [20].

Directly from the Phoenix mission itself, Figure 5 shows what are interpreted as spheroids of saline liquid water, which formed and subsequently grew over weeks on a strut of the Phoenix lander after salty mud splashed on the struts during landing [18]. One spheroid is even shown to have "dripped" from the strut, after darkening on sol 31 and disappearing by sol 44 in Figure 5, which coincides with peak RH and temperature for the mission[3]. A future experiment as part of the European Space Agency ExoMars mission will include bringing known quantities and species of perchlorates to the Martian surface to directly test for the formation of liquid brines in the Mars atmosphere [28].

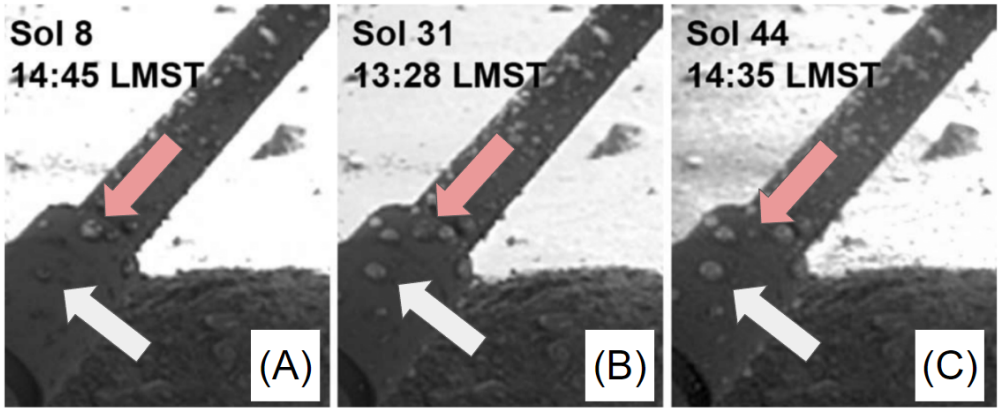

Figure 5: Spheroids on the strut of the Phoenix lander, interpreted as liquid brine droplets which formed through deliquescence of perchlorate salts [18]. Across subfigures (A), (B), and (C), the spheroid indicated by the white arrow grows in size, indicating continual formation of liquid water by deliquescence. Between subfigures (A) and (B), the spheroid indicated by the red arrow darkens. By sol 44 in subfigure (C), it has dripped off the strut. The thin part of the strut is 3.05 cm in diameter for scale.

2.4.2 Freezing Point Depression and Implications at Mars Temperatures

Increased uptake of water from the atmosphere during deliquescence by a salt is a consequence of the lowered vapour pressure characteristic of a salty solution [26]. Another consequence of this lowered vapour pressure is depression of the freezing point of such a solution. As mentioned above,

[3]Martian days are about 40 minutes longer than Earth days and are referred to as *sols*.

saturation vapour pressure (also called equilibrium vapour pressure) is a function of temperature, and freezing will occur when the saturation vapour pressure over ice matches the saturation vapour pressure over liquid water, that is, $e_i = e_s$. Normally, for pure water, e_s will intersect e_i at 0°C, as is shown in Figure 6. However, since dissolved salts reduce the saturation vapour pressure of the liquid solution for a given temperature compared to pure water (i.e. $e_{s,\text{ salty}} < e_{s,\text{ pure}}$), illustrated in Figure 6 by the vertically shifted red line, intersection with the saturation vapour pressure of water ice occurs at a colder temperature than for pure liquid water.

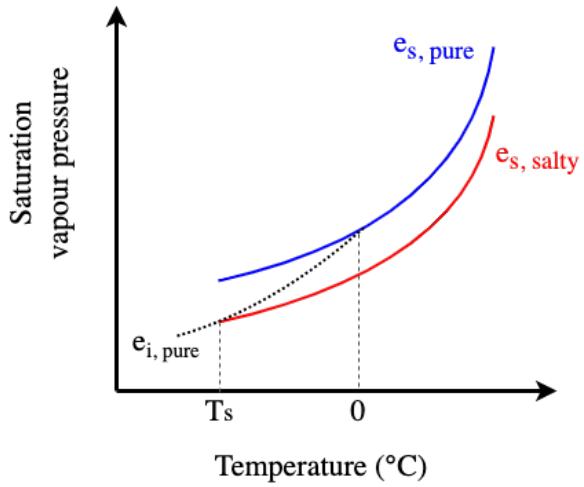

Figure 6: Graphical representation of the mechanism by which reduced saturation vapour pressure of salty solutions depresses freezing point. The saturation vapour pressure of salty solutions intersects that of ice at a lower temperature than 0°C.

Freezing point depression exhibited by perchlorate solutions has implications for the stability of liquid water on Mars. For instance, while surface temperatures modelled at the Phoenix landing site (ranging from just above -20°C to below -70°C [19]) prohibit the formation of pure liquid water, the freezing point and subsequent melting point of a magnesium perchlorate brine was found to be -67°C and -62°C, respectively [6]. Moreover, the diurnal temperature range is modelled to be less extreme below centimetres of regolith at the ice table than at the surface. One thermal model based on *in situ* surface measurements from the Phoenix Thermal and Electrical Conductivity Probe (TECP) [20] simulated the expected temperature range at the ice interface underneath 4.5 cm of Martian regolith during sol 55 of the Phoenix mission (mid-summer) to fluctuate only between -43°C and -53°C. This is illustrated in Figure 7. This range is fully above the freezing temperature of a saturated perchlorate brine [6], meaning saturated brines would be stable as liquid

here due to lowered freezing temperature.

The phenomenon of freezing point depression applies to brines which form through deliquescence and also through straightforward physical contact between perchlorate crystals and water ice. As such, an additional prospect to deliquescence for sustained liquid water on Mars in the subsurface is physical contact between perchlorate mixed into the regolith and water ice at the shallow ice table [7].

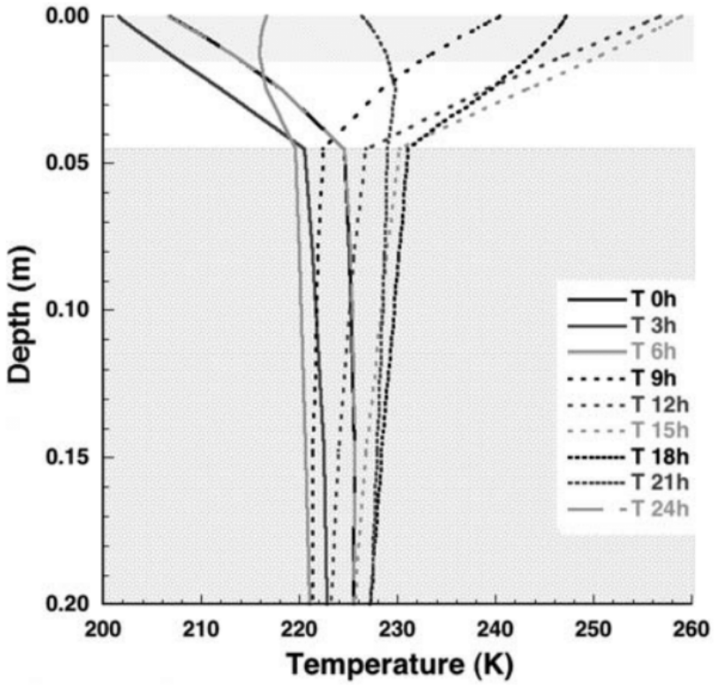

Figure 7: Modelled temperatures of subsurface of the Phoenix site over sol 55 of the mission, where the lower grey portion represents the ice table [19]. The temperature range at the ice table is modelled to be between -43°C and -53°C, which is pertinent for the experiments presented in Chapter 4.

2.4.3 Perchlorate Concentration

Figure 8 shows a phase diagram for magnesium perchlorate concentration based on modelling and experiments [10]. Regardless of concentration, a perchlorate brine will turn to ice at -67°C; this was observed in past experiments involving perchlorate deliquescence mentioned above [6]. However, this transition can occur at warmer temperatures for concentrations lower than the eutectic concentration, which is the concentration exhibiting the highest magnitude of freezing point depression. The eutectic concentration for magnesium perchlorate is 44% (wt%). In Chapter 4, experiments

will feature samples of Martian regolith simulant mixed with perchlorate in varying concentrations by weight, deposited over ice. Since the geometry of the setup is the same, each resultant liquid solution will have a different perchlorate concentration, resulting in different freezing points of the solution. The results have implications for the presence of liquid water on Mars.

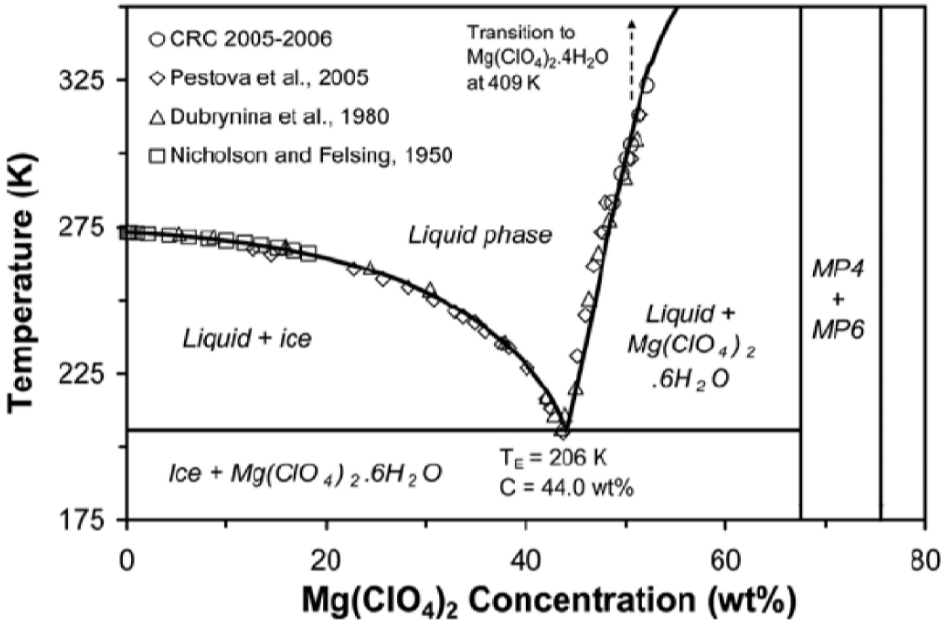

Figure 8: Phase diagram of magnesium perchlorate based on modelling and experiments [10]. As perchlorate concentration in solution increases, the freezing temperature decreases up to the eutectic concentration of 44%.

2.4.4 Liquid Transport in Martian Regolith

Once deliquesced, there is interest in characterizing the dispersion or transport of liquid within the Martian subsurface. Should liquid form, it could be responsible for transporting ions throughout the subsurface and concentrating perchlorates in patches [22]. In 2022, a minor experiment was done which demonstrated significant transport capability of liquid brines in simulated Martian regolith. In a small container, about 2 cm (200 g) of superfine-grade MMS-1 simulated Mars regolith [29,30] was deposited, with a perchlorate dusting evenly distributed on top with a total mass of 2 g (1% that of the regolith sample). Over a weekend at York University, in a humid environment, the perchlorate was allowed to deliquesce and disperse. Two moisture-sensing probes, to be described in full in Chapter 4, were embedded in the sample with kapton tape over the probe prongs such

that one instrument was sensitive to moisture at a depth of 1 cm and one at 1.5 cm. Figure 9 shows the moisture probe signals over the weekend, and Figure 10 shows the resultant images of the sample after liquid transport. Here, conductivity probe signal at a given depth, in units of mV, can be taken to roughly represent relative quantities of liquid water [4].

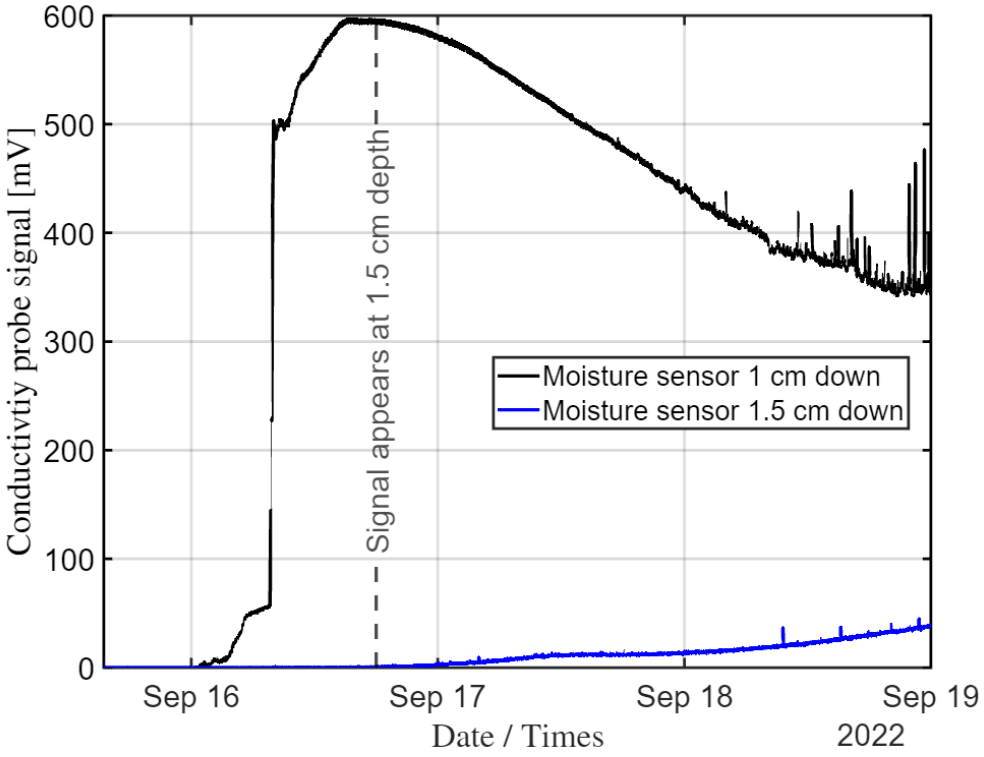

Figure 9: Moisture signals indicating transport of perchlorate brine downwards throughout the sample. The liquid transported about 1 cm down 8 hours after first depositing the perchlorate onto the regolith, indicated by the onset of signal from the moisture probe at that depth. It took an additional 16 hours to transport 0.5 cm further downwards, indicated by onset of signal from the deeper probe.

After the perchlorate on the surface deliquesced, the liquid solution had transported downwards to a depth of 1 cm about 8 hours after the very start of the experiment, as shown in Figure 9. It then took about 16 hours more (24 hours total) for the liquid to subsequently reach 1.5 cm down, indicated by the onset of signal from the lower probe and, it turns out, a decrease in overall liquid signal from the upper probe. Figure 10 shows uniform liquid dispersion (indicated by darker regolith) throughout the top 1 cm of subsurface, with greater depths reached in patches. The transport shown here was only after one weekend; over many millions of years, perchlorate would well disperse itself through the Martian subsurface provided liquid solutions form.

[4] There are important caveats to this, as is discussed in Chapter 4.

(a) Dispersion of perchlorate brine filling the entire top 1 cm of regolith.

(b) Alternative view of Figure 10a.

Figure 10: Evidence of downwards transport of deliquesced perchlorate brine from the top surface of simulated Martian regolith. These images correspond to the data presented in Figure 9. The darkened regolith unambiguously indicates where liquid transported to throughout the sample.

3 Deliquescence on Simulated Martian Regolith

This section discusses advancements made in continuing some of the previous laboratory advancements described in Section 2. As discussed, deliquescence of perchlorate within the Martian subsurface is of a potential mechanism by which liquid water could exist on present-day Mars [6, 10, 18]. The presented experiments attempt to reproduce the hypothesized conditions under which liquid water would form through deliquescence in a realistic cross-section of the Mars surface and subsurface under Mars atmospheric conditions.

3.1 Experiment, Measurement, and Analysis Methods

3.1.1 Planetary Simulation Chamber

All experiments took place at York University inside a vacuum camber from Angstrom Engineering, shown in Figure 11. The chamber is cylindrical, with a diameter and length of 1.3 m for an internal volume of about 1.7 m^3. Experiments generally rest on a platen, covered by a shroud, each of which can be heated or cooled. The chamber is evacuated by a mechanical vacuum pump, or by cryo pump, in which case vacuum below 2×10^{-7} torr can be achieved. The chamber has multiple feedthroughs for electronics harnesses and liquid and gas plumbing.

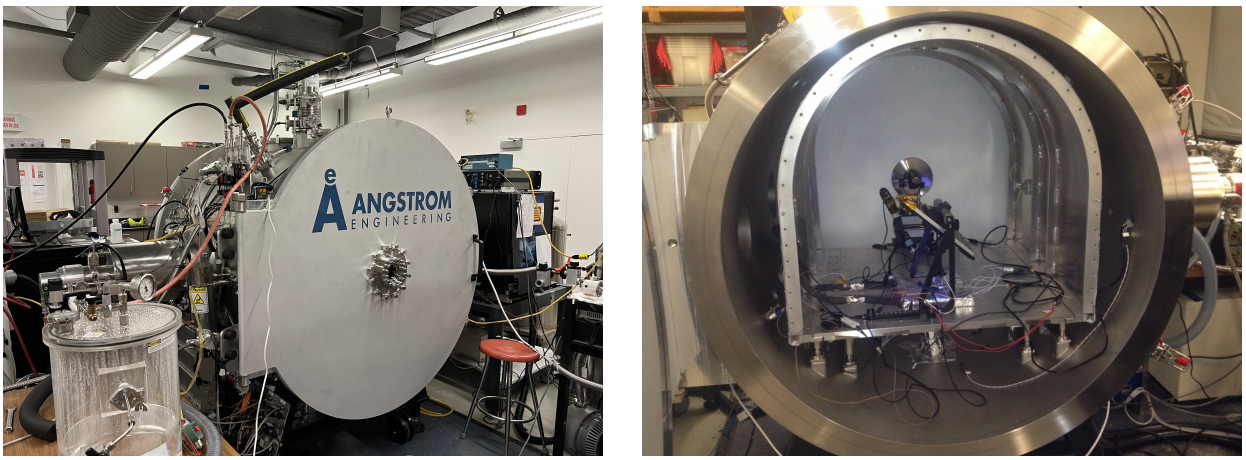

(a) Chamber exterior and bubbler for humidity control.

(b) Chamber interior.

Figure 11: Planetary simulation chamber exterior and interior at York University. The interior of the chamber is 1 m in diameter.

3.1.2 Environmental Control

Figure 12 shows a schematic diagram of the environmental control infrastructure inside the vacuum chamber. The subsections below discuss details.

Pressure and Humidity: Mars-measured pressure and humidity is maintained in the chamber by the simultaneous extraction and supplying of gas by proportional-integral-derivative (PID) control loops running on the lab PC. As gas is extracted through a mechanical pump with an adjustable valve, dry nitrogen or dry carbon dioxide gas can flow into the chamber through an Alicat MCP100SLPM-D-DB15K mass flow controller with a flow rate governed under PID control, controlling the pressure in the chamber to ± 0.05 Torr at 7 Torr. Pressure was measured by an Inficon CDG025D capacitance diaphragm pressure gauge. Simultaneously, an additional Alicat mass flow controller (also under PID control) allows humid carbon dioxide into the chamber after it passes through a Plexiglass bubbler filled with distilled water, which is visible in the bottom left portion of Figure 11a. The humid carbon dioxide passes through a Whatman 6722-5000 Hydrophobic PTFE filter (0.1 μm). Humidity in the chamber was measured by two Vaisala DMT152 capacitive sensors, and was controlled according to frost point temperature to ± 1°C at -60°C frost point.

Temperature: To simulate Mars-measured temperature cycles, all samples (or their containers) were actively cooled using liquid nitrogen, which flows through a 4 × 6 in. heat exchanger, which itself is a 1/4 in. copper tube embedded inside a 1/4 in. thickness aluminum plate. An Omega kapton resistive heater (19.2 Ω) was placed on top of the cooling plate, and on top of that was placed a 4 × 6 in. aluminum plate for the sample (or its container) to rest on. This assembly was covered in insulation. Figure 12 shows these layers, but note that the drawing is not to scale. The liquid nitrogen flow was controlled using a solenoid valve governed by a Love Controls temperature controller on a duty cycle. To achieve a temperature setpoint, the liquid nitrogen duty cycle was set such that the temperature would drop below the setpoint; current is then supplied to the kapton heater using a Stanford Research Programmable Temperature Controller 10 (PTC-10) under PID control to reach the setpoint. The plate temperature is measured by the PTC-10 using an Omega Type T thermocouple fixed to the upper aluminum plate. The temperature could be controlled to within ± 1°C, but temperature gradients of 3 K were seen across the plate. Other thermocouples,

also Omega Type T, were measured by a National Instruments PXIe-4353 Temperature Input Module and monitored by a PC (the PXIe-4353 is not shown in Figure 12 to minimize crowding). These were either fixed to the upper aluminum plate (with their own independent measurement to account for gradients) or placed elsewhere according to the experiment at hand.

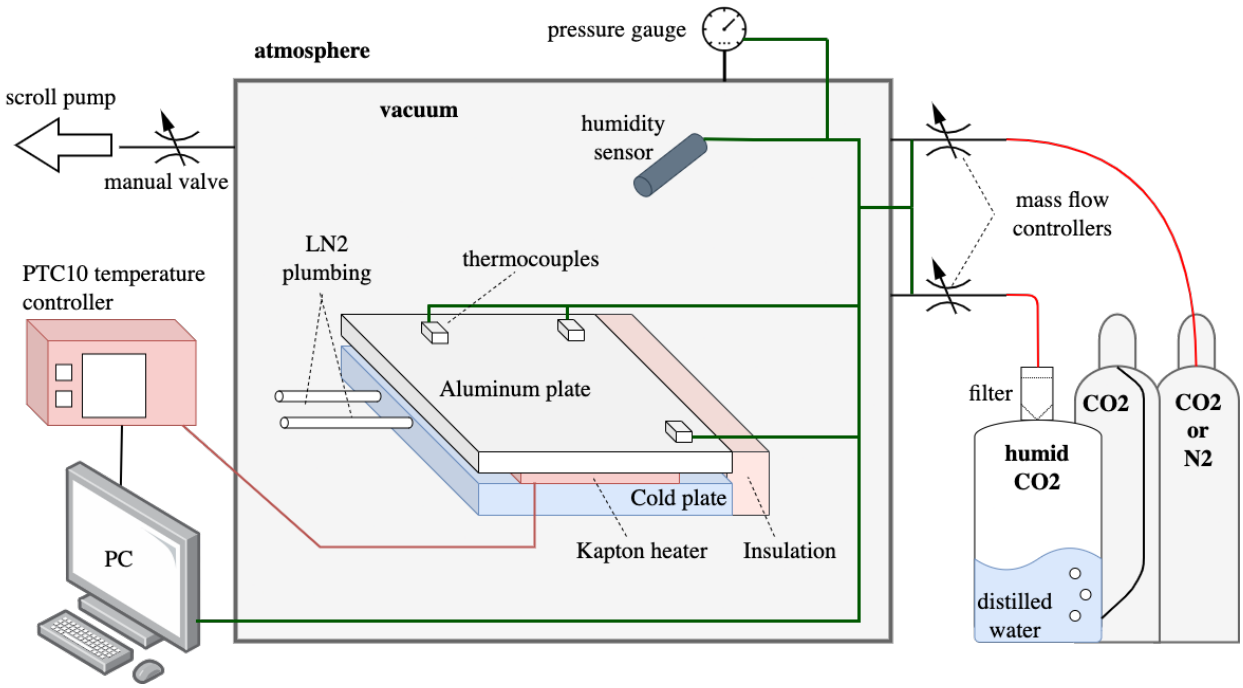

Figure 12: Schematic drawing of the environmental control infrastructure. The large grey enclosure represents the large vacuum chamber shown in Figure 11.

3.2 Raman Spectroscopy

3.2.1 Raman Scattering

When monochromatic radiation is incident on some material, it can either be absorbed, transmitted, or scattered by the molecules which comprise the material. During transmission, the photons pass through the material. In the case of absorption, the energy of a photon matches the energy difference between the ground state and an excited state of a molecule, and the absorbed photon gives energy to the molecule. In the case of scattering, the photon energy need not match the energy difference of a molecule's energy states; instead, the photon polarizes the electron cloud around the molecule, thus creating a "virtual" state, which is unstable, and quickly results in the radiation of a photon back out. Most of the time, the molecule returns to the original state, and

the scattered photons are of the same wavelength as the incident light [31]. This is an elastic process called Rayleigh scattering, and is seen when the distortion of the molecule's electron cloud is the only interaction between photon and molecule [31]. Raman scattering, alternatively, is the inelastic process by which scattered photons are of a shifted wavelength relative to the incident photon due to some energy transfer between the incident photon and the molecule. This occurs when the photon-molecule interaction induces a transition to a higher (quantized) vibrational mode, after which the molecule transitions to a vibrational energy state different from the original state. Either direction of energy transfer is permissible, i.e., the molecule can return to either a higher or a lower vibrational state than originally. In the case that the molecule returns to a higher vibrational state than previously, this type of Raman scattering is called Stokes scattering, and the scattered photon has lost energy to the molecule and has a longer wavelength than the incident photon. In the inverse case, where the molecule returns to a lower level than before, this is termed anti-Stokes scattering, and the scattered photon has a shorter wavelength than the incident photon.

Whether a molecule which undergoes Raman scattering results in a Stokes or anti-Stokes wavelength (or wavenumber) shift depends on the original vibrational energy of the molecule, which itself depends on thermal energy [31]. At temperatures relevant for studying the surfaces of Earth or Mars, a majority of molecules will be at the lowest vibrational state, which thus return to a higher state if Raman scattering occurs [26]. Hence, Stokes wavelength shifts are favoured over anti-Stokes shifts when employing Raman spectroscopy at ambient conditions near the surface of Earth or Mars.

3.2.2 Raman Wavenumber Shifts

Generally, the various wavenumber (or wavelength) shifts of the scattered photons from a sample are represented on a spectrum. The unique wavenumber shifts which correspond to the constituent molecules of the sample can be used to discriminate the composition of a sample, or its phase. This makes Raman scattering effective in studying water, as O-H vibrational stretching modes depend on hydrogen bond strength, and bond strength varies according to the phase of the water. Water ice, liquid water, and bound water of magnesium perchlorate hexahydrate all have distinct Raman wavenumber shifts between 2800 cm^{-1} and 3800 cm^{-1}, as shown in Figure 13. While reporting in wavenumber shift (in cm^{-1}) is more commonly done, reporting Raman spectra in wavelength is

also permissible, and is done in this thesis.

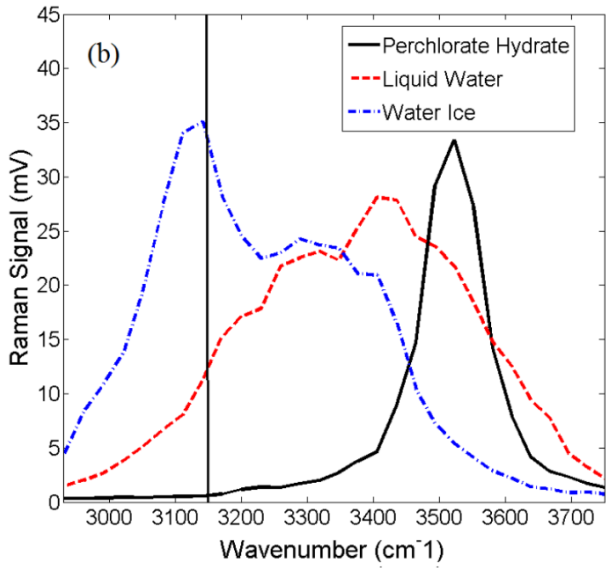

Figure 13: Raman spectra of water ice, liquid water, and bound water of magnesium perchlorate hexahydrate [6]. Each substance is distinguishable by shape of the spectrum and by wavenumber shift. The x-axis could also be in units of wavelength of scattered photon.

3.2.3 Raman LIDAR

A Raman spectroscopy apparatus, designed for both range-resolved atmospheric measurements and close-range measurements, was previously developed at York University. The design was based on the LIDAR (light detection and ranging) instrument of the NASA Phoenix Mars mission [1]. Discussion of the apparatus here will be limited; see the dissertation from Nikolakakos [26] for an in-depth description. In brief, an incident beam was sent towards a sample from outside the experiment chamber (described in Section 3.1.1) from a Q-switched Nd:YAG laser at 266 nm, with a repetition rate of 20 Hz. After passing through a fused silica window into the chamber and reflecting off a mirror, backscatter photons from the sample reflect back off the mirror and out of the chamber. This process is shown schematically in Figure 14. The scattered photons are then collected with a telescope and focused on an optical fibre, which are then passed through a grating spectrometer before landing on an array photomultiplier to be counted. This information is compiled into spectra like those shown in Figure 13. Since photon counting is done at the array photomultiplier, the vertical axes for the presented spectra are in units of MHz.

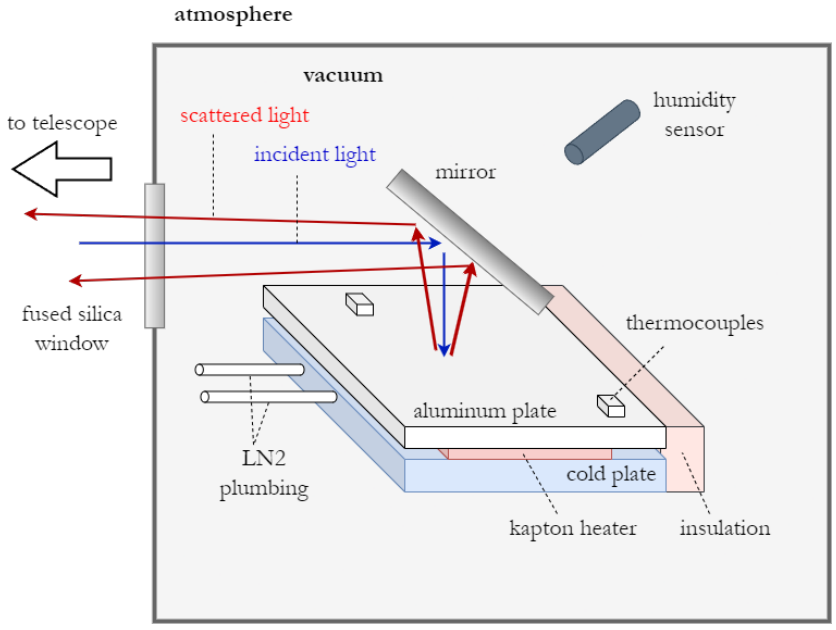

Figure 14: Simplified schematic of the environmental chamber shown in Figure 12 indicating the laser Raman beam path.

3.3 Example Experiment - Deliquescence of Magnesium Perchlorate

The example experiment below is a precursor to the MSc research presented later in this chapter. A major difference is that in the example experiment below, there is no simulated Mars regolith for the perchlorate to rest on.

A fine dusting of magnesium perchlorate-hexahydrate was placed in the centre of the aluminum sample plate shown in Figure 12 (and more specifically, underneath the laser ligthpath as in Figure 14, which is a simplified version of Figure 12). The pressure and frost point temperature in the chamber were reduced from Earth atmosphere to 7 torr and -55°C frost point, respectively. The temperature of the sample plate was then ramped down from room temperature to about -80°C while capturing visible light images and Raman spectra. Figure 15 shows the temperature and relative humidity over the course of the experiment. Black dotted lines indicate notable timestamps which correspond to particular subfigures within Figures 16 and 17. Additionally, subfigures 16a - 16e and subfigures 17a - 17e correspond temporally if they have the same letter index and appear in the same spatial location on the page. Figures 16a and 17a show the initial perchlorate sample in a camera image and Raman spectrum; the dry perchlorate hexahydrate peak is characterized

by a Raman-shifted backscatter at about 293 nm, as shown. The temperature was then decreased from 0°C to -51°C. Deliquescence can be seen to begin at -51°C, as evidenced by the disappearance of grains in Figure 16b and the slight increase in backscatter signal near the 292 nm wavelength in Figure 17b, which indicates the presence of liquid water. A temperature plateau was maintained so that more perchlorate could deliquesce and a stronger signal could be acquired, though note that the plateau is contrived and not accurate to Martian conditions. As shown in Figure 16c, this process allowed for considerable deliquescence; Figure 17c shows a strong liquid water signal at this stage along with a significantly reduced magnitude of the bound water (dry perchlorate) peak at 293 nm. The temperature was then further reduced. The onset of freezing occurred at -67°C. This was confirmed visually in Figure 16d and in spectrum as shown in Figure 17d, where the characteristic ice shoulder has appeared at around 290 nm. By the time the sample plate reached -80°C, ice crystals dominated the visual images and the spectra (Figures 16e and 17e, respectively).

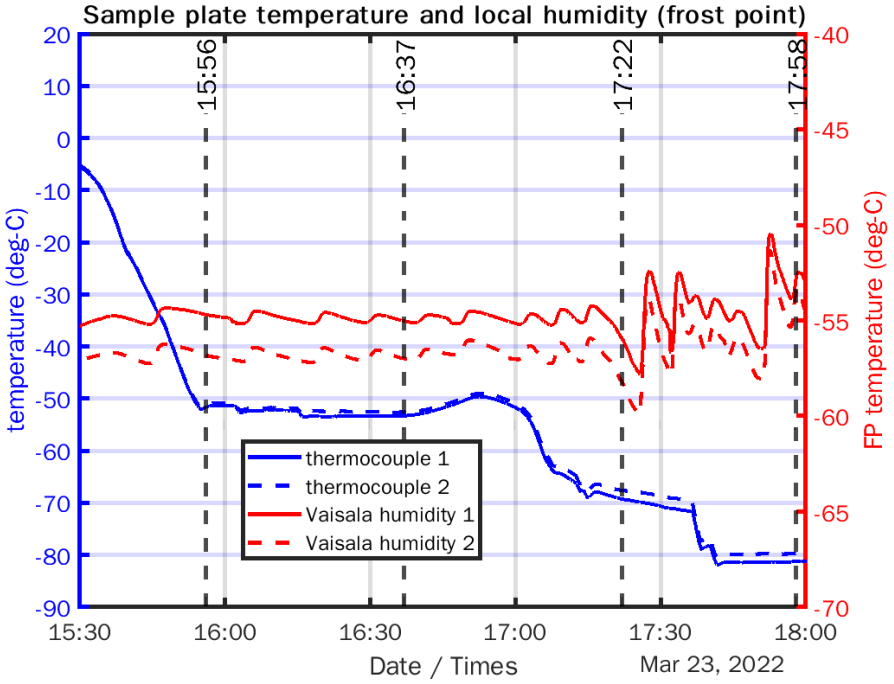

Figure 15: Planetary simulation chamber data for example deliquescence experiment.

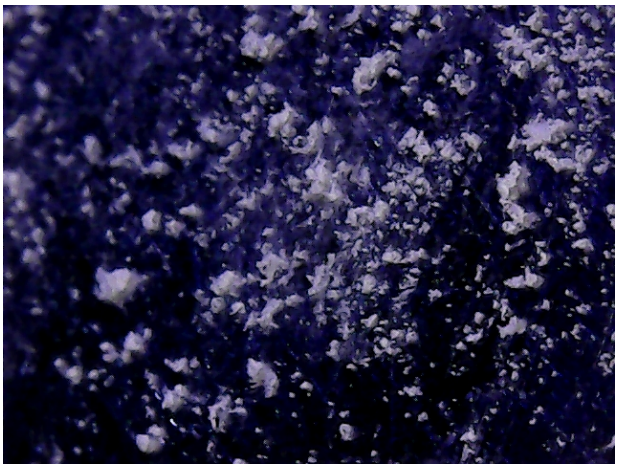

(a) Starting perchlorate sample. The smallest grains will deliquesce first; compare with Figure 16b.

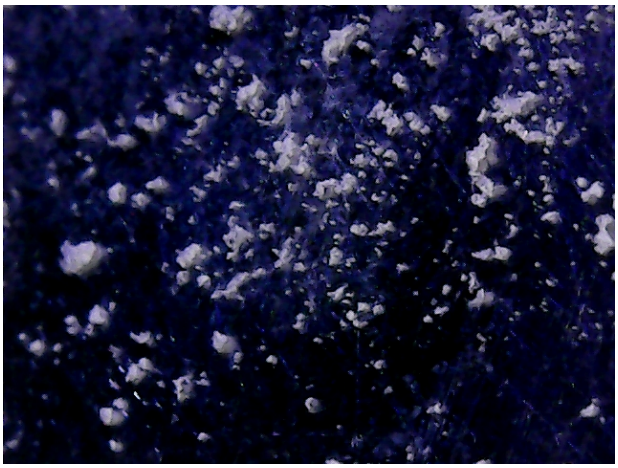

(b) Perchlorate sample at onset of deliquescence at 15:56 (-51°C). Disappearance of grains is evident.

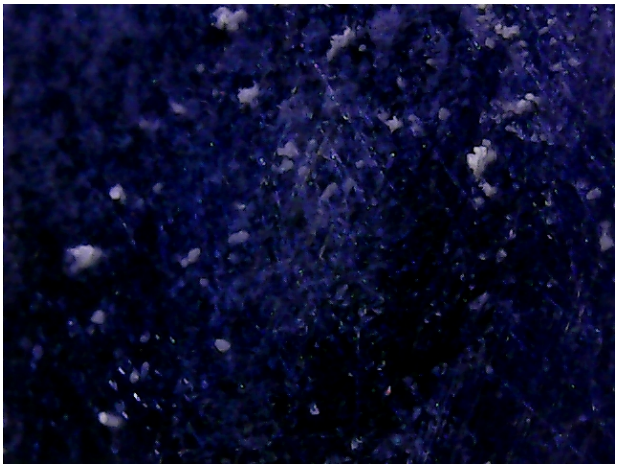

(c) Perchlorate sample at full extent of deliquescence at 16:37 (still -51°C). Freezing has not yet occurred.

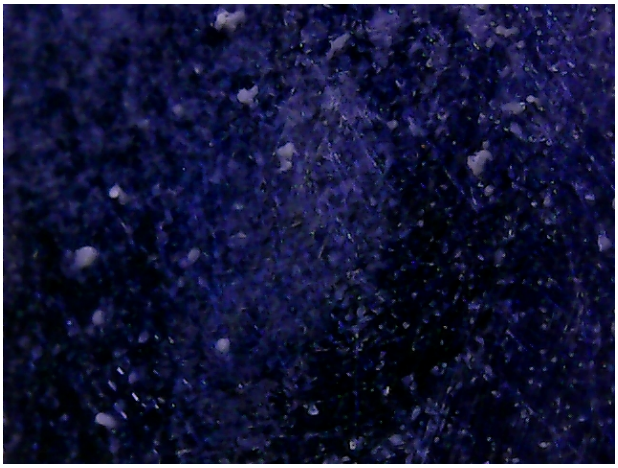

(d) Perchlorate sample at onset of ice signal in Raman spectra at 17:22 (about -67 °C).

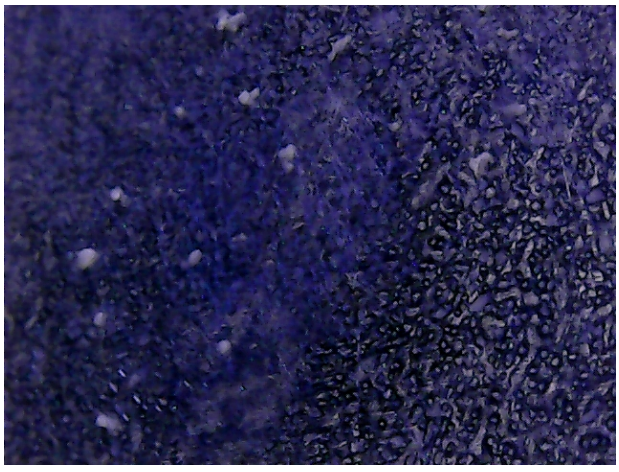

(e) Frozen sample at close of experiment at 17:58 (-80°C).

Figure 16: Visible light images of perchlorate sample undergoing deliquescence. The field of view is about 1 cm across for scale.

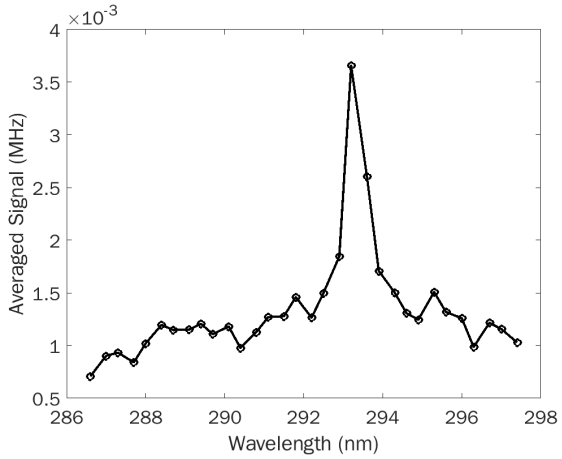

(a) Raman spectrum for perchlorate hexahydrate at the start of the experiment prior to deliquescence.

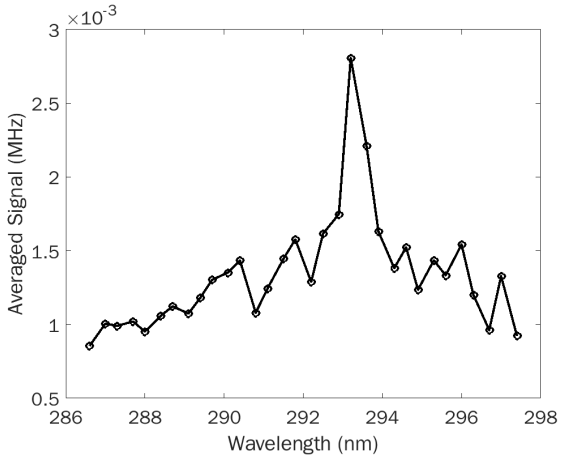

(b) Raman spectrum at onset of deliquescence at 15:56 (-51°C). Liquid signal increasing around 292 nm.

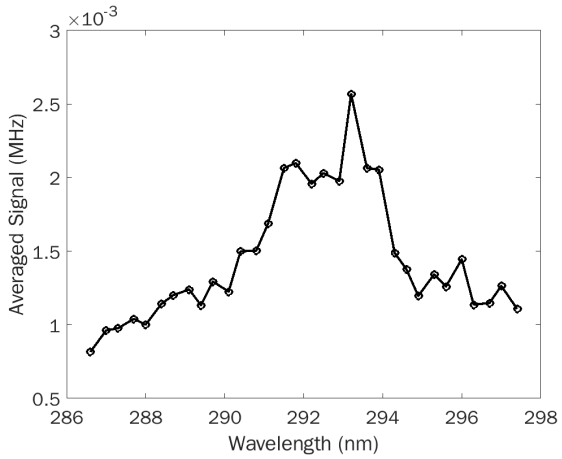

(c) Raman signal corresponding to full deliquescence at 16:37 (still -51°C). Water signal clearly visible on left side of perchlorate bond water peak.

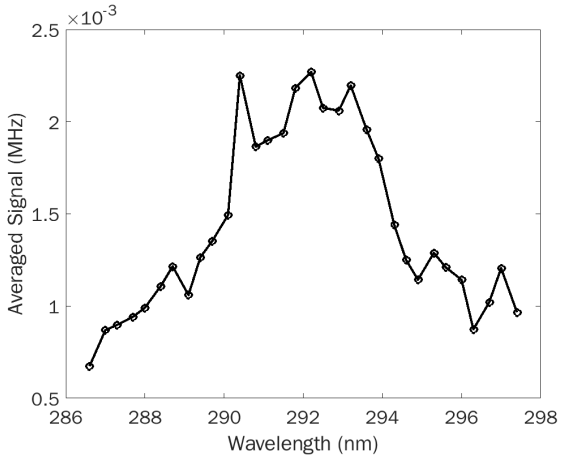

(d) Raman signal at onset of ice signal in Raman spectra at 17:22 (about -67 °C). Ice shoulder at far left now visible, and solid perchlorate bound water signal is diminished.

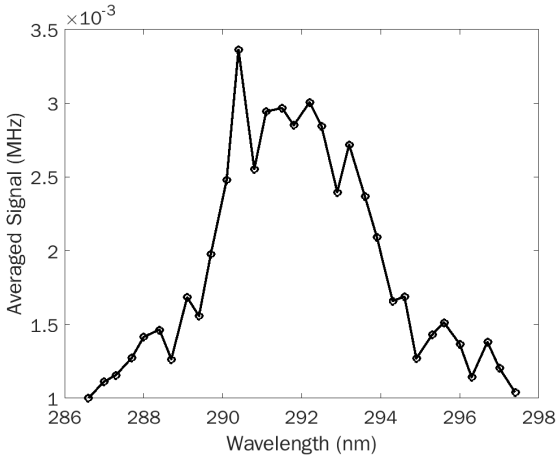

(e) Raman signal for frozen sample at close of experiment at 17:58 (-80°C).

Figure 17: Raman spectra perchlorate sample undergoing deliquescence. The incident laser wavelength was 266 nm.

3.4 Experiment Design

The experiments described below are of near identical format to the example experiment discussed in Section 3.3, where, at Mars pressure and humidity, the temperature of a sample is decreased such that it passes through the DRH of magnesium perchlorate hexahydrate. The primary difference between the tests described below and the example experiment above characterizes the intended advancement in demonstration: Rather than on an actively cooled plate, deliquescence of perchlorate grains is sought on a sample of Martian regolith simulant (also referred to below as simulated Martian regolith).

3.5 Deliquescence on Martian Regolith Simulant - Results

3.5.1 Mars Humidity (-55°C Frost Point) on Quartz Sand

As a next step from the successful demonstration of deliquescence at Mars environmental conditions, the same test was conducted on a small pile of quartz sand, about 3 cm across by 3 mm deep at the centre of the pile. The pile was placed in the centre of the cooling plate under the path of the incident laser beam like in Figure 14, with a light dusting of magnesium perchlorate hexahydrate on top. The pressure and relative humidity in the chamber were reduced from Earth atmosphere to 7 Torr and -55°C frost point, respectively, as indicated by the temperature and humidity plot in Figure 18, which covers the duration of the experiment. Subfigures within Figure 19 show camera captures at different stages in the experiment, which correspond to the timestamps of Figure 18 where indicated in the captions. Figure 20 shows key Raman spectra. In Figure 19, the sensing component of the thermocouple is visible in the top left of each image, and is about 1 mm across. Two thermocouples read out temperature of the sample: one underneath the pile, about 2 mm deep ("in sand" in the legend of Figure 18) and one right at the surface of the sand in an attempt to log the temperature at the top surface ("on surface").

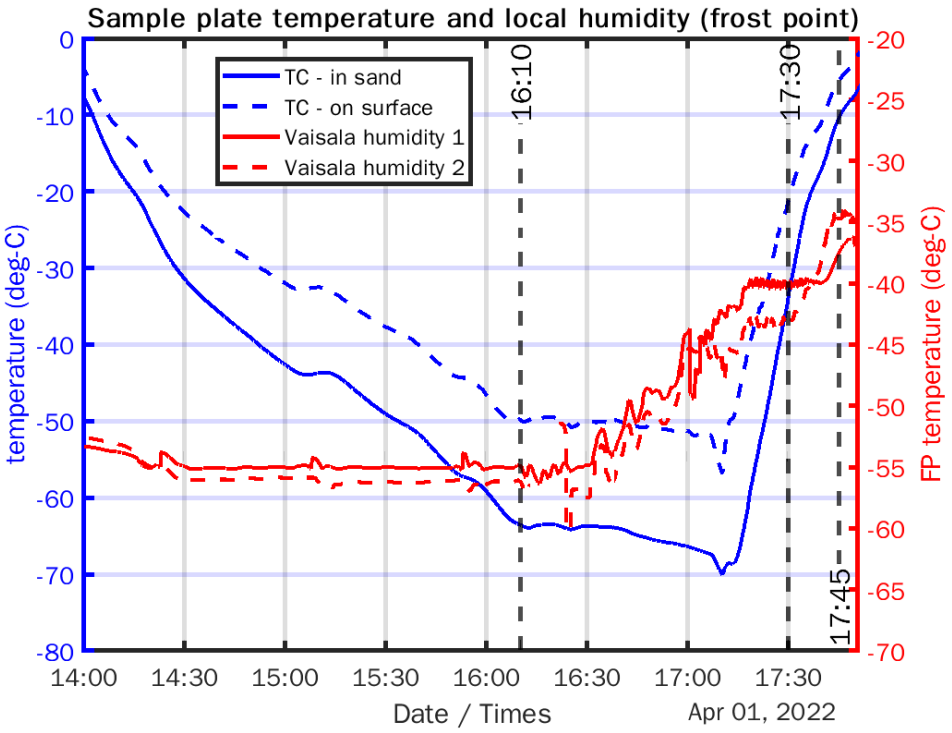

Figure 18: Planetary simulation chamber data for example deliquescence experiment on quartz sand.

Figure 19a shows the initial state of the sample. The temperature of the sand was then cooled as the frost point was maintained. As shown in Figure 19b, by 16:10, upon reaching -50°C temperature at -55°C frost point, no apparent deliquescence has occurred, as would be expected from previous tests. The temperature was then held at this point (with the laser off to prevent heating) for about 30 minutes with no apparent deliquescence of perchlorate in camera captures or in Raman spectra. Rather than taking the surface temperature even lower (and further enabling frost deposition onto the cold plate, thus reducing available water vapour), water vapour was added to the chamber to increase the relative humidity in an attempt to achieve deliquescence. Eventually, deliquescence was seen (Figure 19c) but only after the temperature of the sand was raised to above the frost point temperature at 17:30 (at this point, the sample container temperature was also above the frost point temperature). Figure 20 shows laser Raman LIDAR captures before, during, and after the apparent deliquescence, though note that the resulting brine from deliquescence seeped below the upper surface of quartz sand and was not directly detected by the Raman LIDAR. Instead, deliquescence is evident in the camera captures, and is implied in the decreased magnitude of spectral signal around the dry perchlorate bound water peak at 294 nm scattered wavelength.

Since deliquescence only occurred during the warming period, it appears the perchlorate resting atop the sand never reached the requisite cold temperature during cooling to meet the DRH before the local humidity became too low due to frost deposition. By the time the top surface reached -50°C, the cold plate itself was well below the frost point temperature. Hence, there was not adequate water vapour surrounding the perchlorate, and only sublimated frost coming off the plate during warming provided the necessary moisture for deliquescence to occur.

(a) Starting perchlorate sample atop sand. The tip of a thermocouple ("on surface" in legend) is visible in the top left.

(b) Capture at 16:10, where no deliquescence has occurred despite apparently reaching -50°C at -55°C frost point humidity.

(c) Capture at 17:30, showing onset of deliquescence only upon warming, as frost sublimated from the container.

(d) Capture at 17:45, at completion of deliquescence only after significant warming.

Figure 19: Camera images of perchlorate sample undergoing deliquescence, but only during significant warming, on sand. The thermocouple sensing head shown in the top left of each subfigure is about 1 mm across for scale.

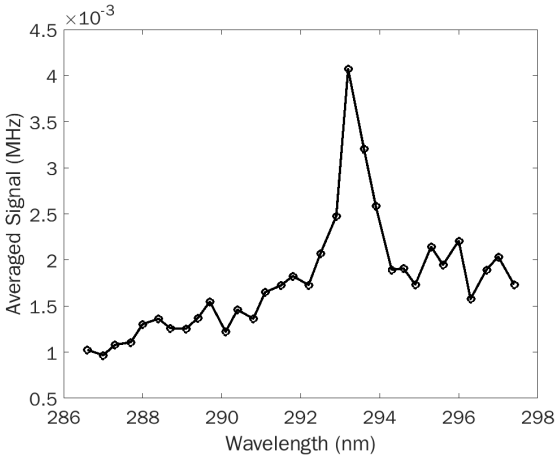

(a) Starting perchlorate sample atop sand.

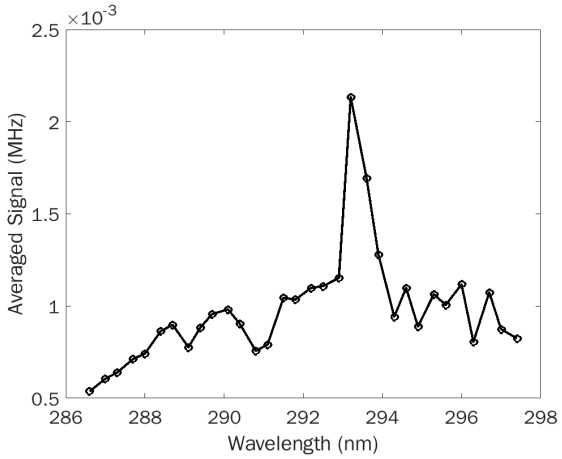

(b) Spectrum at onset of deliquescence only upon warming at 17:30, releasing water from plate.

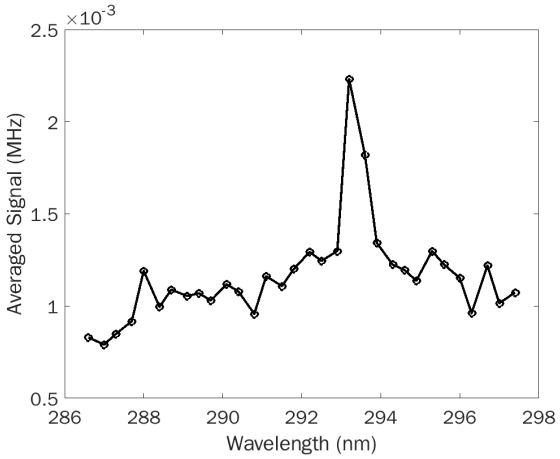

(c) Final state of sample at 17:45, with deliquescence only after significant warming.

Figure 20: Raman spectra which correspond to the camera images in Figure 19; liquid seeped beneath the sand, and deliquescence is not easily confirmed using these spectra. The incident laser wavelength was 266 nm.

3.5.2 -35°C Frost Point on Simulated Martian Regolith

After attempting deliquescence at -55°C frost point on quartz sand, an experiment was done at the much more humid environment of -35°C frost point. A small pile of simulated Martian regolith (henceforth referred to as just "regolith") (Mojave Mars Simulant, MMS-1 [29], [30]), about 2 cm across and 2 mm tall at the centre of the pile, was placed in the centre of the cooling plate under the path of the incident laser beam of Figure 14, just as in the previously discussed test using quartz sand. The rest of the experiment proceeded in the same manner, except this sample was contained within an enclosed box with a lid. Additionally, there was a small pipe inserted into the

box which allows for drawing of air over the sample from a manual valve and pump outside the chamber ensuring the air inside the box is replenished with moisture from the greater chamber.

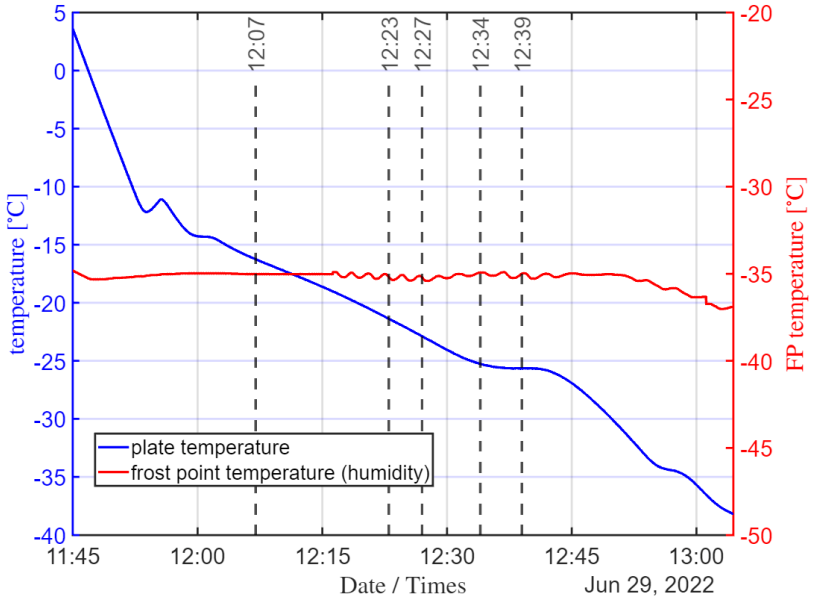

Figure 21: Planetary simulation chamber data for deliquescence experiment at -35°C over regolith.

Figure 22a shows the initial perchlorate sample on the regolith pile and on the plate, indicated by the lighter and darker arrows, respectively. At this point, the temperature was still cooling just past -15°C while the humidity was held steady at -35°C frost point. Chamber air was being drawn over the regolith at about 0.1 L/min. By 12:23, once the temperature of the plate reached -21°C, first deliquescence was seen on the plate, visible in Figure 22b. A few minutes later, by 12:27, by the time the plate temperature reached about -23°C, first deliquescence was seen on the edge of the regolith pile, indicating temperature difference of a few degrees between the plate and the edge of the regolith pile. This is shown in Figure 22c, where some perchlorate grains are seen to have disappeared (lighter arrow), and no apparent perchlorate grains remain on the metal portion (darker arrow). By 12:34, it is apparent in Figure 22d that deliquescence of perchlorate on regolith is working its way inwards, or rather, that the centre portion of the pile is taking longer to cool than the outer portions. Finally, by 12:39, all the perchlorate on the regolith pile has deliquesced. The plate temperature at this point is -26°C, indicating about a 5°C difference in temperature between the centre of the regolith pile and the plate.

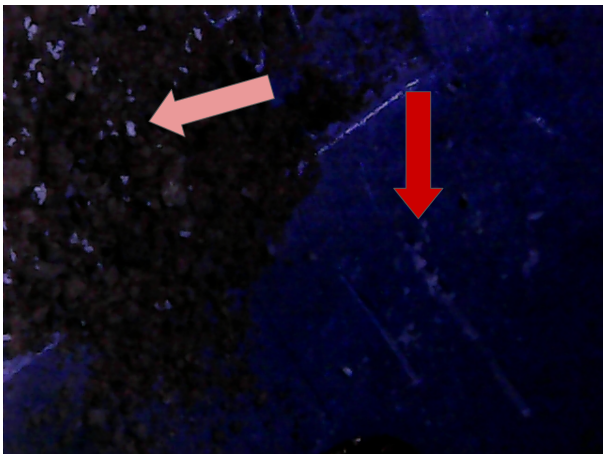

(a) Capture at 12:07, before deliquescence was observed in either the perchlorate on bare metal (dark arrow) or on regolith pile (light arrow).

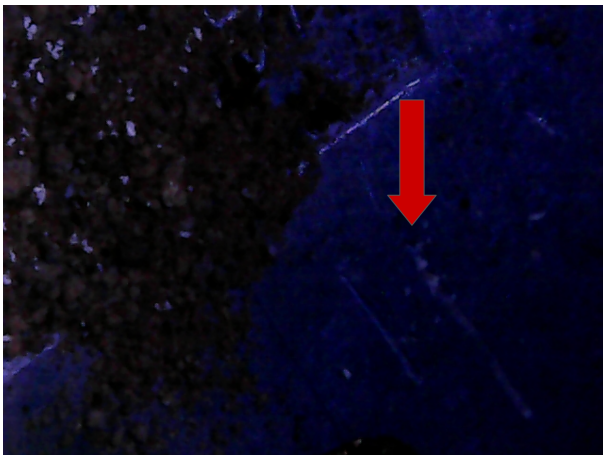

(b) Capture at 12:23, where the temperature of the plate reached -21°C and deliquescence was first observed on the plate.

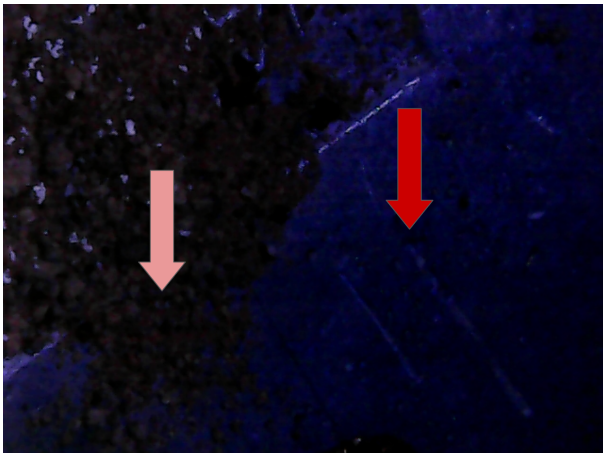

(c) Capture at 12:27, where deliquescence has completed on the plate, and deliquescence has just began at the edge of the regolith pile.

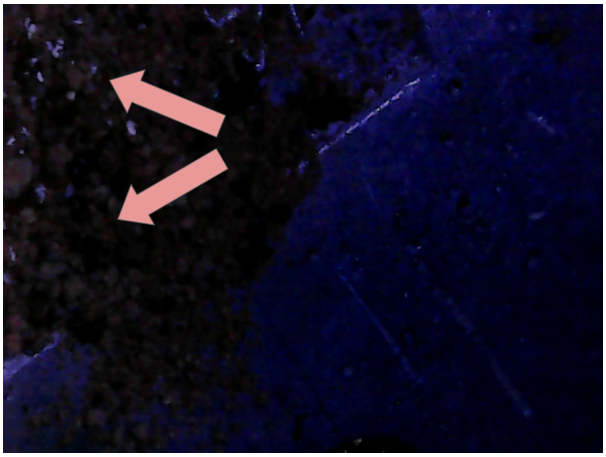

(d) Capture at 12:34, as the onset deliquescence on the pile moves inwards.

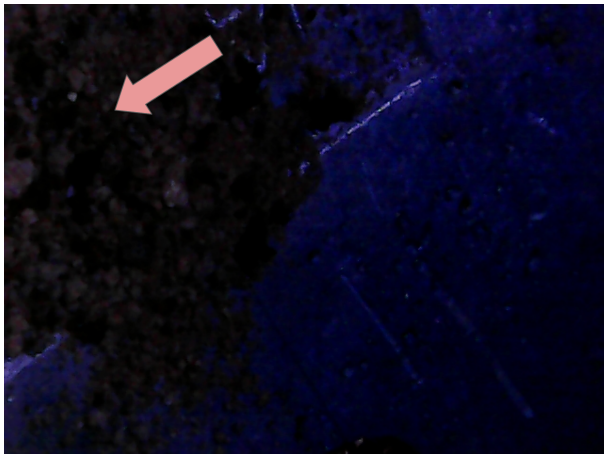

(e) Capture at 12:39, where deliquescence has completed on the regolith pile. The plate temperature is now about -26°C.

Figure 22: Camera images from -35°C frost point deliquescence experiment on simulated Martian regolith. The field of view is about 2 cm across.

In addition to camera captures, Raman spectroscopy was attempted as an additional means of detecting deliquescence in this experiment. However, it turns out that the Martian regolith simulant severely depletes signal strength while also adding significant contamination around key features, and so the spectra are not shown. Absorption of signal is due to iron in the regolith mixture, which is known to absorb ultraviolet light [26]. Hence, for this experiment and future experiments on simulated Martian regolith, visible inspection of the sample by camera was deemed superior to Raman spectroscopy (addressing this shortcoming is listed in Future Work below in Section 3.6).

3.5.3 -35°C Frost Point on Simulated Martian Regolith - Alternate Cases

The previous test at -35°C frost point temperature was then repeated twice, in one case where there was no air from the greater chamber drawn through the sample box, and a separate case where there was no lid capping the sample box, thus not shielding the regolith from the surrounding chamber's infrared radiation. These two tests ultimately show that both air draw over the sample and a lid to shield infrared radiation are required for a demonstration of this nature.

No air draw: Figure 23 shows the pressure and humidity data from the iteration where no moisture-replenishing air was drawn through the enclosed sample box over the regolith, and Figure 24 shows the corresponding camera captures. The rest of the experiment procedure is unchanged.

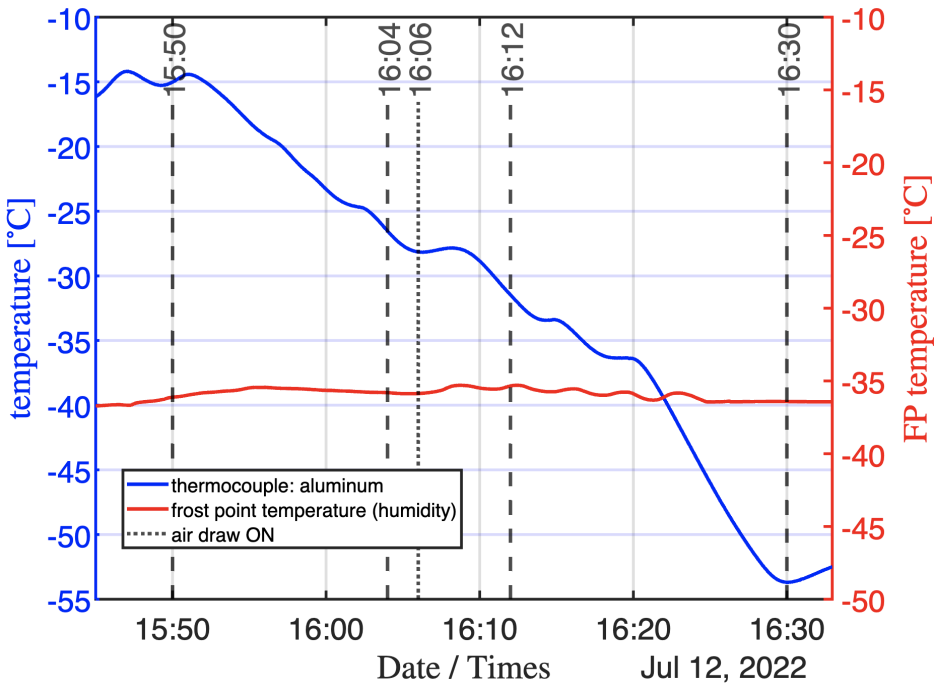

Figure 23: Planetary simulation chamber data for deliquescence experiment at -35°C over regolith with no air drawn over sample.

As shown in Figure 24b at 16:04, despite the temperature of the plate reaching below -25°C, no deliquescence was seen on the plate, whereas in the previous experiment (Section 3.5.2, Figure 22b), deliquescence on the plate occurred at -21°C. At 16:06, the air draw was reintroduced, and immediately deliquescence occurred on the plate (Figure 24c). The rest of the experiment proceeded as in Section 3.5.2 once air flow was reintroduced. Another difference was that some perchlorate remained on the regolith pile at the very centre by the close of the experiment, which can be attributable to slightly greater thickness of the pile at that location. A thicker portion of regolith would see a larger temperature difference compared to the plate than a thinner portion due to compounding effects of insufficient thermal contact between grains. Ultimately, a warmer temperature at that location would prohibit deliquescence before frost deposition disallowed it entirely regardless of regolith temperature, which is evidently an issue in the next experiment shown below.

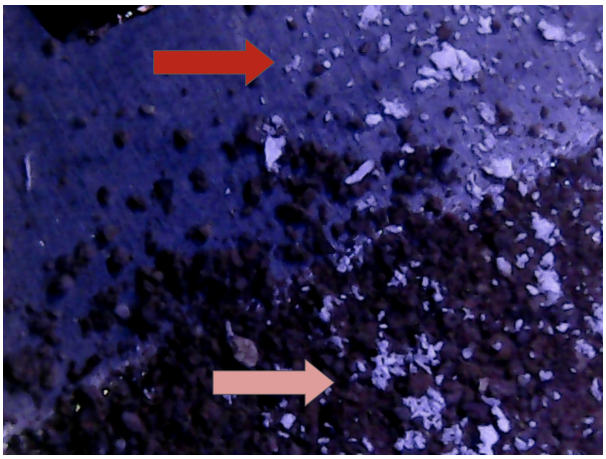

(a) Capture at 15:50, at a temperature before any deliquescence is expected anywhere for -35°C FPT.

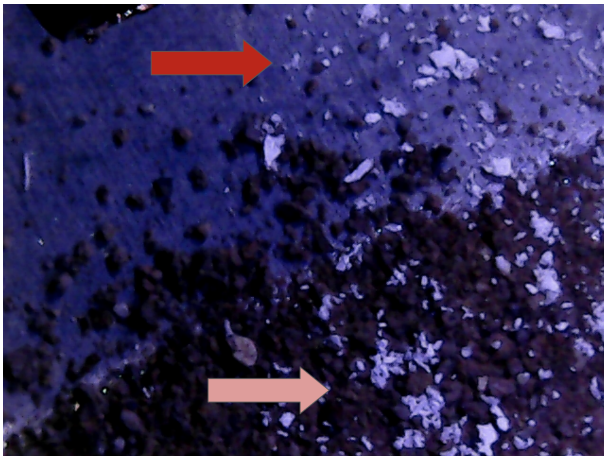

(b) Capture at 16:04, where no deliquescence on plate (dark red arrow) has occurred despite the plate reaching well below the requisite temperature of -21°C.

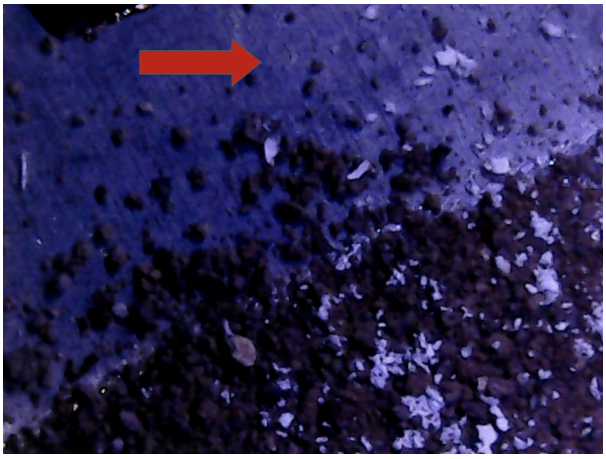

(c) Capture at 16:06, at the instant where the air draw was reintroduced, and deliquescence on the plate immediately kicks in.

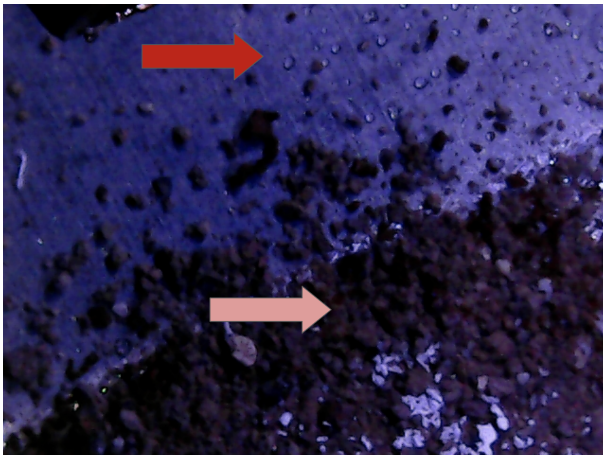

(d) Capture at 16:12, as deliquescence quickly follows on the regolith pile from the outside in as in previous tests.

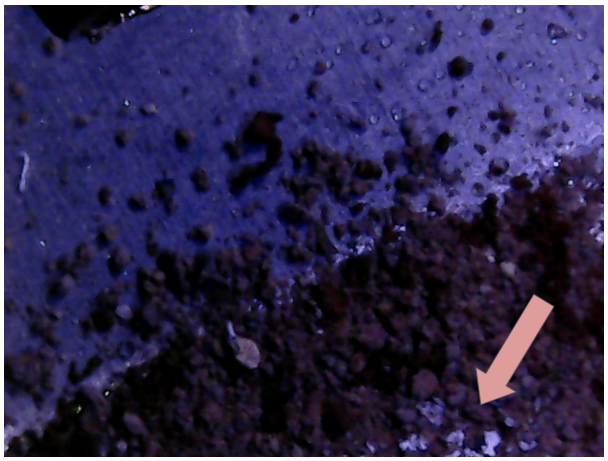

(e) Capture at 16:30. The centre of the pile never cooled sufficiently, so some perchlorate remains un-deliquesced.

Figure 24: Camera images from -35°C FPT deliquescence experiment on simulated Martian regolith. The field of view is about 2 cm across.

No infrared blocking: Figure 25 shows environmental data for a second case, where there was no cooled lid to shield the regolith from the greater chamber's infrared radiation. However, there is now at least ample water vapour due to being open to the chamber environment. As usual, Figure 26 shows camera captures which correspond to the timestamps of Figure 25.

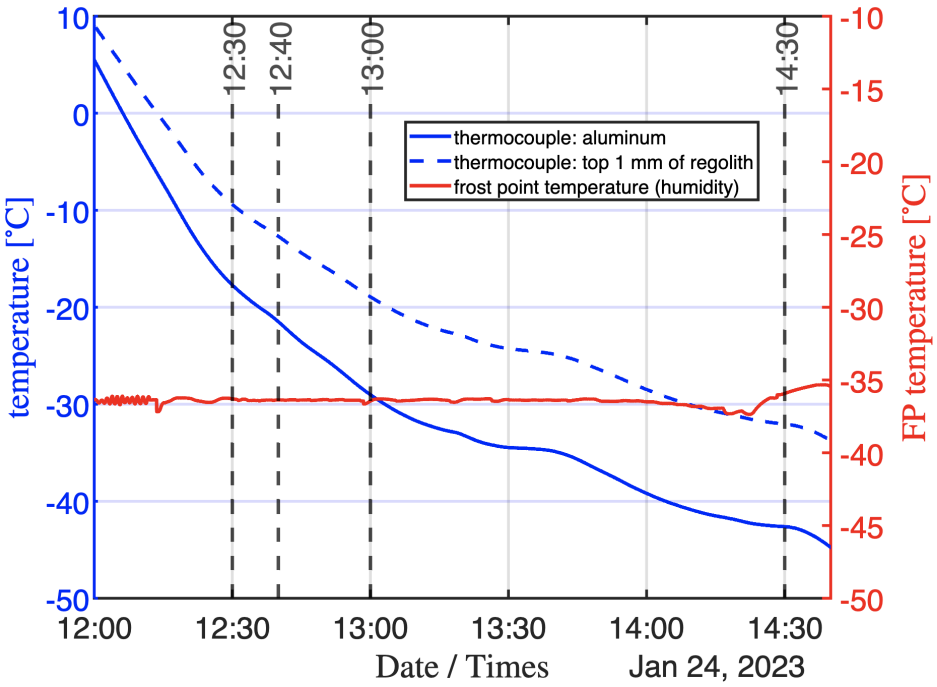

Figure 25: Planetary simulation chamber data for deliquescence experiment at -35°C over regolith with no lid, and thus no infrared blocking.

The experiment was set up and conducted in the standard way. Figure 26a shows the initial perchlorate on both the actively cooled aluminum (dark arrow) and on the regolith (lighter arrow), both exposed to infrared from the chamber environment. By 12:40 (Figure 26b), right as the temperature reached -21°C during cooling, the perchlorate on the plate deliquesced, which is in exact agreement with previous tests. However, as indicated across Figures 26c and 26d, the perchlorate on the regolith never deliquesced. By the time the top 1 mm of regolith reached below -20°C, the aluminum was already dipping below the frost point, as seen in Figure 25, causing frost deposition. If we surmise that the surface of the regolith is even warmer than the top 1 mm of subsurface, it follows that the perchlorate never would become cold enough to reach the DRH before deposition began extracting moisture out of the surrounding environment. This problem would only be exacerbated at colder temperatures, like -50°C.

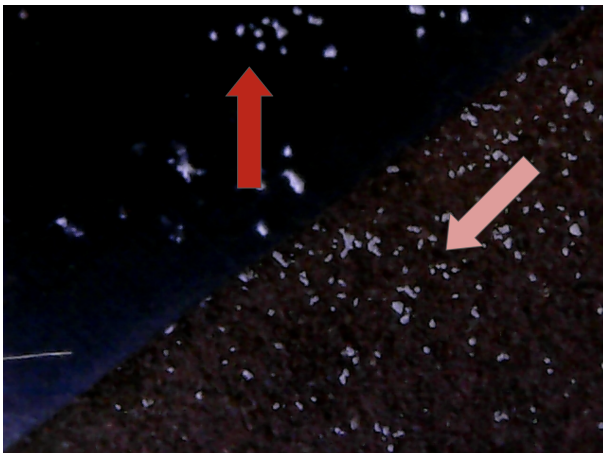

(a) Capture at 12:30, showing initial set up where no deliquescence is yet expected. Perchlorate is present on both regolith (light arrow) and actively cooled aluminum (dark arrow).

(b) Capture at 12:40, as deliquescence on the aluminum begins precisely where expected at -21°C for -35°C FPT (red arrow).

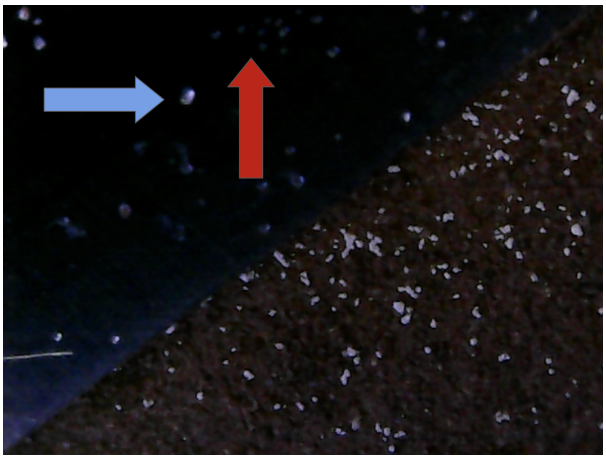

(c) Capture at 16:12, where full deliquescence of dry perchlorate has completed (red arrow) and some perchlorate brine begins to freeze (blue arrow).

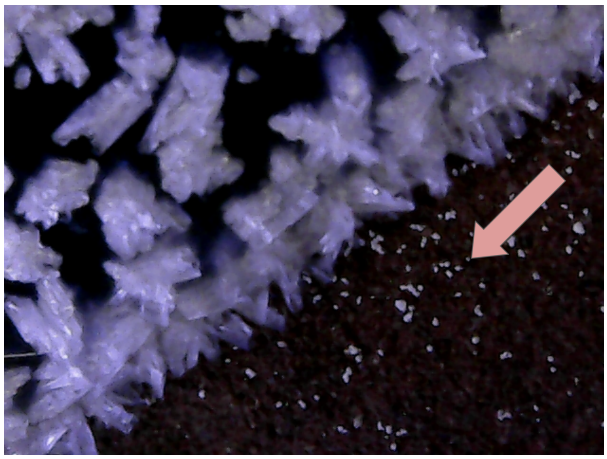

(d) Capture at 14:30. The plate is so cold that massive frost formations are seen, but the perchlorate on the regolith never deliquesced.

Figure 26: Camera images from -35°C frost point temperature deliquescence experiment on simulated Martian regolith with no lid. The field of view is about 2 cm across.

3.5.4 Mars Humidity (-55°C Frost Point) on Simulated Martian Regolith

The above experiments demonstrated that both air draw of chamber air over the sample as well as infrared shielding by a cooled lid are required to sufficiently cool a sample of simulated Martian regolith while providing ample moisture to achieve deliquescence of perchlorate grains. In an attempt to translate this to achieve a demonstration of this at Mars conditions, the successful test at -35°C frost point was re-done at Mars humidity. The sample was prepared in the same manner as in Section 3.5.2. The experiment procedure was also the same, with the only difference (importantly)

being that the humidity level in the chamber (about -52.5°C frost point) far more closely resembles the humidity from the Phoenix landing site on Mars [20].

Figure 27 shows temperature and humidity data for this experiment, again with timestamps which correspond to the camera capture subfigures of Figure 28, which has dark and light arrows to highlight perchlorate on just aluminum and on regolith, respectively. Initially, at 17:00, no deliquescence is expected since the plate temperature (and thus the relative humidity) is not near the critical level for -52°C frost point temperature. By the next timestamp (Figure 28b), there is no change, despite reaching -51 °C plate temperature. At this temperature, if resting on an actively cooled plate, perchlorate deliquescence is expected; recall the example experiment in Section 3.3, where at -55°C frost point, deliquescence occurred around -51°C plate temperature.

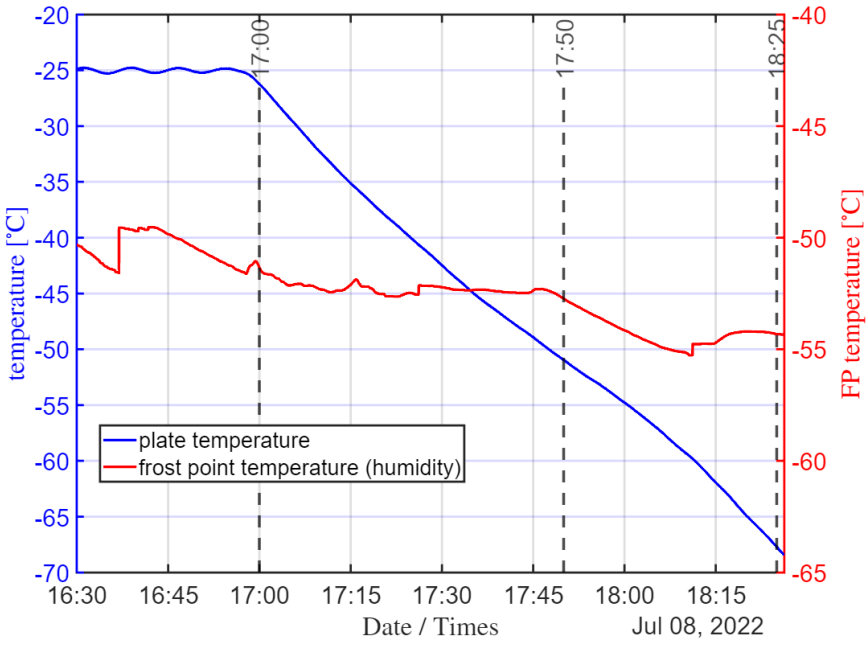

Figure 27: Planetary simulation chamber data for deliquescence experiment at -52.5°C FTP, down to -55°C FTP, over regolith.

For this test, humidity is actually more generous than in Section 3.3, or on Mars for that matter, being itself at -52.5° frost point, which would theoretically require a warmer critical temperature of the sample for deliquescence to occur than at -55°C frost point. In fact, not even the perchlorate on the cold plate has deliquesced (as indicated by the dark red arrow), indicating it may be in contact with a warmer regolith grain, or balanced atop the rough artifact in the plate surface in such a way

that it is not sufficiently cooled. By 18:25, there is still no change (Figure 28c), despite attempts to cool the regolith pile considerably so that it (or rather, the perchlorate grains resting on top) can pass through the requisite temperature such that the DRH is met. This suggests either a very large temperature gradient between the sample plate and the regolith (nearing 20°C difference, which is possible at low temperatures such as these), or, as has been shown above in previous experiments, the local humidity has been reduced too greatly by deposition of water vapour onto the plate which occurs when the temperature of the plate drops below the frost point. Either case presents practical challenges, and prohibits demonstration of deliquescence on a sample of regolith where previously (at -35°C frost point humidity, Section 3.5.2 above), it was achievable.

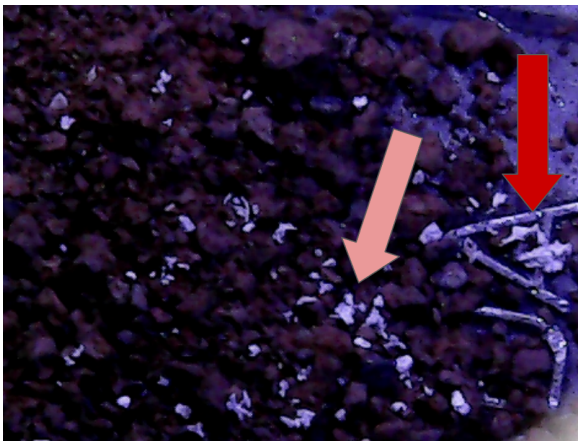

(a) Capture at 17:00, showing initial state. Some perchlorate is balanced atop an artifact in the plate, and may be in contact with regolith grains.

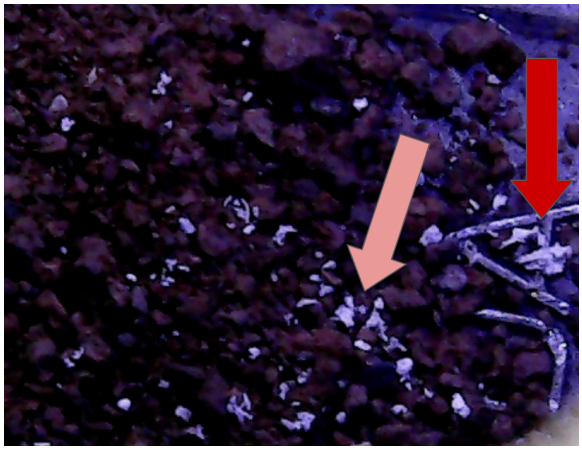

(b) Capture at 17:50, at a temperature where deliquescence would routinely have already occurred on a cold plate, but none has.

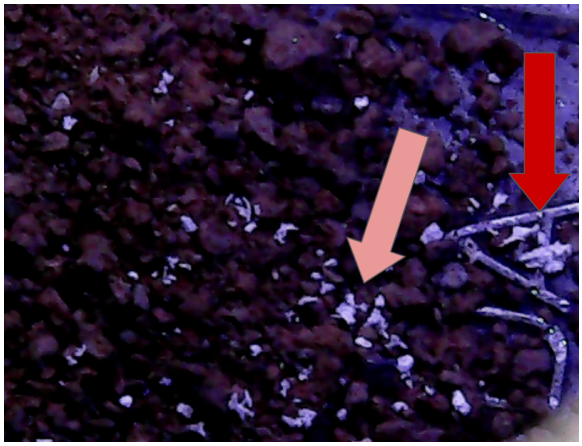

(c) Capture at 18:25, at the coldest point in the test (below -65°C), with no deliquescence seen whatsoever.

Figure 28: Camera images from -52.5°C frost point humidity deliquescence experiment on simulated Martian regolith. The field of view is about 1 cm across.

3.5.5 Mars Humidity (-55°C Frost Point) on Simulated Martian Regolith - Updated Apparatus

Having determined the necessity of superior cooling (including infrared shielding), and replenishing air flow to counteract deposition as the sample container cools below the frost point temperature, the experimental apparatus was updated to that shown schematically in Figure 29. Two experiments which utilized this apparatus are then presented; the left-most portion of the apparatus, which is an additional small container which can measure the humidity of the gas leaving the sample box, was only added for the second experiment discussed below. The different stages are illustrated in detail in Figures 30 through 32.

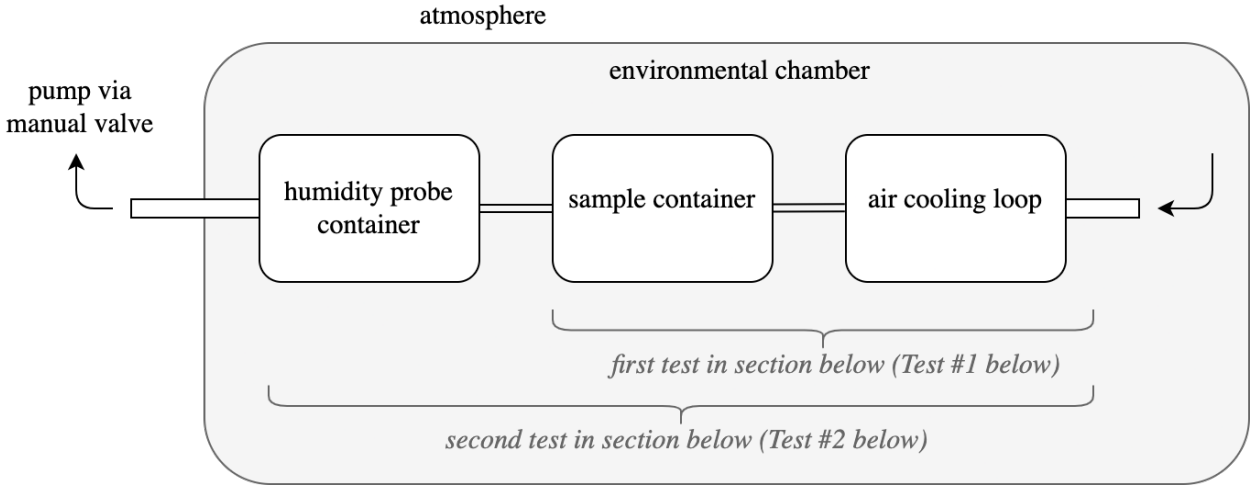

Figure 29: Schematic of updated apparatus for demonstrating deliquescence on simulated Martian regolith.

The custom-machined primary stage, which holds the regolith and perchlorate sample, is shown in Figure 30 from the side and from the top. The cross-section of simulated Mars subsurface rests entirely enclosed in an aluminum container, which is temperature controlled using the same heat exchanger as previously. A perchlorate dusting sits atop the regolith pile, both of which are now expected to have reduced temperature discrepancy with the interior temperature of the container walls, since the regolith is now in contact with all inner surfaces of the rectangular, actively-cooled aluminum container except the lid, which shields the sample from chamber infrared radiation. This lid is in strong thermal contact with the body of the container, and so is nearly the same temperature as the side walls. Air is drawn over the sample from a pump outside the chamber through one main channel (which first passes through a cooling loop, Figure 31), which is intended

to spread out over the sample by a series of small holes which open from a small depression into the sample area, as illustrated in the top-down view of Figure 30b, and as visible in the real life images of the machined parts in Figure 33.

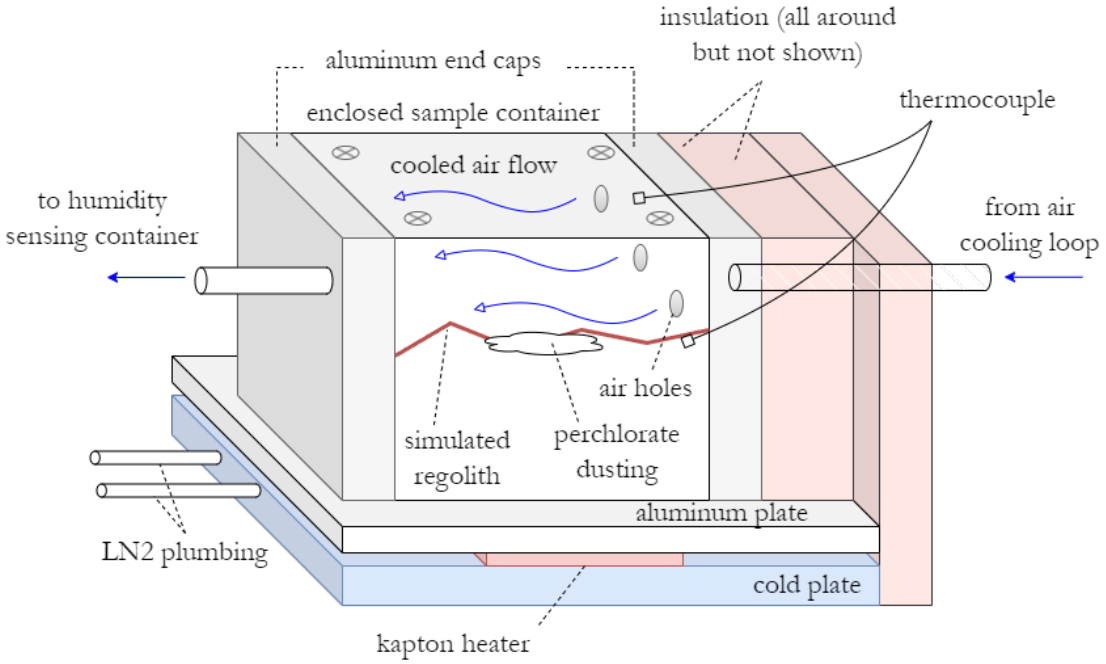

(a) Sample-holding stage of the updated apparatus.

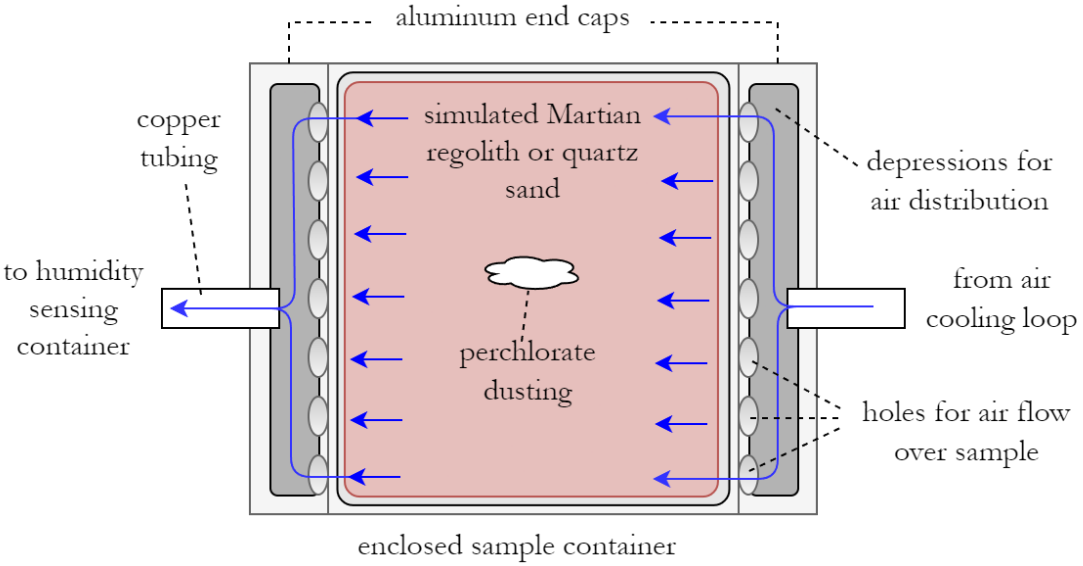

(b) Top-down view of the same, showing intended cooled air flow.

Figure 30: Sample stage of updated apparatus. The enclosed sample container, not counting the aluminum end caps, has outer dimensions of 90 × 90 × 40 mm. The inner depression where the regolith simulant rests has dimensions 70 × 70 × 30 mm.

Thermocouples are used for measuring temperature of the sample and of the container. In the case

where thermocouples are used inside, holes were drilled in the container and re-sealed with kapton tape and aluminum tape after threading in the thermocouple. Air which passes over the regolith and perchlorate first passes through the air cooling loop shown in Figure 31, which is just a loop of copper tubing (1/4 in. in the first test, then 1/8 in. in the second) wound around a cooled aluminum cylinder. A second liquid nitrogen loop was established for independent temperature control of the cooling loop, the aluminum cylinder for which was in contact on the top and bottom with liquid nitrogen cold plates. A Vaisala DMT152 capacitive humidity sensor was placed near the air intake. Cooled air from this stage is connected to the sample stage with copper tubing, fixed with Swagelok compression fittings, and sealed with Torr Seal epoxy resin sealant.

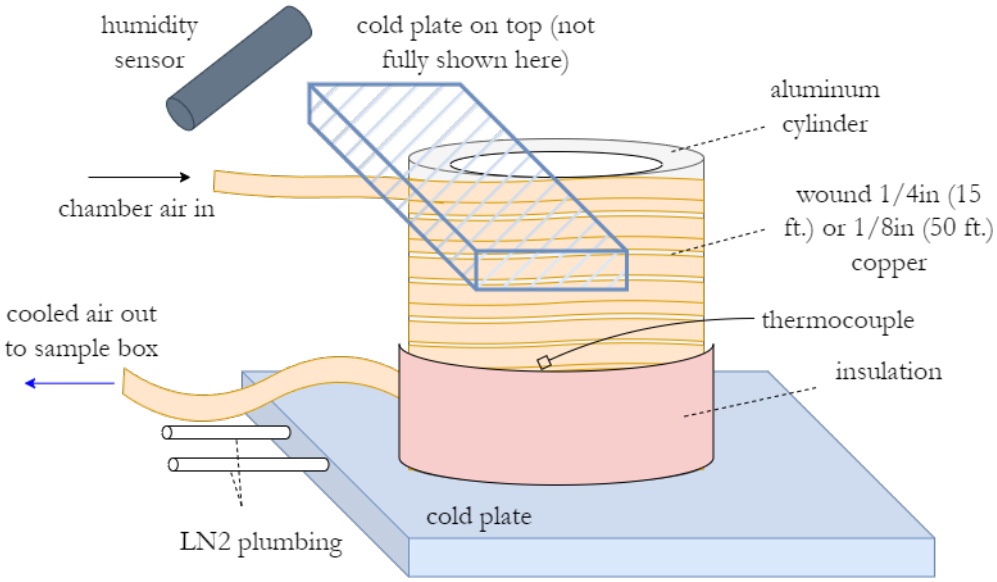

Figure 31: Diagram of air-cooling stage of updated apparatus. Air which passes over the sample first passes through a length of cooled copper tubing, which was either 15 ft. long at 1/4 in. outer diameter (OD) or 50 feet long at 1/8 in. OD.

The above stages were used for the first experiment described in Section 3.5.6 below. For the second experiment discussed, a third stage was added, which is an additional enclosed container with another Vaisala DMT152 humidity probe for sensing the humidity of the air leaving the sample enclosure. This is illustrated in Figure 32.

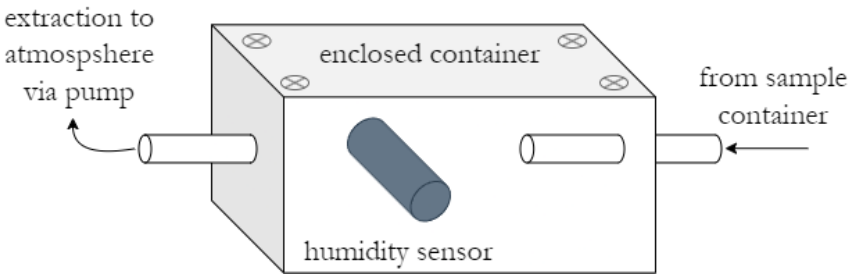

Figure 32: Humidity-sensing stage of updated apparatus, which has interior dimensions of 4 in × 4 in.

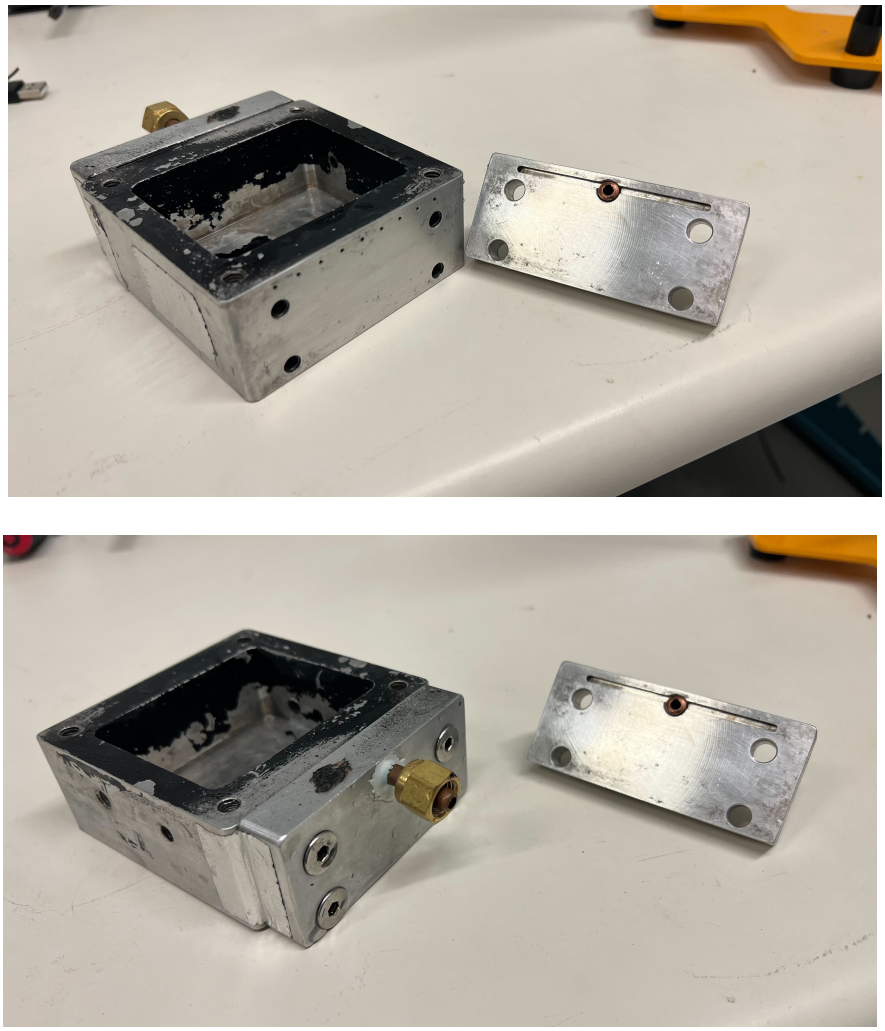

Figure 33: Real images of the enclosed sample container and aluminum end caps illustrated in Figure 30. This is the sample-holding stage, featuring holes in main unit plus depressions in end caps for air flow.

3.5.6 Mars Humidity (-55°C Frost Point) on Simulated Martian Regolith - Updated Apparatus Results

Test #1 - Sample Holding Stage and Air Cooling Stage: A first experiment was conducted using only the right-most stages of Figure 29, illustrated in detail in Figures 30 and 31. 15 ft. of 1/4 in. copper tube was used for the air cooling stage. On the floor of the sample container was placed a very thin layer of simulated Martian regolith; this was as thin as possible while maintaining total coverage to try to get the regolith as cold as possible, so the layer was only single-digit regolith grains thick. A perchlorate dusting was deposited on top, and once the sample container was closed, all surfaces were insulated with blocks of closed-cell insulation. Figure 34 shows the temperature and humidity data for the experiment, including measurements from thermocouples taped with kapton tape to the floor of the sample container, the outer surface of the container lid, and to the air cooling loop near where the loop feeds the sample container.[5] Humidity in the chamber was kept near -55 °C frost point for the duration of the experiment, and the air cooling loop was kept near -55 °C temperature. For this experiment, there are no live means of detecting deliquescence of perchlorate, and instead, deliquescence was checked for at the conclusion of the test.

Initially, there was no cooled air flow as the regolith temperature was dropped. Once the temperature of the regolith approached -45°C, air flow was opened at approximately 0.1 L/min through the sample container. At this point, as shown in Figure 34b, the onset of cooled air flow caused a distinct change in slope of the temperature trend, indicating a warming contribution as a result of the air flow. This appears to have kept the perchlorate grains too warm overall to have reached the appropriate relative humidity for deliquescence despite the regolith itself reaching about -52.5°C by the end of the test, and being inside the expected critical relative humidity range (i.e. above 60%) for about 45 minutes overall. At the close of experiment, no perchlorate grains whatsoever had undergone deliquescence.

[5]Figure A.1 in the Appendix shows another experiment of similar nature to this, which is included to prove that the inner walls of the container and the outer insulated lid showed the same temperatures throughout the experiment to within 0.5°C.

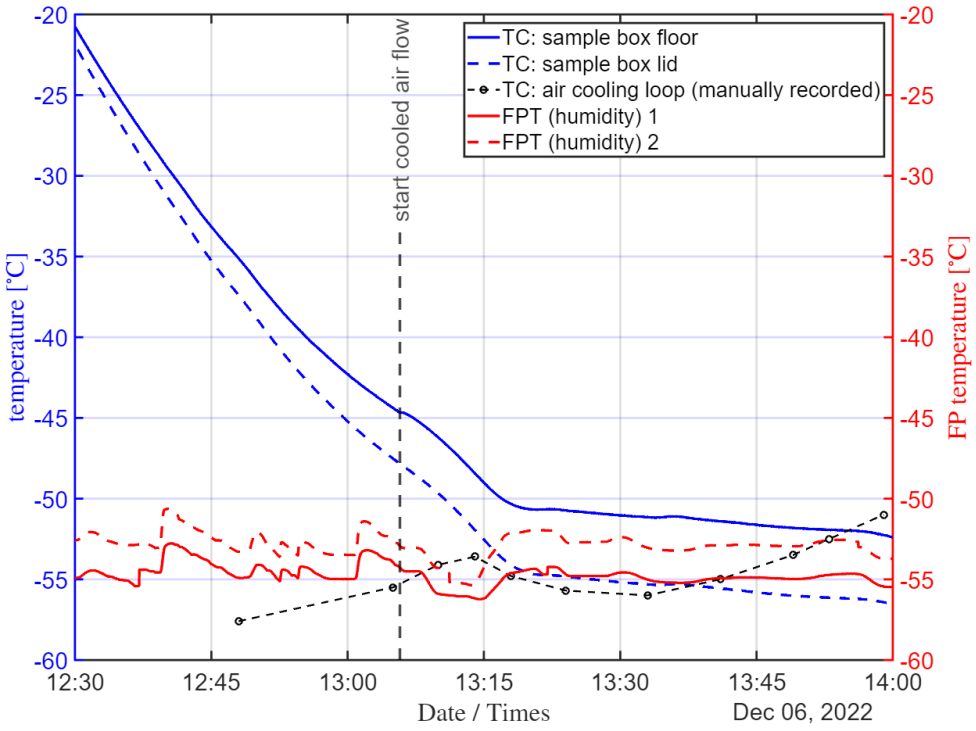

(a) Full set of environmental data.

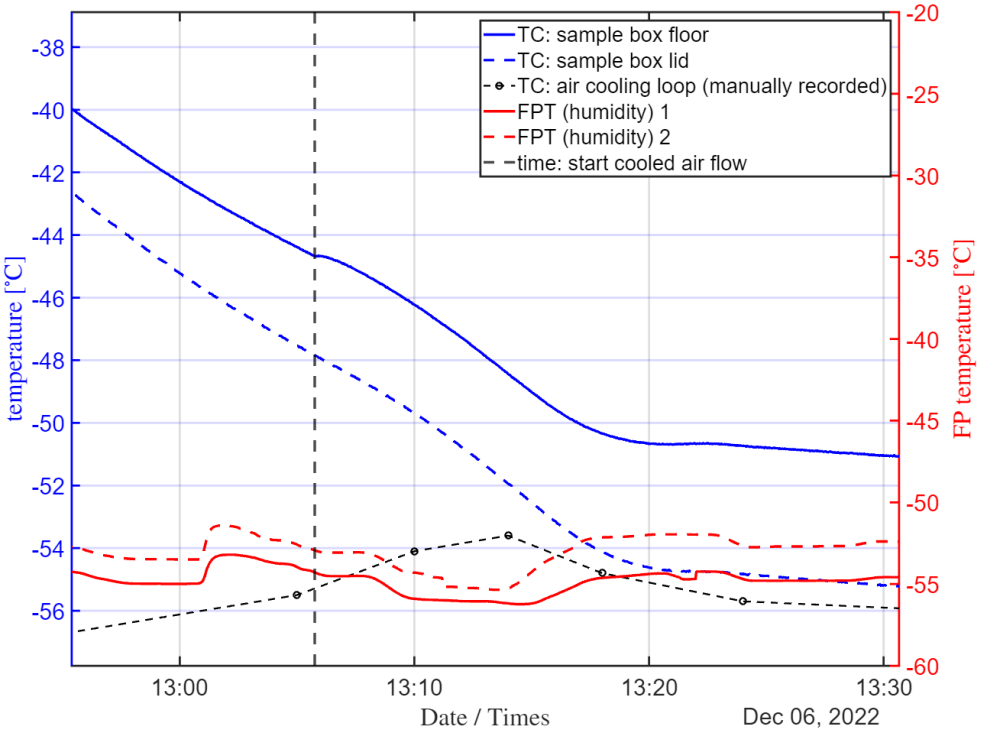

(b) Zoomed in capture of temperature increase from introduction of cooled air flow.

Figure 34: Planetary simulation chamber data for deliquescence experiment at -55°C frost point using updated apparatus and thinner regolith sample.

Test #2 - All Three Stages: The experiment described above was redone with with the full set of apparatus stages described in Figures 29 through 32, which includes humidity sensing of the air which passes through the sample container. This experiment was conducted in the same manner, except here there was no thermocouple inside the sample container for measuring the regolith temperature, and the regolith temperature is instead inferred to be lagging the lid temperature to within 5°C during cooling, as is seen in multiple previous tests, including the one immediately above and another shown in the Appendix in Figure A.1. Additionally, cooled air flow was on for the whole experiment, and the cooling loop was updated to include 1/8 in. diameter copper tubing rather than 1/4 in., and the total loop length was extended to over 50 ft. from the original 15 ft.

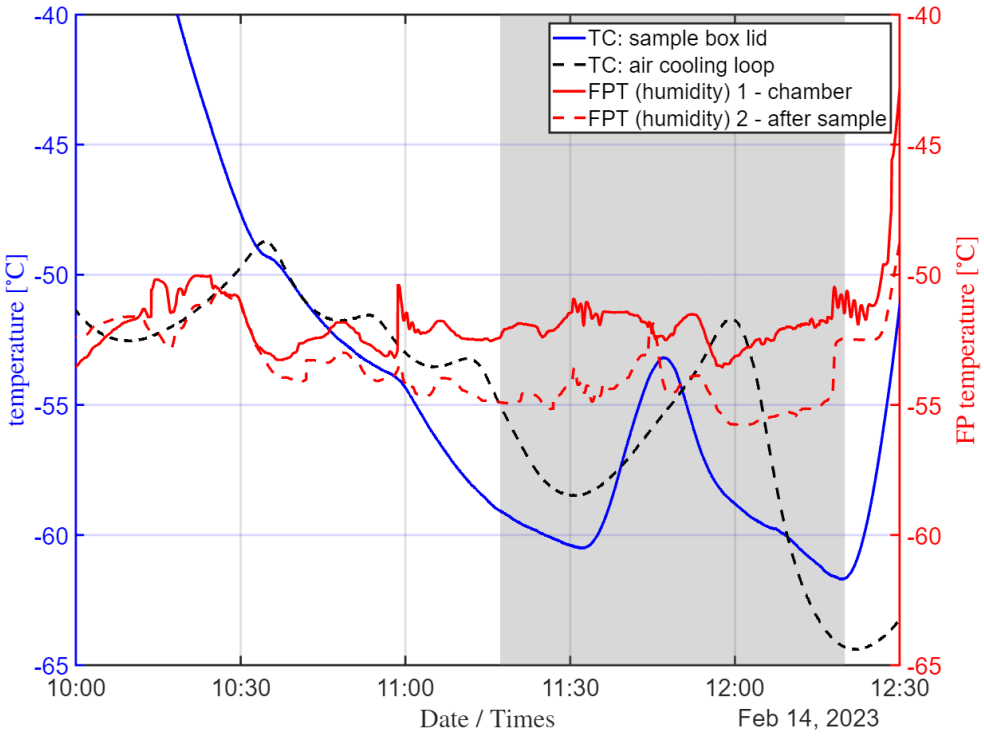

Figure 35: Planetary simulation chamber data for deliquescence experiment at -55°C frost point using all stages, including post-sample humidity sensing. Within the grey zone is where deliquescence was expected to occur based on past experience and theory, yet no deliquescence occurred.

The grey region of Figure 35 indicates a period where the regolith has the best chance of deliquescing given past experiments where deliquescence occurs at 60% relative humidity (-51°C at -55°C frost point). Here, with the sample box lid nearing -60°C, past experiments would suggest the regolith has reached at least -55°C (e.g. Figure A.1 in the Appendix). However, as revealed by the end of the experiment, no deliquescence occurred at any point, suggesting that the air cooling loop

was still insufficient to properly cool the air such that the introduction of the air flow wouldn't immediately warm up the perchlorate grains. Additionally, the cold surfaces required to cool the sample material and the moisture-replenishing air likely removed excessive moisture from the air through deposition. The latter is supported by the marked drop in humidity from the chamber through to the small container past the sample container: In Figure 35, the dotted red line, "FPT 2," after the sample enclosure is about 3°C frost point lower than "FPT 1," whereas the inverse is true for the same device calibrations in Figure 34. This indicates substantial drying of the air as it passes through the cold cooling loop and sample container.

3.6 Chapter 3 Discussion: Deliquescence on Simulated Martian Regolith

3.6.1 Sample Geometry

On Mars, perchlorate was measured to exist in concentrations of up to 0.6% (wt%) in the regolith at the Phoenix landing site [5]. After millions of years, a fair assumption is that this perchlorate is well-distributed throughout the regolith. Hence, the experiments described above, which featured magnesium perchlorate hexahydrate sprinkled directly on top of a regolith sample, are thus not realistic for what is hypothesized to actually occur on present day Mars. However, towards an eventual fully realistic demonstration of deliquescence under Martian conditions, it is thought to be the step which changes the fewest conditions from the successful deliquescence at Martian atmosphere and temperature of perchlorate on bare metal, shown in Section 3.3. Besides, the demonstration of deliquescence on Martian regolith in these experiments is not entirely unlike[6] a planned European Space Agency mission called ExoMars, which will attempt to observe the same process in a controlled sample box on a rover on the Martian surface [28]. In addition, once deliquescence is demonstrated on top of a sample of regolith, additional information could easily be obtained in that same experiment about potential transport of liquid brines within the sample. This could be done through laser Raman LIDAR measurements of perchlorate at different layers of regolith post-transport after some light excavation; more on this in **Future Work** below.

[6]There is of course one very obvious and substantial difference.

3.6.2 Temperature

Deliquescence of perchlorate at Mars humidity and temperature can almost be done routinely if on bare aluminum (Section 3.3). However, as shown in experiments which featured some material (simulated Martian regolith or quartz sand) underneath the perchlorate grains (Sections 3.5.1, 3.5.4, and 3.5.6), reaching the DRH becomes substantially more challenging. In fact, even if perchlorate is only contacting metal, but is awkwardly elevated with little surface area in actual contact with the plate (Figure 28a), deliquescence does not occur, illustrating significant disparity in temperature (and thus RH) that is introduced once you change the medium upon which the perchlorate rests and the geometry of the contact between the perchlorate and the medium. This underscores the importance of adequate sample cooling and infrared shielding, illustrated most blatantly in the second experiment of Section 3.5.3: This relatively humid -35°C frost point demonstration showed deliquescence occurring as expected on metal, but not on adjacent regolith, despite having deliquesced on regolith in past tests under nearly identical conditions. The only difference in this case was that there was no cooled lid to keep the top surface cold enough to reach the DRH before deposition began removing moisture from the air.

3.6.3 Air Effects

Upgrading the apparatus to better cool a sample of regolith in a tightly enclosed container seemed approachable, but new challenges were introduced in maintaining the appropriate humidity, as demonstrated specifically in the first experiment of Section 3.5.3. Once the sample was enclosed, replenishing air flow was critical in facilitating deliquescence. At temperatures between -20°C and -30°C, the difference in temperature between the regolith and the air was not so much as to overly warm the sample once commencing airflow. However, as we approach temperatures around -50°C, air temperature appears to be a significant factor. The size and characteristics of the overall vacuum chamber present challenges related to this, as the outermost walls of the chamber cannot be cooled, and will always be heating the air, making it challenging to cool the entire volume of air to Martian temperatures. Attempts were made to cool the air drawn over the sample by means of a long, thin cooling loop, but this did not provide the solution, as the air was either not cold enough after passing through the loop, or it would lose significant moisture through deposition if

the temperature of the loop was below the ambient frost point temperature.

3.6.4 Implications for Liquid Water by Deliquescence on Mars

Though practical challenges in demonstrating deliquescence on simulated Martian regolith at Mars environmental conditions were identified, these specific results do not yet have implications for whether the formation of liquid water by deliquescence occurs on Mars. Indeed, there remains substantial evidence that deliquescence of magnesium perchlorate occurs on Mars [6, 9, 10, 18] (and Section 3.3). Instead, these results illustrate practical challenges of demonstrating the hypothesized process on Earth, and inform future work.

3.6.5 Future Work

Progress has been made towards the ultimate desired demonstration. While the experiments shown highlight the primary practical challenges, they are intended to represent tens of other experiments whereby other conditions were modified or tested in an attempt to reach the DRH for perchlorate on regolith. These other tests include different cadences and rates of air flow, ramping or holding of temperatures, depth of regolith, and sample container geometries, which are not discussed in detail in this report. These additional trials are recorded and will support plans for future work.

With the available materials, accurate sensing of the cooled airflow temperature is challenging; often, thermocouples read the temperature of some nearby surface (like the inner walls of the sample container or cooling tube) due to infrared exchange rather than the temperature of weak airflow. Significantly thinner thermocouples than the ones available for these experiments may give more explicit confirmation whether or not the replenishing air is being effectively cooled. Since we suspect that it is not, a longer cooling loop could yet be implemented in future tests so that it does not need to be cooled any further than -55°C, eliminating the risk of extracting moisture from the chamber air prior to the air meeting the sample. Ideally, if a small vacuum chamber were to be used, all the air in the chamber could be cooled so that both the effects of air warming the sample plus insufficient available air moisture would be mitigated.

Once deliquescence is achieved, future tests should explore the movement of the perchlorate solution through the regolith, as discussed in Section 2.4.4. This could be by using an embedded moisture detection probe (like those discussed in Chapter 4) at some depth or by excavating the sample and detecting perchlorate, newly dispersed beneath the surface, using laser Raman scattering. A key observation would be transport of perchlorate solution all the way to the ice table about 5 cm below the surface. However, in order to do this using laser Raman scattering, a means of mitigating signal absorption of UV light by iron and the significant contamination due to other materials in the regolith mixture would be necessary.

4 Melting and Freezing at the Ice-Regolith Interface

This section addresses the primary goal of this MSc research, which was to determine whether a layer of liquid water would form at the top of the ice table while in contact with regolith mixed with perchlorate, as was found at the Phoenix landing site. In addition to deliquescence, contact between perchlorate in the Martian regolith and water ice at the ice table was suggested as potential means of stable brines on Mars [7]. However, detecting liquid underneath an existing layer of simulated Martian regolith presents the challenge of a broken line-of-sight from above to the ice layer. Excavating or otherwise disturbing the simulated regolith such that a laser beam for Raman LIDAR could strike the ice layer and scatter is theoretically viable, but this would greatly disturb (and potentially alter) the sample mid-experiment with the addition of a warm excavating tool, altered sample geometry, warming from the laser on remnant regolith grains, and the inability to restore the sample to its previous state and continue the experiment over multiple temperature cycles. Hence, an alternative method was devised using a commercially available soil moisture detector which could be embedded in a simulated Martian subsurface cross-section.

4.1 Experiment, Measurement, and Analysis Methods

4.1.1 Dielectric and Resistive Liquid Water Detection

Two primary means of sensing liquid water in soil exploit principles of resistance and dielectric permittivity. Resistive detectors use liquid water as a type of variable resistor, as electricity can conduct along ions in wet soil and bridge two prongs, causing a readout voltage theoretically proportional to the amount of water. However, in terms of quantifying water volume within soil, a resistive approach can be prohibitively susceptible to changes in ion concentration depending on what information is sought [32]. For instance, deploying the same probe into different soils may yield different resistive readings without an actual change in water volume if there is a difference in salinity within the soil. Dielectric probes such as a capacitance sensors, on the other hand, are less dependant on ion content [32]. This type of probe measures the charge-storing capacity of the surrounding material, and exploits the fact that the dielectric constant of liquid water is much higher than other common materials in soil, and so it is more sensitive just to changes in water content. Generally, dielectric probes are packaged as one unit, whereas resistive probes require

multiple prongs.

4.1.2 Liquid Detection Implementation

In terms of calibration to absolute liquid water volume across various soils, dielectric (e.g. capacitive) probes are less susceptible to ion concentration than resistive probes [32], and are more widely used in terrestrial hydrology [33]. However, as it relates to exploring simple phase transitions of water, which is the case in the below experiments, low-cost resistive probes can be as informative as dielectric probes. Hence, a resistive probe was chosen due to low cost and form factor.

4.1.3 Instrument Description

Figure 36 shows the probe used for the following experiments, which was originally designed as an inexpensive hobbyist soil moisture detector. Its circuit schematic is also shown.

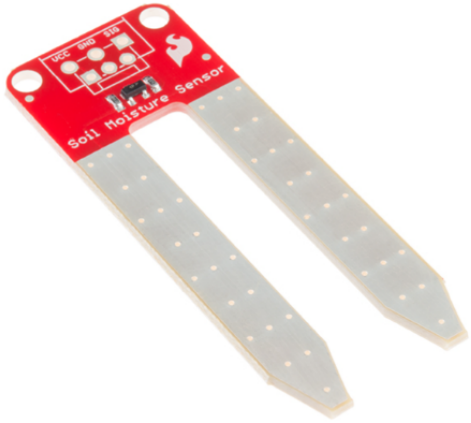

(a) Conductivity probe used in the below experiments.

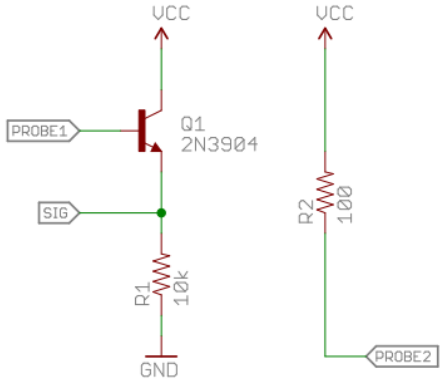

(b) Circuit schematic of the probe.

Figure 36: Conductivity probe and associated circuit schematic, which provides a voltage at the signal output (SIG) roughly proportional to the amount of liquid water bridging the probe prongs

The probe circuit is an NPN transistor with one prong shorted to the base of the transistor, and another prong connected to the power supply through a series resistor. When there is electrical conductivity (i.e. liquid water) between the prongs, a voltage is seen at the base of the transistor. As current flows through a resistor in series with the emitter and ground, the voltage formed at **SIG** is read out in units of mV to a logging program.

4.1.4 Planetary Simulation Chamber

All experiments took place in the planetary simulation chamber as described in Section 3.1.1.

4.1.5 Experiment Apparatus

The sample set up was as shown in Figure 37. The conductivity probe was embedded in a layer of distilled water ice about a centimetre in thickness. Two thermocouples (TCs) were embedded in the ice as well. Each thermocouple was of type-T and 20 AWG wire gauge. TC1 was embedded half exposed to the regolith, though still frozen into the ice, in an attempt to read as accurately as possible the uppermost portion of the ice layer. TC2 was embedded about a millimetre below that. In each experiment, a layer of simulated Martian regolith (Mojave Mars Simulant, MMS-1 [30]) was deposited on top of the ice in a layer about 1 cm thick. In each case the regolith had a controlled concentration (wt%) of magnesium perchlorate hexahydrate mixed in. The precise thickness of the regolith layer was not critical for this experiment, as the temperature of the ice is actively controlled and the mixed-in perchlorate was uniformly distributed. The conductivity probe was embedded in the ice such that the prongs enter perpendicular to the ice surface, and any liquid that forms along that layer would bridge the prongs. The taped portions shown in Figure 37 are intended to limit readout to only volumes around the ice interface, and not somewhere in the upper portions of the regolith (e.g. due to liquid transport upwards).

The whole sample is contained within a solid aluminum box with a detachable lid in order to minimize temperature gradients within the simulated regolith or ice. The entire box sits on an aluminum plate which sandwiches a resistive kapton heater between itself and a cooling plate for temperature control of the box, and by extension the ice. The ice (and ice surface) is actively cooled from the sample container itself, and not subject to radiative or other thermal mechanisms, say, from the top down through the regolith.

4.1.6 Experiment Overview: Ice-Regolith Interface

Sample Preparation: Samples of simulated Martian regolith with varying concentrations (wt%) of magnesium perchlorate hexahydrate (5%, 3%, 1%, and 0.6%) were prepared by first deliquescing

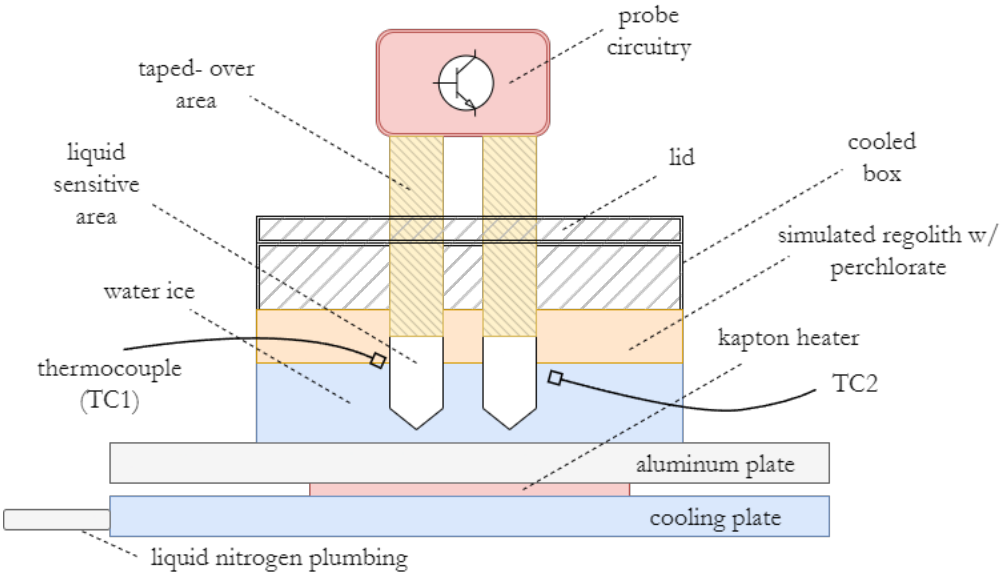

Figure 37: Diagram of ice-regolith liquid detection experiment apparatus. As part of the experiment set up, the moisture-sensing probe is frozen directly into the simulated ice table. The regolith simulant perchlorate mixture is then placed on top prior to evacuating the chamber.

the perchlorate into the simulated regolith in a humid environment and allowing the resulting liquid solution to disperse overnight. The sample was then fully dried using low pressure and heat in the vacuum chamber, and then thoroughly mixed together using mortar and pestle and other mixing implements for several minutes. After freezing the conductivity probe and thermocouples in the ice as per Figure 37, the ice was taken to a very low temperature (below -70°C) to avoid sustained liquid water upon depositing the simulated regolith-perchlorate mixture onto the ice. After depositing the solid mixture, a lid was then placed on top of the box with pieces of aluminum tape covering any large openings in order to keep the entire regolith sample as cool as possible.

Uncertainty in Concentration: Each sample was prepared using about 20 g initial mass of Mars regolith simulant. The measurement uncertainty in the perchlorate concentration added to the regolith to prepare the mixture is 0.01 g, hence, in percent, the uncertainty in the perchlorate concentration is around 0.05%, which is not thought to impact conclusions presented herein. Additionally, results are presented with the assumption that the mixing procedure above resulted in samples where the perchlorate is evenly distributed throughout the regolith.

Pressure and Humidity: At this point the planetary simulation chamber was pumped down to about 7 torr as with all previous experiments to simulate the Martian surface pressure. Since the chamber pumps caused significant noise in the conductivity probe readout voltage, active pressure control was not implemented in contrast to the experiments described in Chapter 3. The pressure over the course of any experiment discussed below rarely surpassed 8 torr despite not implementing active pressure control, though pressure changes on the scale of a few torr is not thought to have significant impact on these results. Precise humidity control was also not thought to be a dominating factor for these experiments, so it wasn't actively controlled, nor could it be controlled under the current set up without active pressure control.

Temperature Cycling and Data Collection: In each experiment, the temperature of the ice surface was cycled multiple times through warmer and colder temperatures, as would be seen on Mars. The maximum and minimum temperatures for a given set of cycles were actually varied at times in an attempt to discern any dependency in the freezing temperature of the solution on temperature history.

A common sequence is as follows: During first warming, the ice eventually passes through the melting temperature for a given concentration of perchlorate, and a voltage is seen on the output of the conductivity probe relatively proportional to the amount of liquid which bridges the prongs through melting (though it is understood that unaccounted for changes in ion concentration can prohibit absolute water volume quantification). As the ice is subsequently cooled, the liquid layer will partially freeze, decreasing the voltage readout from the probe. Once the sample is fully frozen, the conductivity probe will read zero voltage. This is then repeated over multiple melting and freezing cycles as would occur daily on Mars.

A Note on Sensor Operation: It should be explicitly stated that in the experiments discussed below, the conductivity probe is not relied upon to provide absolute water volume quantification; instead, we look only for the points at which conductivity signal disappears completely during cooling (indicating that liquid bridging the prongs has frozen entirely) or that conductivity signal is recovered during warming (indicating that some liquid is now bridging the prongs). By extension,

this instrument does not have explicit sensitivity to all possible liquid water present (e.g. remnant water around the prongs themselves which does not bridge them, or other pockets). However, the assumption is that the temperature of the prongs, being well-embedded in the ice, is well-coupled to the actual ice temperature, and that the detection of presence or absence of liquid water between the prongs is representative on the whole ice-regolith interface of the simulated Martian cross-section.

4.2 Melting and Freezing at the Ice-Regolith Interface - Results

Before presenting results, the following should be noted:

1. In the 5% perchlorate concentration experiment presented first, the first melting phase (Figure 39b) exhibited a melting temperature far warmer than is reasonably expected given subsequent melting temperatures and other experiments, and so it is omitted. This is presumably attributable in some way to the practical implications of being freshly mixed and/or freshly deposited on ice, as similar observations were made in other experiments not presented here. This observation is not thought to significantly impact conclusions.

2. Shortly before or after critical temperatures, very small precursor or remnant signals were observed which quickly would drop back to zero. For the purposes of these analyses, if there are multiple small signals within one minute of each other either preceding or succeeding a substantial period of liquid signal, only then will that be counted as the onset (or loss) of a liquid signal. Generally, these precursor or remnant signals begin or end within about 2°C of obvious, substantial signal, so the uncertainty in temperature measurement for melting or freezing for a given cycle is set to ±2°C.

3. For a given concentration, the final reported temperatures of melting and freezing is the mean over multiple cycles. The associated uncertainty is given by the usual expression for uncertainty of the mean:

$$\delta_{\text{mean}} = \frac{\delta_{\text{measured}}}{\sqrt{N}}$$

where δ_{measured} is the uncertainty of each measurement (in this case 2°C) and N is the number of terms in the average (in this case either 2 or 3). Hence, in the case of a reported temperature

where three cycles were averaged, the applied uncertainty is

$$\delta_3 = \frac{2^\circ\text{C}}{\sqrt{3}} \approx 1.2^\circ\text{C},$$

and for the case of two cycles,

$$\delta_2 = \frac{2^\circ\text{C}}{\sqrt{2}} \approx 1.4^\circ\text{C}.$$

4.2.1 5% Perchlorate Concentration

Starting Sequence: A sample of simulated Martian regolith was prepared according to the steps described in Section 4.1.6 with 5% perchlorate concentration (wt%). The experiment apparatus was established according to Figure 37, and the 5% perchlorate mixture was deposited on the ice while the ice was below -70°C. Figure 38 shows a high-level snapshot of the whole experiment, while Figures 39 through 41 show zoomed-in snapshots of interest.

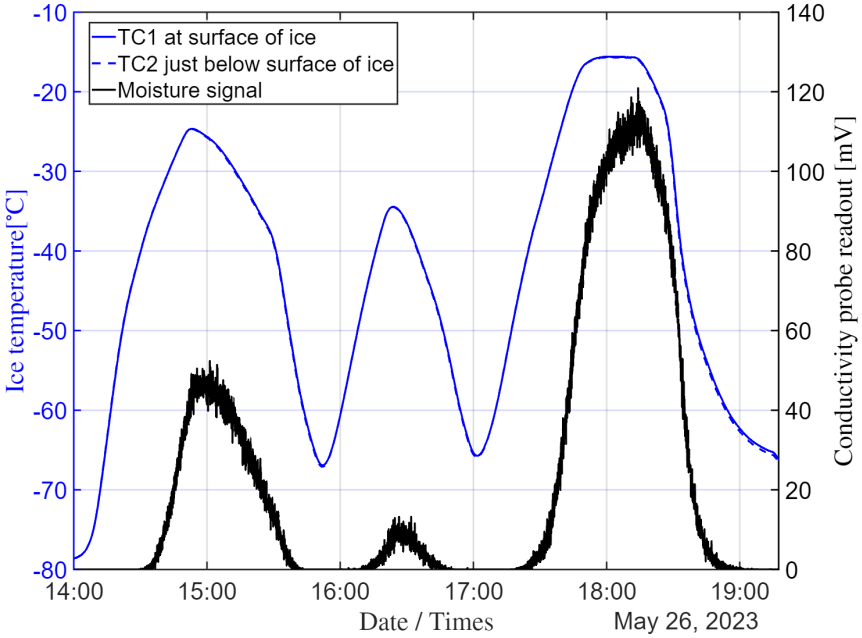

Figure 38: 5% perchlorate concentration full experiment overview.

First Cycle - Figure 39: During the first warming cycle from the initial -70°C, melting occurs only once the relatively warm temperature of -41°C is reached. Note that this value is not repeated in subsequent warming cycles (since this sample is newly prepared), and is omitted. Warming continued until about -25°C in order to form substantial liquid at the ice-regolith interface, as

indicated by the substantial moisture signal around 15:00 in Figure 38. Cooling then commenced, with the intent to drive the temperature below the point where the liquid at the ice-regolith interface is fully frozen. As shown Figure 39d, this occurs at about -59°C, or in other words, some liquid could persist at the ice-regolith interface on Mars until the temperature at the ice reaches -59°C according to this trial. The minimum temperature reached after freezing is not of great significance, since the sample is now fully frozen anyway.

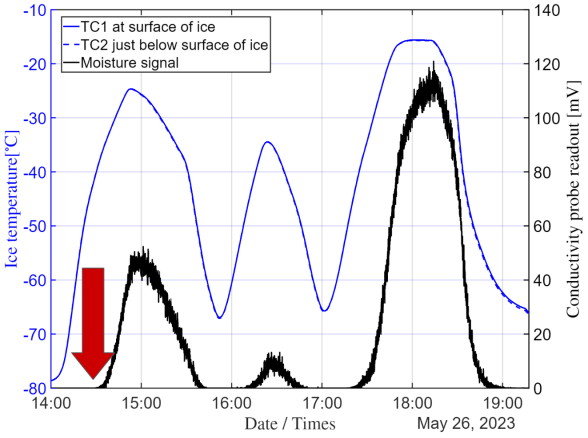

(a) Red arrow locates transition in Figure 39b.

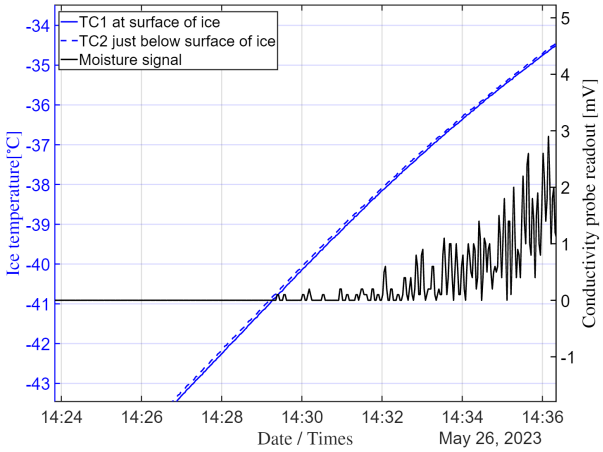

(b) Melting temperature of first cycle.

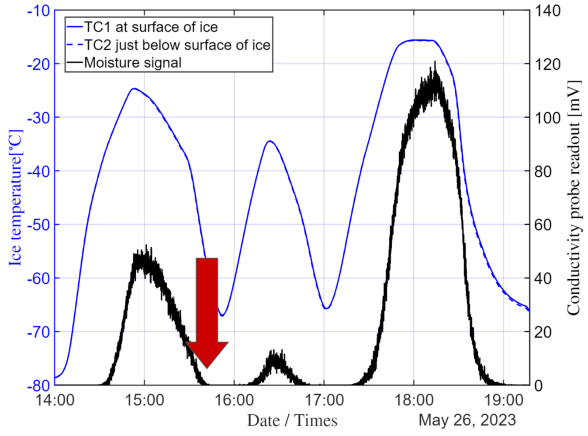

(c) Red arrow locates transition in Figure 39d.

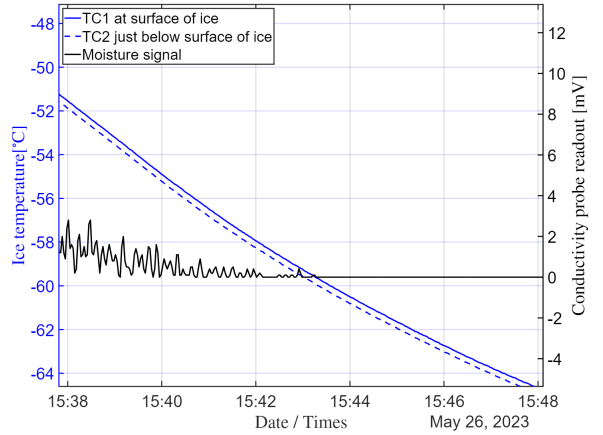

(d) Freezing temperature of first cycle.

Figure 39: 5% perchlorate concentration first temperature cycle.

Second Cycle - Figure 40: The ice was warmed again after the sample was fully frozen to determine at what temperature liquid water would reappear in a simulation of the warming period during a standard summer day on Mars. As shown in Figure 40b, liquid would be recovered between -53°C and -52°C. During this warming cycle, the temperature was raised to only -35°C, which was

mostly arbitrary, save for being intentionally cooler than the first cycle's warmest temperature to try to check for any extreme differences in freezing temperature on account of forming more or less total liquid. Upon second cooling, shown in Figure 40d, full freezing occurred about -56°C, which is only a few degrees warmer than the first temperature of full freezing.

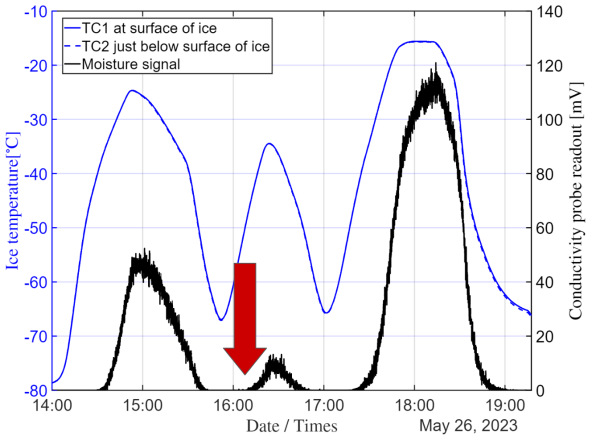

(a) Red arrow locates transition in Figure 40b.

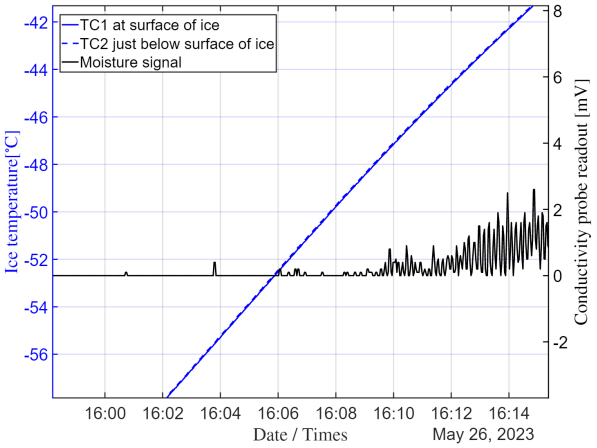

(b) Melting temperature of second cycle.

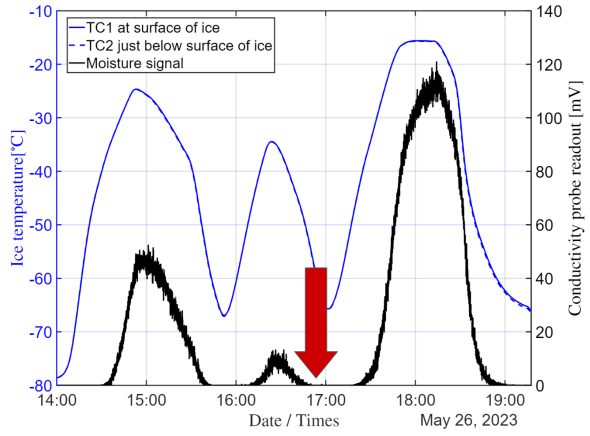

(c) Red arrow locates transition in Figure 40d.

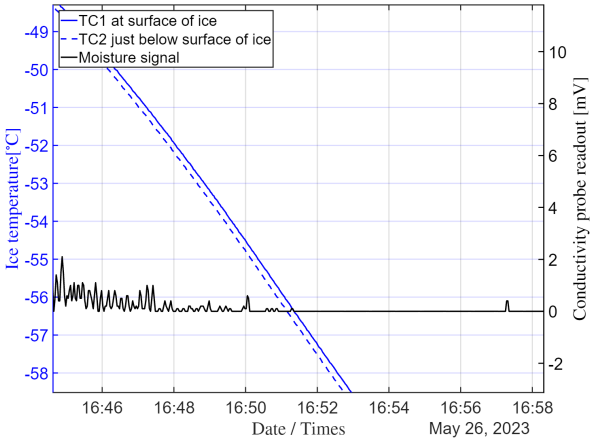

(d) Freezing temperature of second cycle.

Figure 40: 5% perchlorate concentration second temperature cycle.

Third Cycle - Figure 41: During the third and final warming period, melting occurred at about -50°C, which is only about two degrees warmer than the second cycle, signifying consistency aside from the initial temperature cycle, omitted on account of the sample being freshly prepared. Upon cooling, the liquid which had formed during the melting phase became fully frozen at about -64°C.

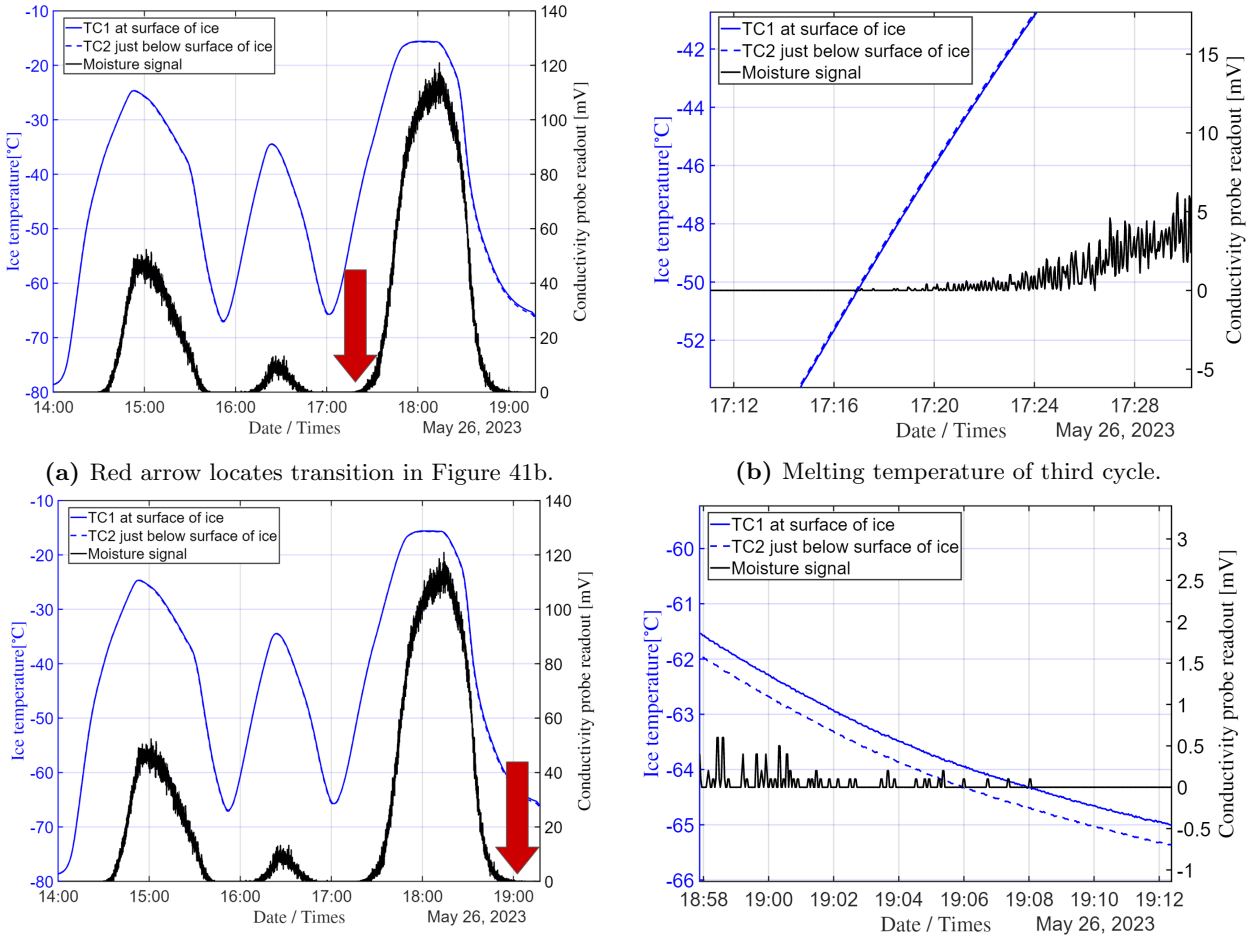

(a) Red arrow locates transition in Figure 41b.

(b) Melting temperature of third cycle.

(c) Red arrow locates transition in Figure 41d.

(d) Freezing temperature of third cycle.

Figure 41: 5% perchlorate concentration third temperature cycle.

Summary - 5% Perchlorate Concentration: For liquid brine formed at the interface between Martian regolith simulant and ice at 5% perchlorate concentration, the average freezing temperature was -61 ± 1.2°C, and the average melting temperature was -51 ± 1.2°C. Thus, at 5% perchlorate concentration in Mars regolith, liquid water would be present for the entirety of a summer Martian sol at the ice-regolith interface based on the simulated temperature range of the ice table on sol 55 of the Phoenix mission (-43°C to -53°C, Figure 7) [19]. In place of averaging, even if the most conservative single cycle result is used (-51°C melting temperature and -56°C freezing temperature), liquid water is present for the entire sol.

4.2.2 3% Perchlorate Concentration

Starting sequence: A sample was prepared in the same way as in the 5% concentration test, but now with 3% perchlorate. The general procedure was the same as previously, except due to increased humidity in the laboratory on this day, the depositing of the regolith sample needed to be expedited and done earlier in the test to avoid deliquescence of perchlorate within the sample in ambient room air, which could have an unknown effect on results. Hence, the regolith was deposited at about -50°C, so each temperature cycle now begins with freezing, not melting. This is not thought to impact overall results. Figure 42 shows a snapshot of the whole experiment, with Figures 43 to 45 showing zoomed-in snapshots of interest.

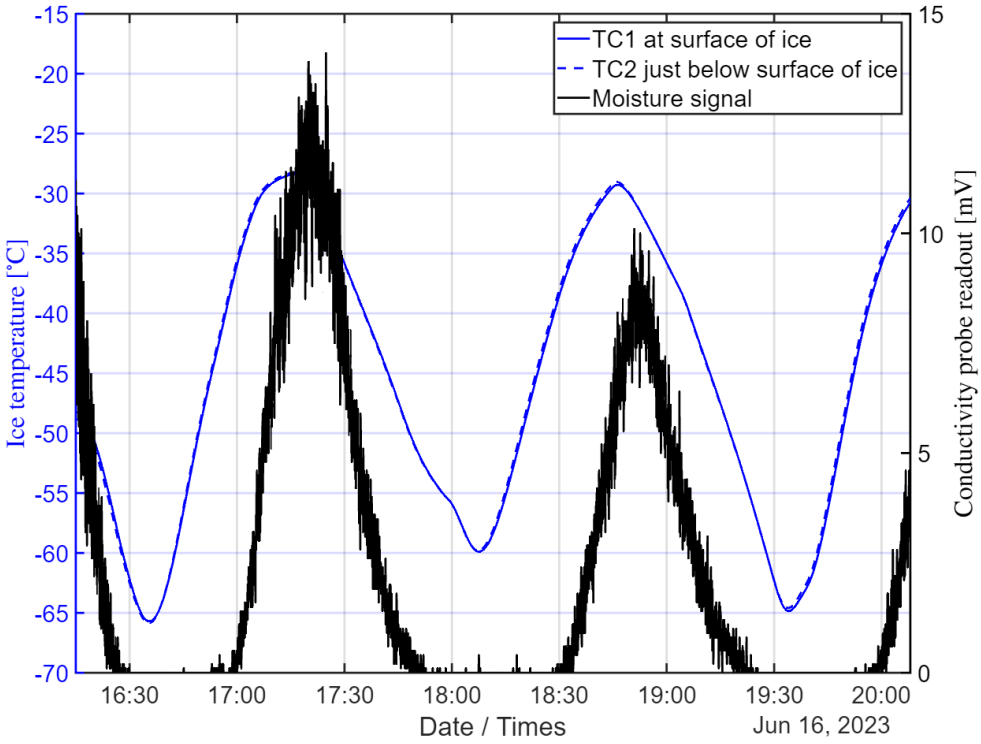

Figure 42: 3% perchlorate concentration full experiment overview.

First Cycle - Figure 43: Upon first cooling, full freezing occurred at -62°C. Subsequent melting occurred when the temperature is brought back up to -39°C, which is outside of simulated ice temperatures 4.5 cm below the surface at the Phoenix landing site.

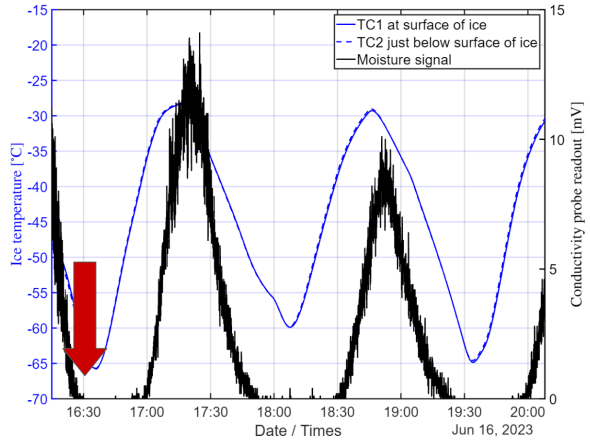

(a) Red arrow locates transition in Figure 43b.

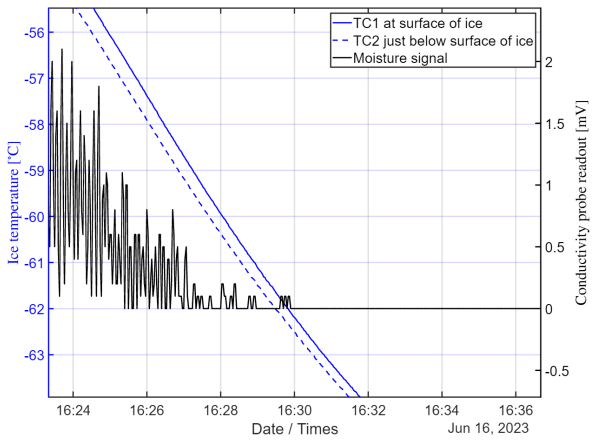

(b) Freezing temperature of first cycle.

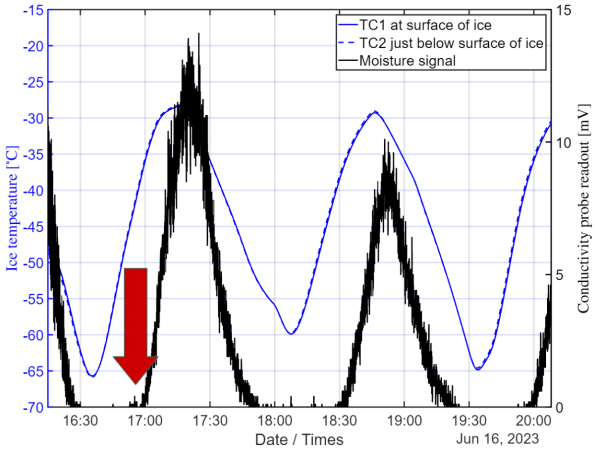

(c) Red arrow locates transition in Figure 43d.

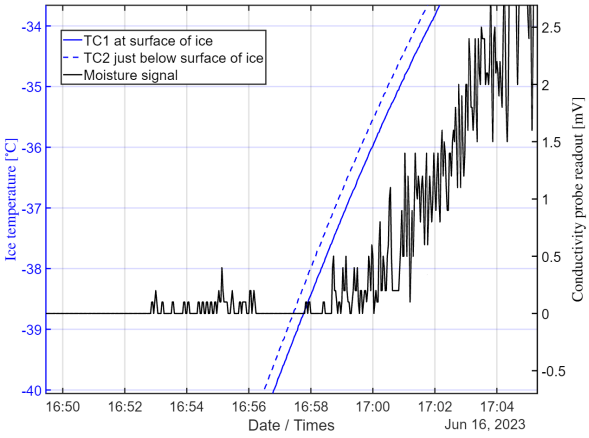

(d) Melting temperature of first cycle.

Figure 43: 3% perchlorate concentration first temperature cycle.

Second Cycle - Figure 44: In a second temperature cycle, full freezing is seen at -53°C, which is a warmer temperature than any melting temperature for 5% concentration, which is expected for a lesser concentration of perchlorate (as per the phase diagram in Figure 8). Upon subsequent warming, melting occurred between -41°C and -40°C, which is slightly cooler than the previous melting temperature, but remains warmer than the warmest simulated Mars ice table temperature which was -43°C. In other words, the temperature at the ice table would not reach high enough to melt the ice in the first place at this concentration.

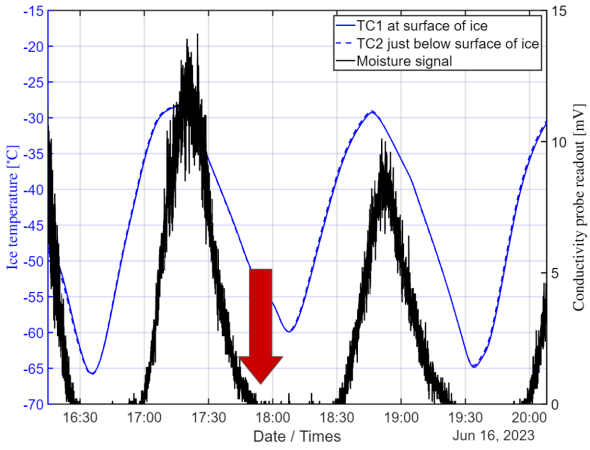

(a) Red arrow locates transition in Figure 44b.

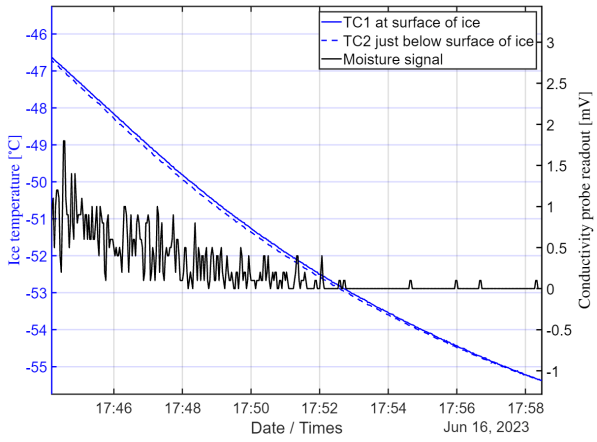

(b) Freezing temperature of second cycle.

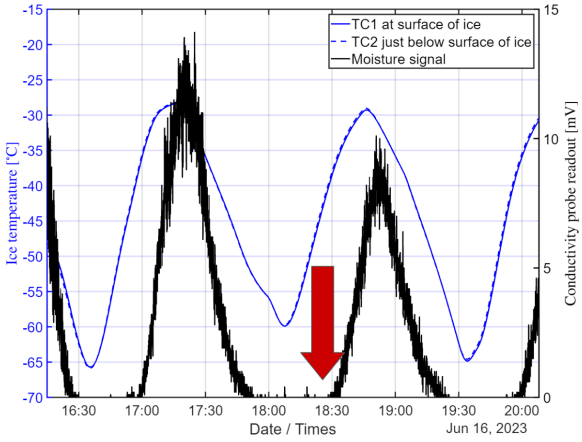

(c) Red arrow locates transition in Figure 44d.

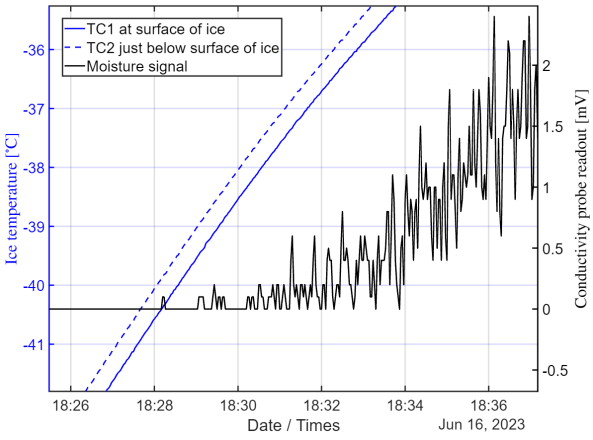

(d) Melting temperature of second cycle.

Figure 44: 3% perchlorate concentration second temperature cycle.

Third Cycle - Figure 45: Upon a final cycle, full freezing occurs at -57°C, which is cooler than the previous test, but still warmer than the average 5% freezing temperature. Melting occurred at essentially the same point as on the second cycle, between -41°C and -40°C.

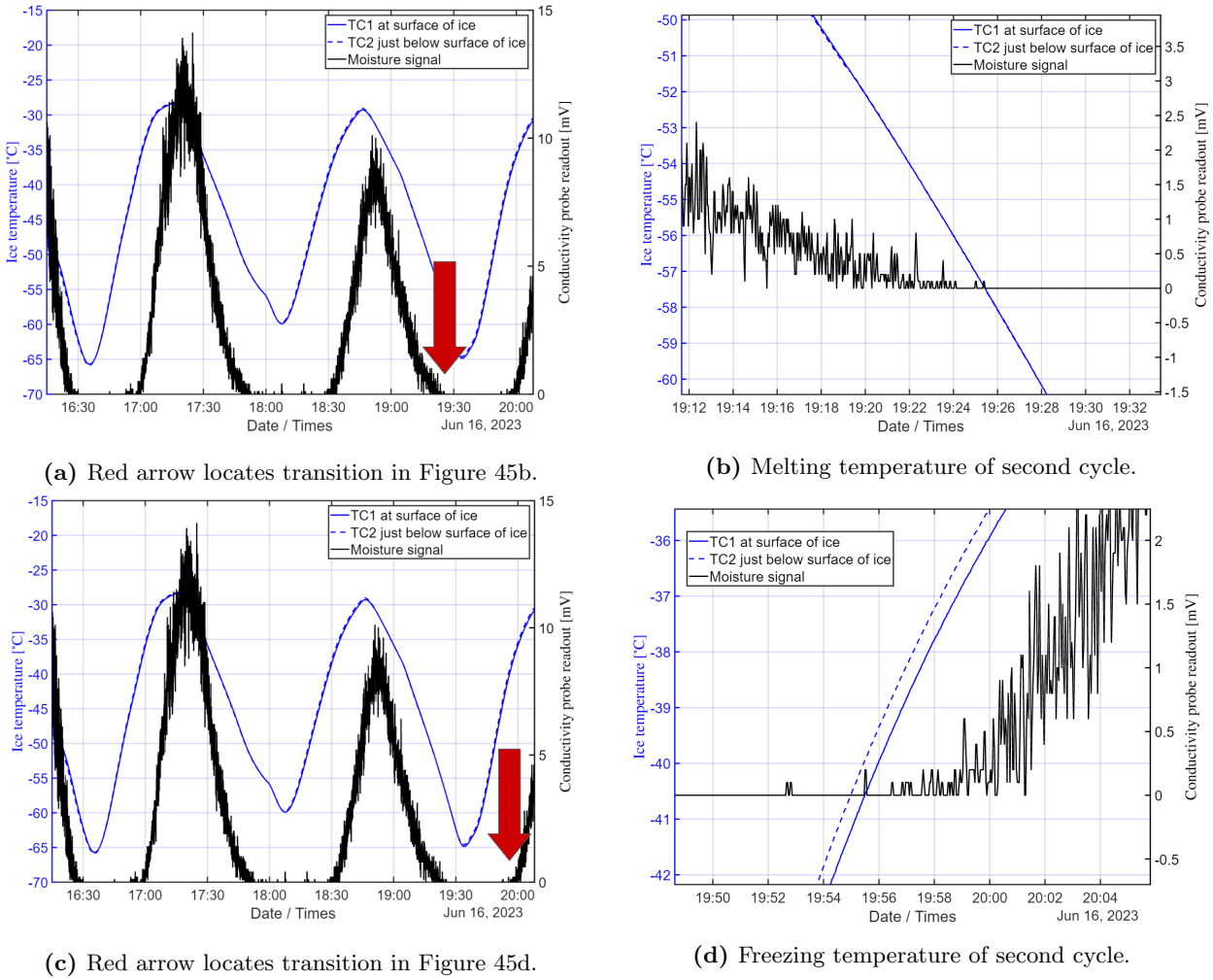

(a) Red arrow locates transition in Figure 45b.

(b) Melting temperature of second cycle.

(c) Red arrow locates transition in Figure 45d.

(d) Freezing temperature of second cycle.

Figure 45: 3% perchlorate concentration third temperature cycle.

Summary - 3% Perchlorate Concentration: For liquid brine formed at the interface between Martian regolith simulant and ice at 3% perchlorate concentration, the average freezing temperature was -55 ± 1.2°C, and the average melting temperature was -40 ± 1.2°C. Thus, at no point would the ice melt during at the ice-regolith interface based on the simulated temperature range of the ice table on sol 55 of the Phoenix mission (-43°C to -53°C, Figure 7) [19]. If, due to a thinner regolith top-layer or warmer sols later in the summer, the temperature does reach above -40°C, melting would occur and liquid water could persist until the temperature once again drops to -55°C.

4.2.3 1% Perchlorate Concentration

In the same manner as the above tests, a sample was created with 1% perchlorate concentration, and was subject to the same experiment. Figure 46 shows a high-level snapshot of the first experiment, with higher detail snapshots in Figures 47 through 48. A second experiment using the same sample on a different day is shown in Appendix B.

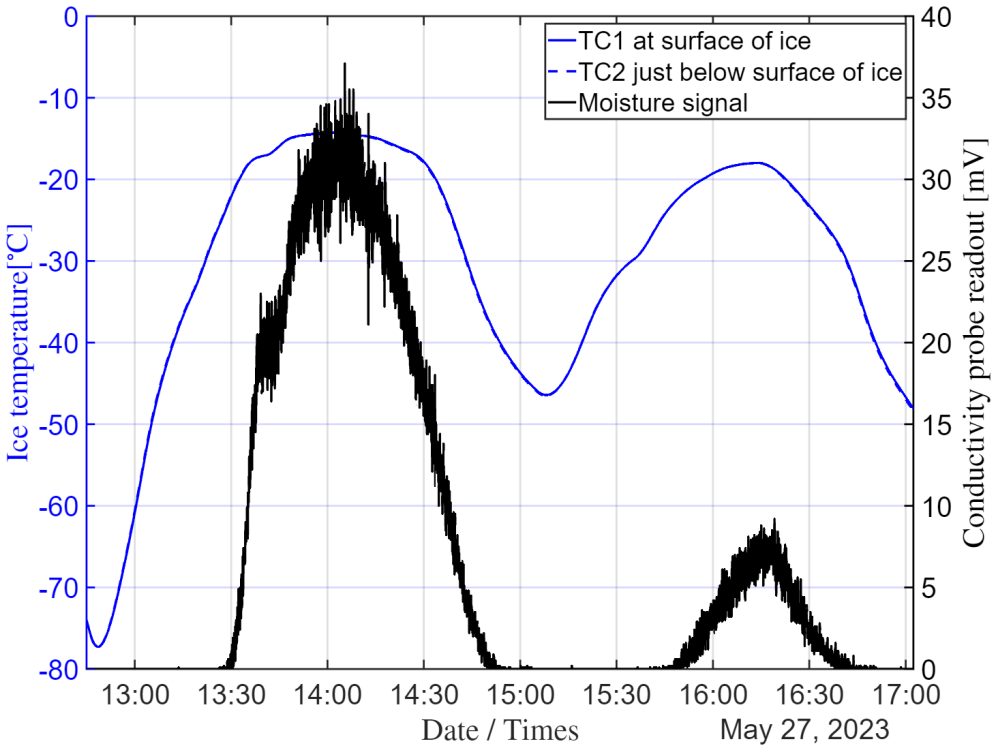

Figure 46: 1% perchlorate concentration full experiment overview - Trial 1 of 2.

First Cycle - Figure 47: For 1% perchlorate concentration, the first melting occurred at about -26°C, which is much warmer than the maximum temperature simulated to be found during the summer at the ice level at the Phoenix landing site. Substantial liquid was eventually recovered as the temperature was raised to about -15°C, which is the warmest temperature also tested during 5% perchlorate concentration experiments (Figure 38). Upon first cooling, full freezing occurred at -41°C.

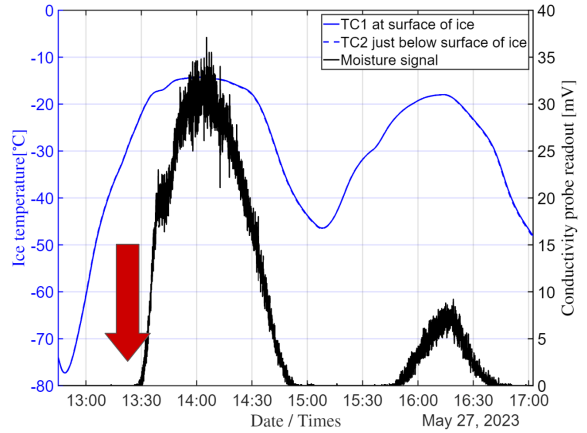

(a) Red arrow locates transition in Figure 47b.

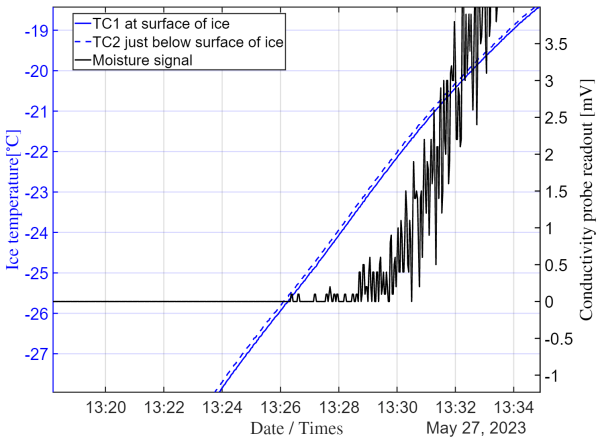

(b) Melting temperature of first cycle.

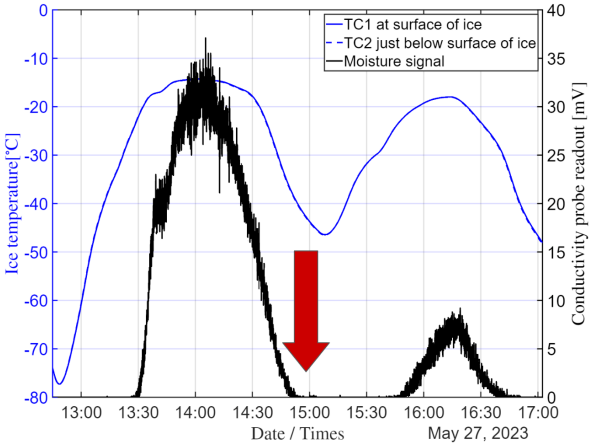

(c) Red arrow locates transition in Figure 47d.

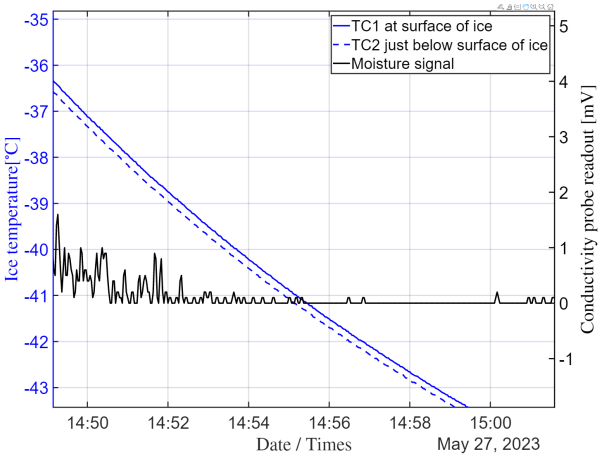

(d) Freezing temperature of first cycle.

Figure 47: 1% perchlorate concentration first temperature cycle.

Second Cycle - Figure 48: Upon a second warming, melting occurred between -25°C and -24°C, which is close to the melting temperature of the preceding cycle. Upon final cooling, despite the maximum signal from the previous warming having only reached about one-quarter the previous magnitude for a similar maximum temperature, the temperature at which full freezing occurred was very similar to the first freezing temperature (-41°C) at -40°C.

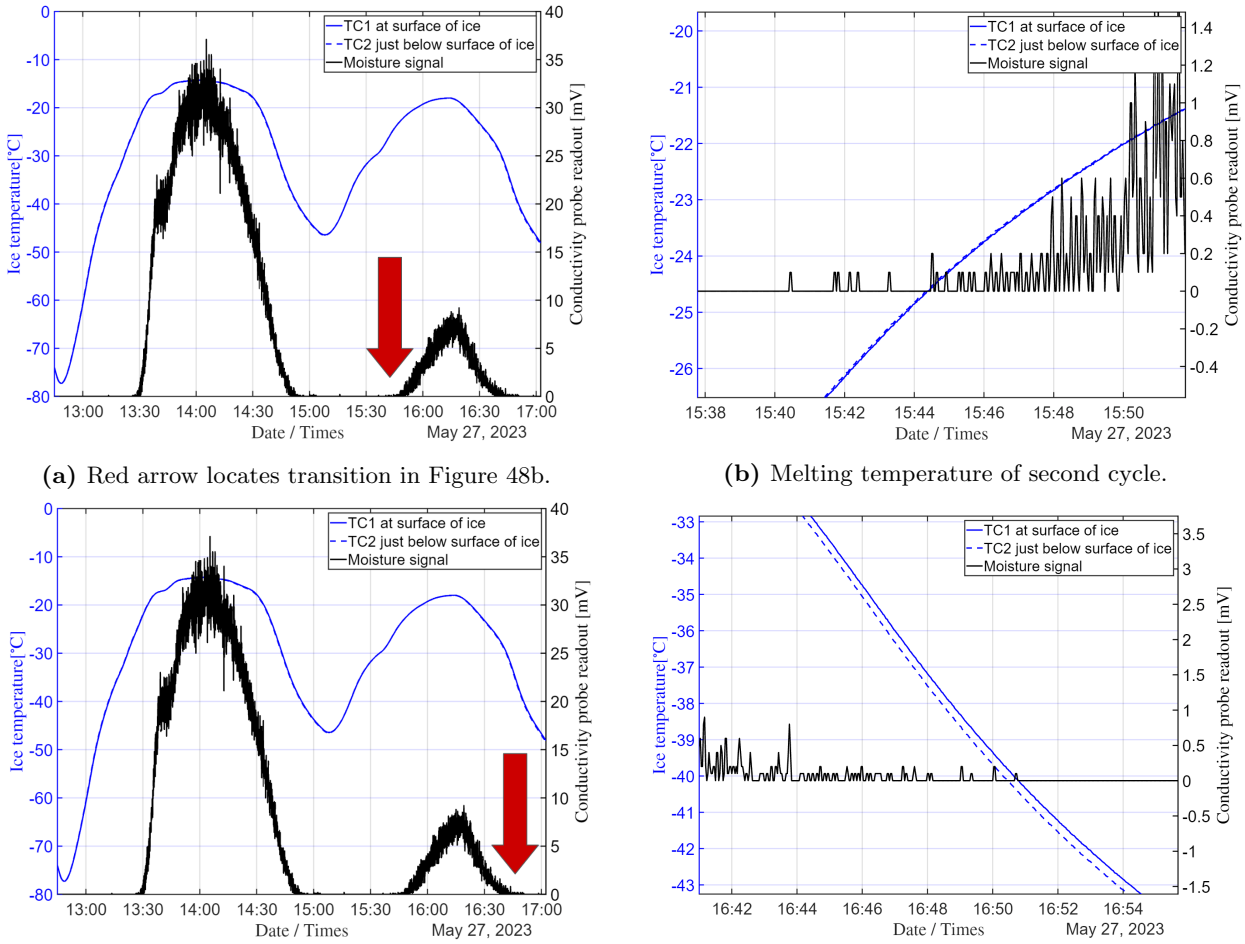

(a) Red arrow locates transition in Figure 48b.

(b) Melting temperature of second cycle.

(c) Red arrow locates transition in Figure 48d.

(d) Freezing temperature of second cycle.

Figure 48: 1% perchlorate concentration second temperature cycle.

Summary - 1% Perchlorate Concentration: For liquid brine formed at the interface between Martian regolith simulant and ice at 1% perchlorate concentration, the average freezing temperature was -41 ± 1.4°C, and the average melting temperature was -26 ± 1.4°C. In a subsequent experiment which was a repeat of this one (Figures B.4 through B.6 in the Appendix), respective average freezing and melting temperatures were -42 ± 1.4°C and -31 ± 1.4°C. The combined average temperatures across both trials were -41 ± 1°C for full freezing and -28 ± 1°C for melting. The melting temperature is not close to the upper bound of the simulated temperature range (-43°C to -53°C, Figure 7) at the ice level below 4.5 cm of regolith at the Phoenix site on sol 55 [19]. Thus, at this concentration, the ice would never melt unless the regolith over the ice table was substantially thinner than 4.5 cm.

4.2.4 0.6% Perchlorate Concentration

Lastly, in accordance with the measured concentration of perchlorate salts in Martian regolith [5], a sample was created with 0.6% perchlorate concentration. Figure 49 shows the full experiment, with higher detail snapshots in Figures 50 through 52. One temperature cycle was bounded by the actual simulated temperatures at the ice level at the Phoenix landing site [19], which is captured in Figure 51.

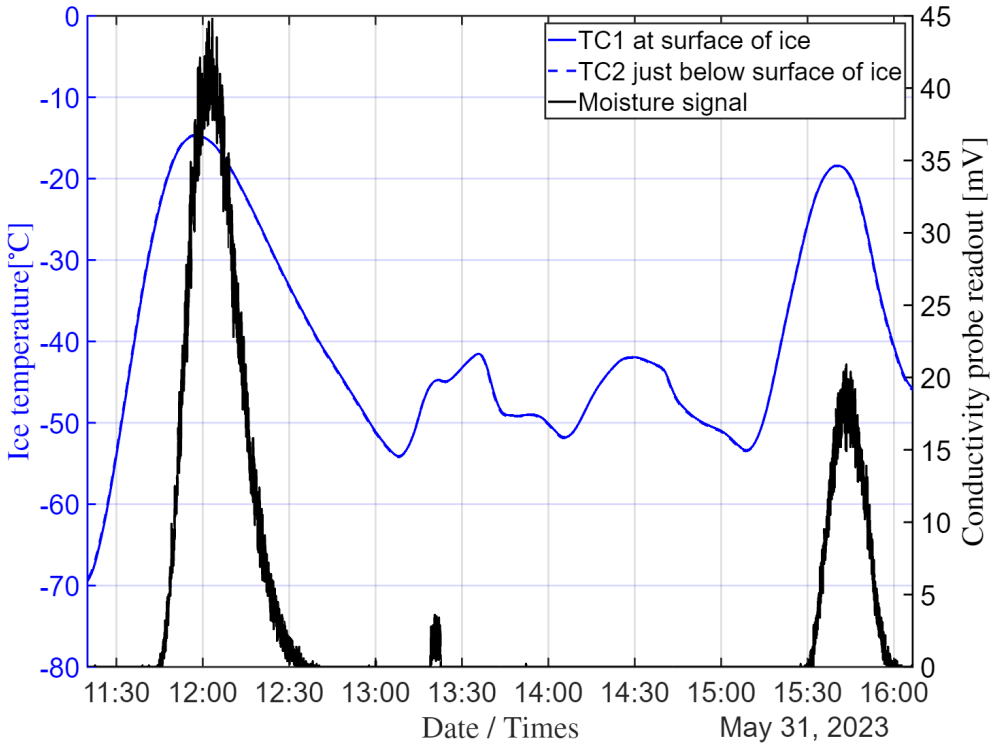

Figure 49: 0.6% perchlorate concentration full experiment overview - Trial 1 of 2.

First Cycle - Figure 50: The 0.6% concentration exhibited melting during the first warming cycle at nearly the same temperature as the 1% concentration, between -25°C and -24°C. Just like at 1%, substantial liquid was seen as the temperature was raised to about -15°C. Full freezing of the liquid then occurred at -40°C on the cooling portion, which, as with 1% perchlorate concentration, is warmer than the warmest simulated temperature at the Phoenix landing site at the ice level.

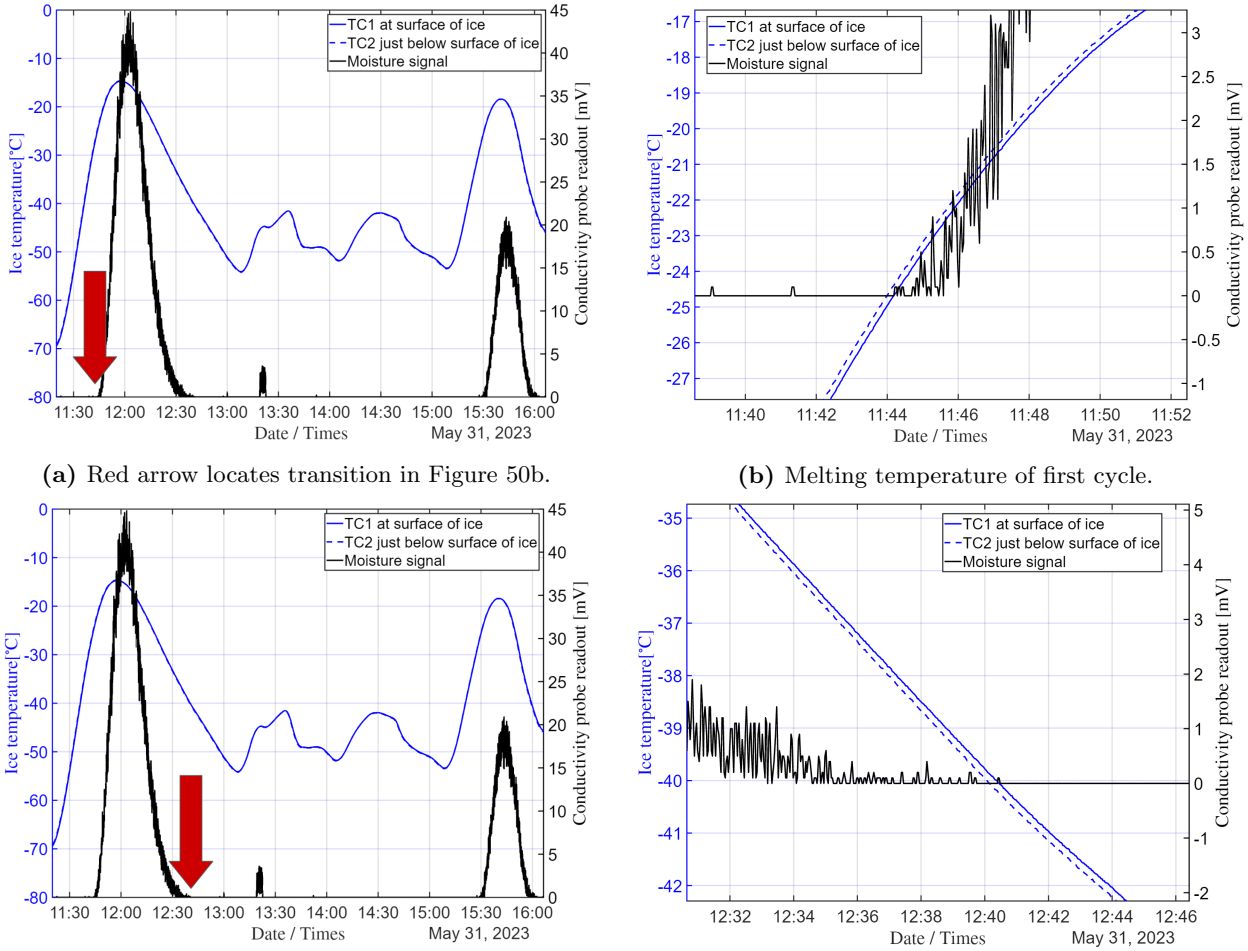

(a) Red arrow locates transition in Figure 50b.

(b) Melting temperature of first cycle.

(c) Red arrow locates transition in Figure 50d.

(d) Freezing temperature of first cycle.

Figure 50: 0.6% perchlorate concentration first temperature cycle.

Martian Temperatures - Figure 51: For the next temperature cycle,[7] the ice temperature was limited to only the temperatures of the ice table simulated at the Phoenix site, specifically -43°C to -53°C [19]. As shown in Figure 51, at no point over the course of the daily temperature cycle does the sample melt (having already frozen around -40°C during the previous cooling cycle).

[7]One cycle, which featured anomalous conductivity probe behaviour between 1300 and 1330, is omitted. We speculate a piece of frost from the lid could have momentarily bridged the prongs here.

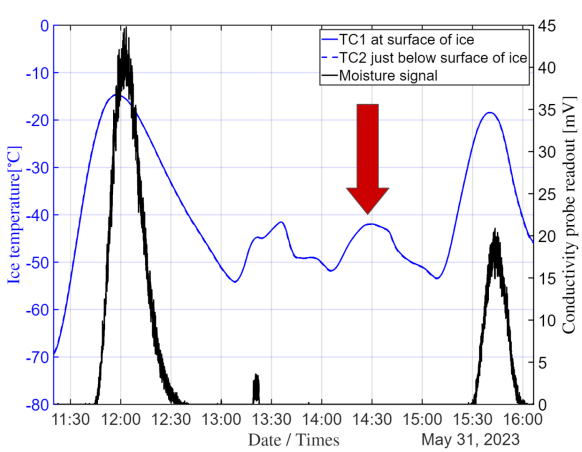

(a) Red arrow locates transition in Figure 51b.

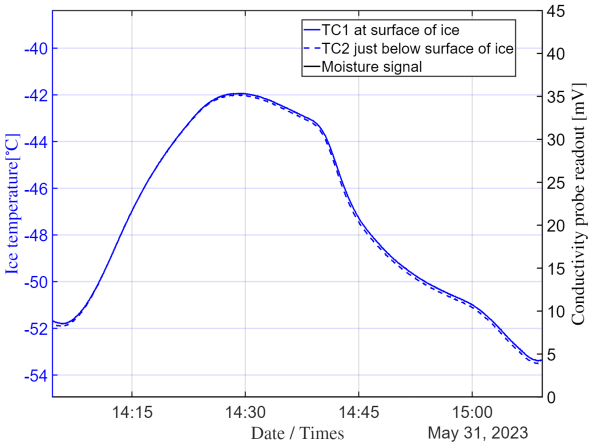

(b) Temperature range of one summer Mars day, with no liquid formed.

Figure 51: 0.6% perchlorate concentration second temperature cycle bounded by daily simulated Martian subsurface temperatures.

Third Cycle - Figure 52: Melting was seen on the last cycle at -27°C, which is slightly cooler than the melting temperature of the first cycle. Upon subsequent cooling, the sample fully froze at -43°C, which is also slightly cooler than the corresponding freezing temperature of the first cycle.

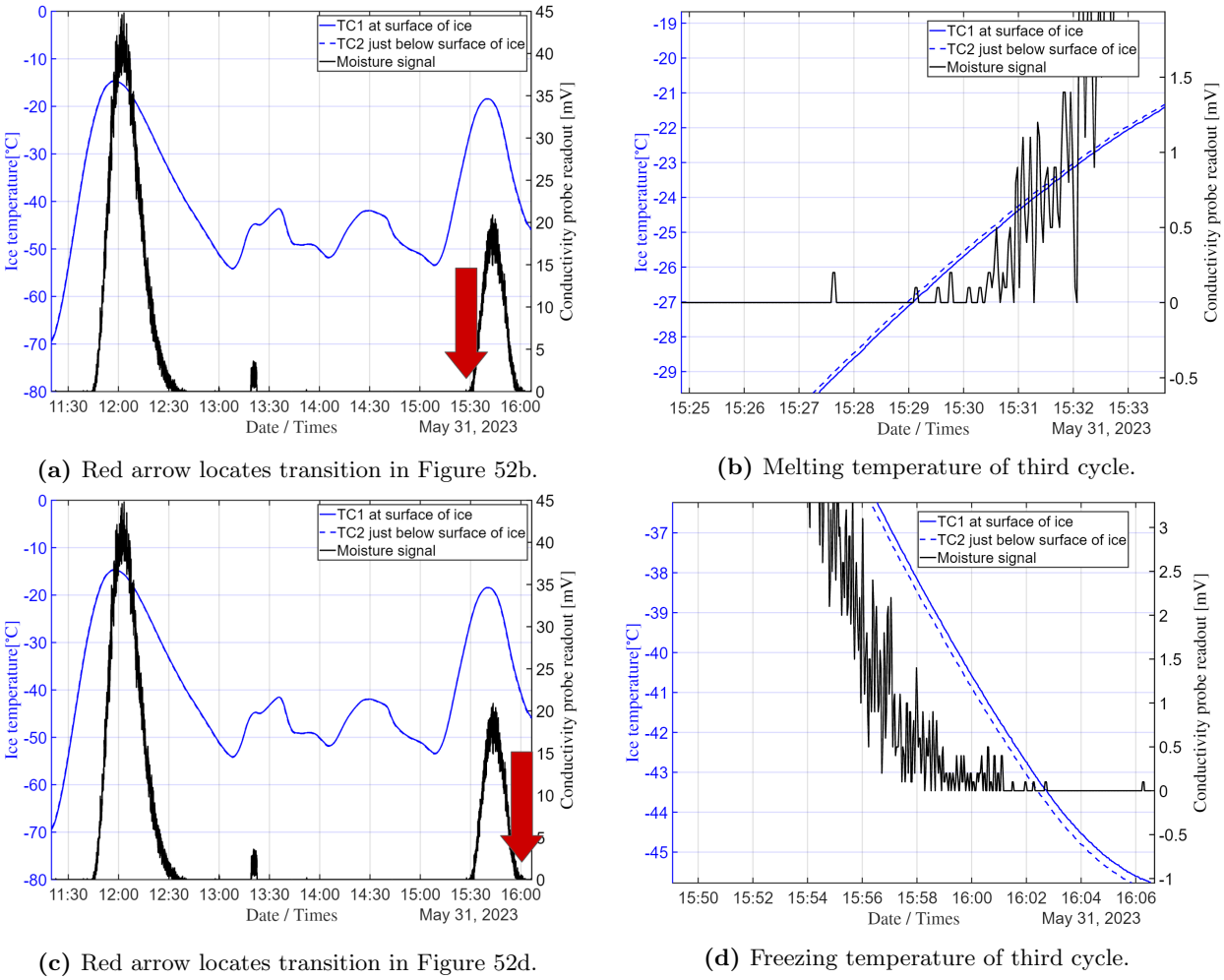

(a) Red arrow locates transition in Figure 52b.

(b) Melting temperature of third cycle.

(c) Red arrow locates transition in Figure 52d.

(d) Freezing temperature of third cycle.

Figure 52: 0.6% perchlorate concentration third temperature cycle.

Summary - 0.6% Perchlorate Concentration: For liquid brine formed at the interface between Martian regolith simulant and ice at 0.6% perchlorate concentration, which is the measured concentration at the Phoenix site [5], the average freezing temperature was -41 ± 1.4°C, and the average melting temperature was -26 ± 1.4°C. In a subsequent experiment which was a repeat of this one (Figures B.7 through B.9 in the Appendix), respective average freezing and melting temperatures were -41 ± 1.4°C and -25 ± 1.4°C. The combined average temperatures across both trials were -41 ± 1°C for full freezing and -26 ± 1°C for melting. Hence, liquid water would not be present under the temperature range of -43°C to -53°C (Figure 7), which was simulated for sol 55 at a depth of 4.5 cm at the Phoenix landing site [19].

4.2.5 Overall Summary of Results

Figure 53 shows each of the critical temperatures from the above experiments against the simulated temperature at the ice table beneath 4.5 cm of regolith at the Phoenix site on sol 55 of the mission, which ranges between -43°C and -53°C (solid black line in each subfigure) [19]. The time scale spans approximately one Martian sol, and the sinusoidal shape of the plot approximates the daily temperature trend. The relative differences in melting and freezing temperatures are in line with expectations for decreasing perchlorate concentrations across tests, since perchlorate solutions of lower concentrations will turn to ice at warmer temperatures than at higher concentrations, as per the phase diagram in Figure 8. Note that the average results for 1% and 0.6% include the additional trials shown in Appendix B.

Liquid water would form at the present-day Phoenix ice table for a perchlorate concentration in regolith of 5%. While the freezing temperature for 3% is sufficiently low for existing liquid to remain unfrozen, as shown in Figure 53b, the melting temperature is too warm for melting to occur in the first place. At even lower concentrations such as 1%, or the measured concentration on Mars of 0.6% [5], the ice would not melt at the ice table under the conditions at the Phoenix landing site in mid-summer, and the freezing temperature for a hypothetical existing liquid is above the warmest simulated temperature anyway.

Figure 53 does not show simulated temperature trends for areas of regolith over the ice table which are thinner than 4.5 cm, where the sinusoid would oscillate between larger extremes [19]. In a case such as this, the regolith need not be much thinner for the solid black line to intercept the dashed 3% melting line, where melting would occur and the liquid would not freeze until the temperature returns to -55°C several hours later. For very thin regolith layers such as 1 or 2 cm, only then is melting likely to occur at 1% or Phoenix-measured 0.6% perchlorate concentrations.

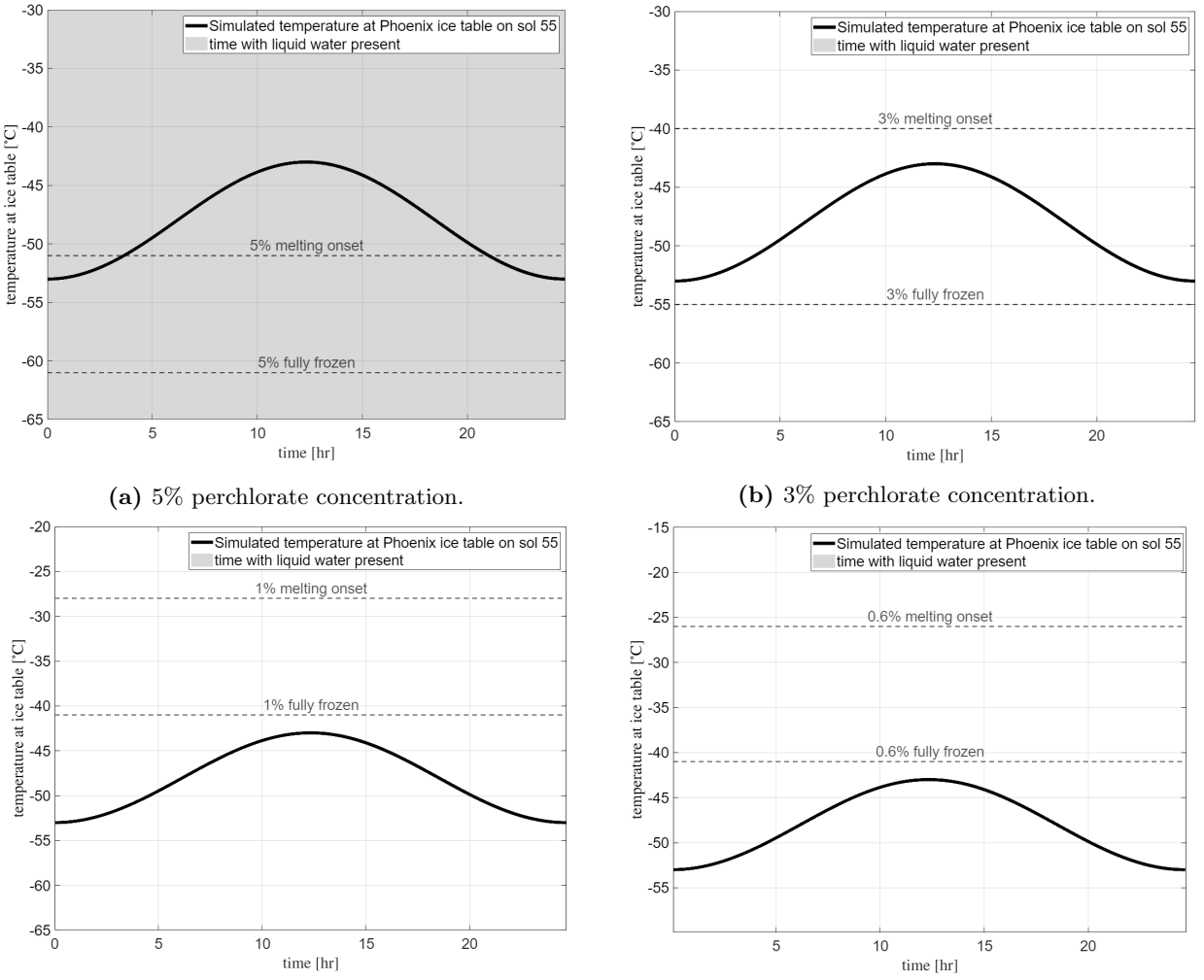

(a) 5% perchlorate concentration.

(b) 3% perchlorate concentration.

(c) 1% perchlorate concentration.

(d) 0.6% perchlorate concentration.

Figure 53: Graphical summary of critical temperatures, indicating that at 4.5 cm depth at the Phoenix site, only 5% perchlorate concentration causes melting and sustained liquid water. Applying uncertainties for the mean critical temperatures for 5% and 3% (±1.2°C), and also for 1% and 0.6% concentrations (±1°C) does not impact conclusions.

4.3 Chapter 4 Discussion: Ice-Regolith Interface

4.3.1 Conductivity Probe Moisture Signal Magnitude and Ion/Water Transport

In general, the warmer the ice temperature during a given cycle, the larger the magnitude of the moisture signal from the conductivity probe. For instance, review the cycles of the 5% perchlorate experiment of Figure 38. The smallest, middle, and largest magnitude moisture peaks were associated with the coolest, middle, and warmest temperature cycles, respectively. However, as mentioned previously, resistive probes may not be suitable for characterizing absolute water vol-

ume due to high sensitivity to ion concentration, which may not be perfectly representative of water volume [32]. For instance, and particularly for higher concentrations of perchlorate (3% and 5%), freezing temperatures sometimes varied substantially (e.g. -62°C to -53°C for 3% perchlorate concentration), meaning the probe was either seeing a different geometry of liquid or ion distribution bridging its prongs, or the actual concentration of perchlorates within the liquid was changing.

Either of these explanations has implications for Mars, as the transport of liquid (once formed) or the transport of ions can be a mechanism by which concentrations of perchlorates can change over time [22].

4.3.2 Implications for Liquid Water at the Ice-Regolith Interface on Mars

The experiment which featured 0.6% perchlorate mixed into the simulated Martian regolith showed no liquid forming between -43°C and -53°C, which are the temperatures simulated to constrain a summer day's temperature range beneath 4.5 cm of regolith [19] at the Phoenix landing site. Hence, perchlorate is not present in high enough concentrations at the Phoenix site for the formation and persistence of liquid brine due to contact with the ice table. However, if pockets exist at higher concentrations than 0.6%, like 3% or 5% (which may in fact be present on Mars [22]), these may be viable locations for liquid water to form and persist entire days. Indeed, as discussed just above, there was possible evidence of liquid (and/or perchlorate ion) movement within the samples of these experiments, which could be means for accumulation of perchlorate into higher concentrations. Aside from pockets of increased concentration, melting could occur at 0.6% or similar concentrations at a site with shallow regolith over ice (around 1-2 cm) where the daily temperature was simulated to surpass the experimental melting temperature [19].

As an aside, these results may have implications for any future *in situ* sampling, since in the case of warming as a result of a spacecraft or other human device, there are potential false-positives for persistent liquid water should enough heat be unwittingly added to the sampling site. If there were a local perchlorate concentration of at least 3% in the regolith around such a warming event, it would not immediately freeze, and could persist until cooler seasons bring the temperature to below -55°C. If concentrations remain constrained to 0.6% or similar, temperatures sufficient for melting

(-26°C) may be introduced by a human-made spacecraft, but a brine made from this extremely localized circumstance would quickly freeze when temperatures returned to normal, even in the summer.

4.3.3 Experimental Limitations and Future Work

The processes which shaped the present-day Martian surface and subsurface occurred over many millions of years of geologic and chemical evolution. In these experiments, the regolith-perchlorate mixture was formed in hours, and instantly deposited onto ice. On Mars, various unaccounted for effects stemming from the timescales and processes involved could further influence the chemical environment of the subsurface, including the formation high-concentration pockets due to ion movement, or different types of ice such as (more brittle) saline ice [18], the implications of which have not been studied. Further, as discussed, a probe reading of zero does not guarantee absolute absence of liquid whatsoever, and so there remains an assumption that the space between the conductivity probe prongs represents the entire layer at the interface of regolith and ice. Additionally, while only phase transitions were of interest for these experiments, the absolute liquid water volume once liquid water signal is seen cannot be measured using the existing apparatus, nor do we measure its transport upwards from the ice layer through the regolith by means of dispersion. Measuring the extent of liquid transport throughout the regolith has potential implications for perchlorate concentration, and the Martian hydrological cycle.

Relatedly, though the conductivity probe used in the presented work is sensitive to freezing and melting at the ice-regolith interface, it would be interesting to repeat the above experiments with a dielectric probe; observing the signal from this probe over the same conditions as these initial experiments should allow for better quantification of absolute water volume, which adds to the story started here. However, this type of probe is usually only one piece, meaning no area where measurements are taken will represent an undisturbed portion of the ice-regolith interface, which contrasts the plateau between prongs of the conductivity probe utilized in experiments above.

5 Conclusions

Experiments have been conducted towards both an advanced demonstration of surface-atmosphere water exchange on Mars, and towards a clearer picture of the stability of liquid water at the ice-regolith interface at the shallow Martian subsurface. Concluding summary is provided for each of the outlined goals for this MSc research.

Research Goal #1: Demonstrate the deliquescence of magnesium perchlorate at environmental conditions equivalent to those on Mars in a sample of simulated Martian regolith with Mars-measured thickness over ice.

Experiments were presented in Chapter 3 which advanced the laboratory's progress in demonstrating the deliquescence of perchlorate on a simulated Martian surface, the demonstration of which is routinely achievable if the perchlorate is resting on bare, cooled aluminum metal. At more humid conditions, at -35°C frost point temperature, the demonstration on top of regolith was achieved. Furthermore, experiments at this humidity honed in on key apparatus parameters necessary for deliquescence, namely, that replenishing airflow is present if the experiment takes place in an enclosed container, and that the top surface is sufficiently shielded from infrared radiation from the chamber environment. Despite updating the apparatus in accordance with this progress, deliquescence at -55°C frost point temperature was elusive due to the fact that by sufficiently cooling the sample and the moisture-replenishing air, we begin immediately extracting moisture out of the air through deposition, prohibiting deliquescence. While the demonstration was not completed before transitioning to the primary goal of this MSc project, these experiments represent significant progress, and the experience gained provides opportunity for further advancement in future studies.

Research Goal #2: Determine if a layer of liquid saline water forms at the ice table which was found at the Phoenix landing site on Mars.

Experiments presented in Chapter 4 investigated whether melting occurs at the ice table 4.5 cm below the surface of Mars, the liquid being a result of contact between perchlorate in the regolith and the ice table. The freezing point of this solution is depressed depending on the salt concentration. Experiments used a conductivity-based moisture detection probe, which would read out non-zero voltage in the presence of liquid water roughly proportional to volume, which was embedded at the interface between the regolith and the ice. The results demonstrated that the 0.6% concentration of perchlorate measured at the Phoenix landing site does not melt the ice at the ice table 4.5 cm below the surface during mid-summer (sol 55 of the Phoenix mission). However, if somewhere on Mars there is the same concentration of perchlorate but the ice table is instead at a shallower depth of 1 or 2 cm (where the temperature is simulated to reach -25°C in the summer), melting would occur, and liquid could persist for hours a day during peak temperatures.

At higher concentrations like 3%, existing liquid water could persist until the temperature reaches -55°C, which is below the coldest simulated temperature under 4.5 cm of regolith, but the temperature to cause melting in the first place is marginal at -40°C, which is warmer than the warmest simulated temperature of -43°C. Hence, 3% is not a sufficient concentration at Phoenix conditions for liquid formation at the ice table. At a high concentration like 5%, liquid is expected for days at a time if the temperature remains constrained between the simulated -43°C to -53°C, since freezing was not seen until the temperature reaches -61°C.

Hence, the research goal is addressed with opportunity for refinement: Liquid water forms at the ice-regolith interface on Mars if either (A) perchlorate is able to concentrate into substantially higher quantities than what was observed at the Phoenix landing site, or (B) for the observed concentration around 0.6%, the ice table rests only 1 or 2 cm below the top surface such that temperatures reach the requisite melting temperature. Opportunities for refinement lie in better characterizing actual liquid/ion volume, geometry, and transport, and thus better constraining freezing temperatures.

Appendix

A Supplementary Experiments - Chapter 3

A.1 Additional Deliquescence Attempt

Another experiment from the set of experiments done throughout the period covered by Chapter 3 is shown in Figures A.1 and A.2. This is included here to show (A) that the regolith temperature inside the enclosure tracks the wall and lid temperatures to about 5°C, and (B) that the lid and wall temperatures track each other nearly exactly. This justifies removing instrumentation from inside the enclosure, mitigating potential warming or leak effects. This experiment did not result in deliquescence for the same reasons those described in Section 3.5.6.

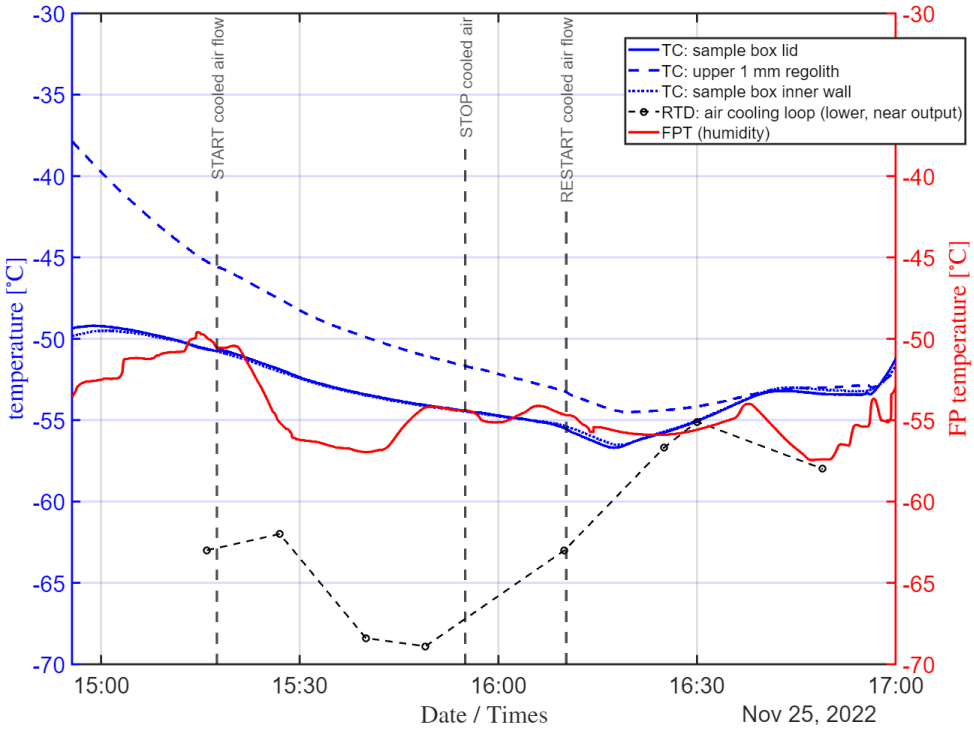

Figure A.1: Planetary simulation chamber data for deliquescence experiment at -55°C frost point using updated apparatus.

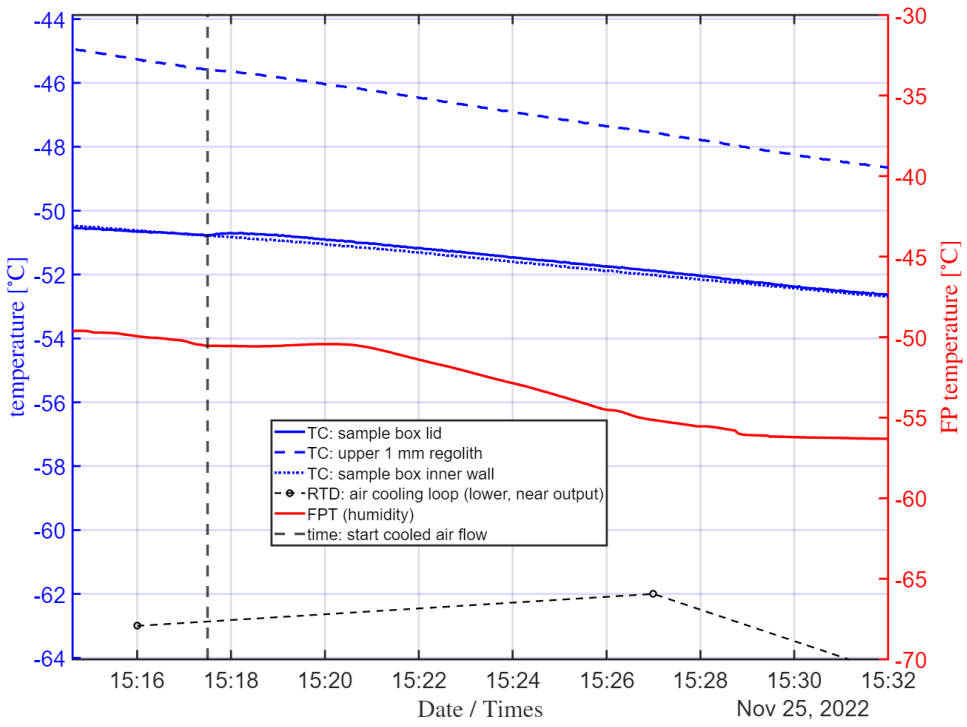

Figure A.2: Slight temperature increase from introduction of cooled air flow.

B Supplementary Experiments - Chapter 4

B.1 Comparison of Laser Raman Spectra and Conductivity Probe Readout

A brief comparison was made between the moisture-sensing conductivity probe and laser Raman LIDAR spectra. Figure B.1 shows the test set-up. There is a clear line of sight from the Raman LIDAR laser output (and scattering receiver) to a sample of magnesium perchlorate hexahydrate sprinkled atop ice between the two conductivity probe prongs. A thermocouple was embedded in the ice near the deposited perchlorate puddle to record the ice temperature. Figure B.2 shows the moisture signal from the conductivity probe for multiple temperature cycles.

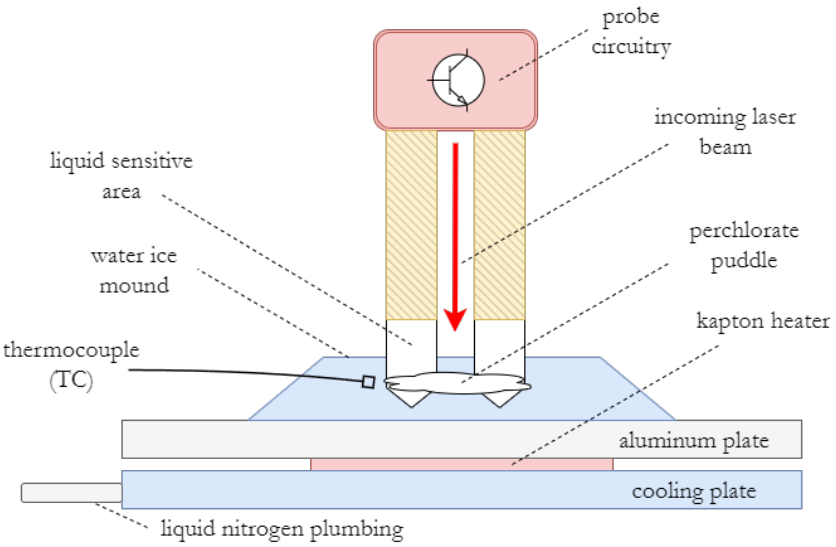

Figure B.1: Apparatus for experiment comparing conductivity probe output with Raman LIDAR signal.

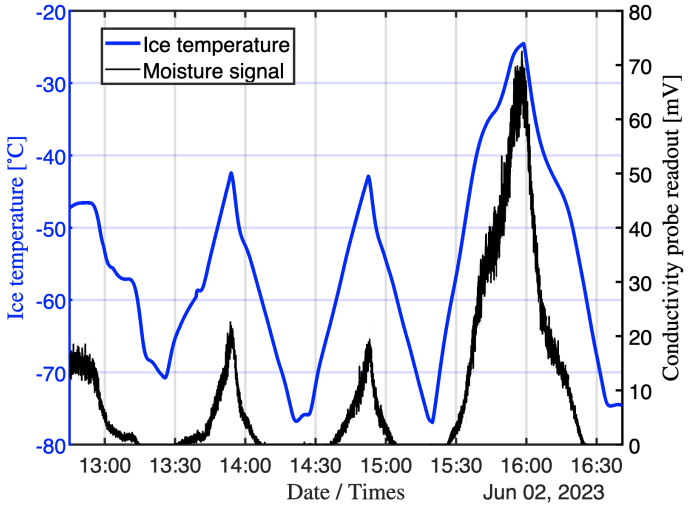

Figure B.2: Conductivity probe moisture signal over multiple temperature cycles while laser Raman data was collected simultaneously.

Figure B.3 shows two Raman spectra, one at 1515 (where the sample is fully frozen below -70°C), and one at 1600, where there is peak liquid content as indicated by the conductivity probe. While minor differences can be identified, the overall shapes are very similar; this is since any detection of liquid over ice will always have significant background ice signal, making absolute quantification of liquid over ice difficult. Spectral unmixing would be required to determine if the Raman spectra allows for detection of water phase transitions over ice with the same temporal acuity as the moisture detection probe. However, a Raman LIDAR system has the additional disadvantage of potentially

warming the ice as trace regolith grains (say, after excavation) absorb the radiation, which could induce premature melting.

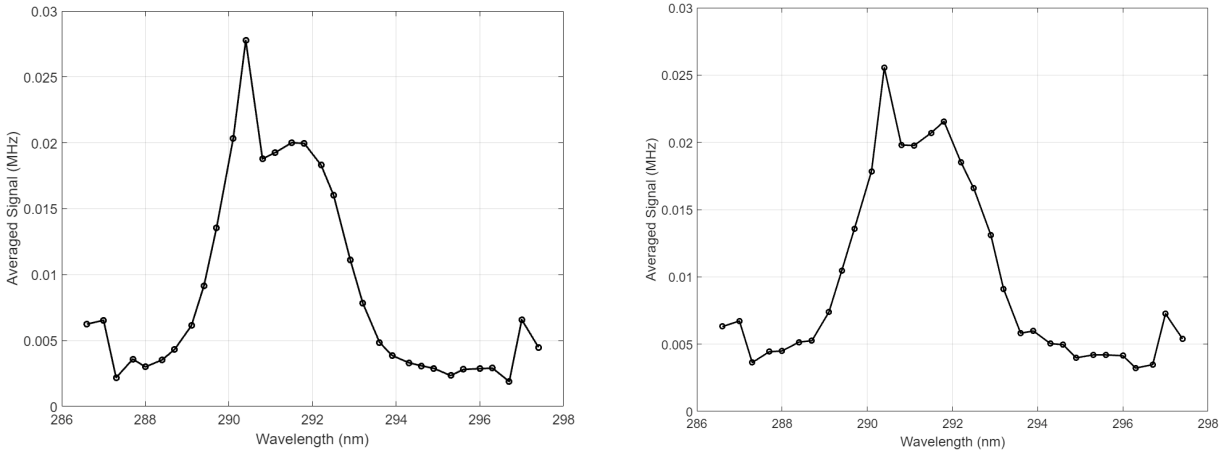

(a) Raman spectrum at 1515 of frozen sample.

(b) Raman spectrum at 1600 at peak liquid content.

Figure B.3: Laser Raman LIDAR scans at points of substantial liquid and ice. The incident laser wavelength was 266 nm.

B.2 Additional 1% and 0.6% Perchlorate Ice-Regolith Interface Trials

Supplementary plots, just like those presented in Section 4.2, are shown for the additional 1% and 0.6% tests in Figures B.4 through B.9. The results are included in the final averaged critical temperatures in the main text. No aspect of the test procedure was changed.

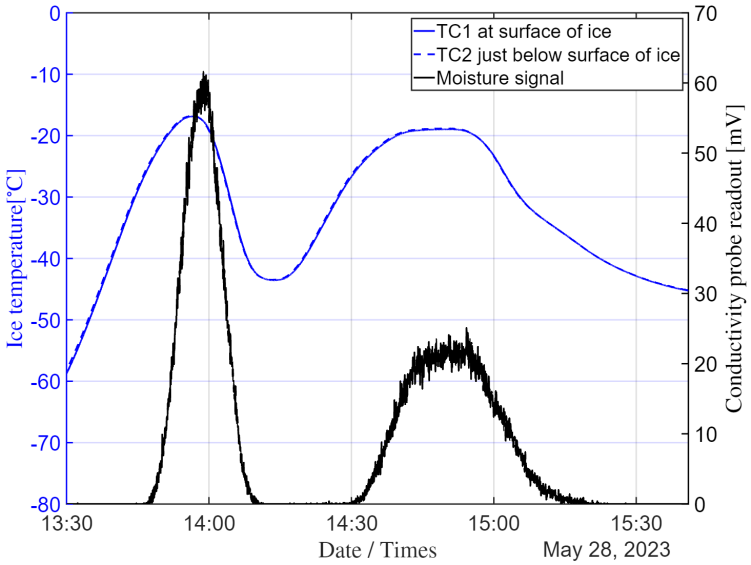

Figure B.4: 1% perchlorate concentration full experiment overview - Trial 2 of 2.

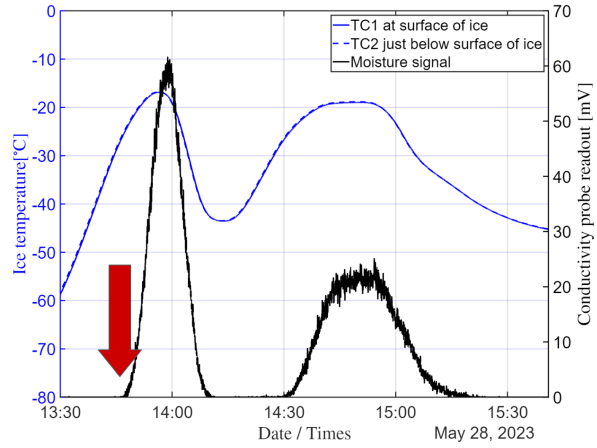

(a) Red arrow locates transition in Figure B.5b.

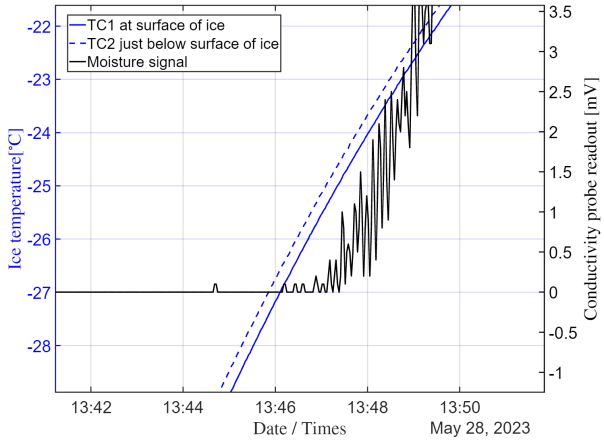

(b) Melting temperature of first cycle.

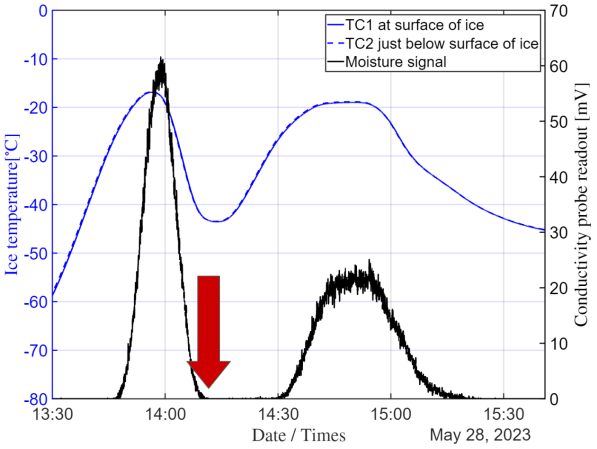

(c) Red arrow locates transition in Figure B.5d.

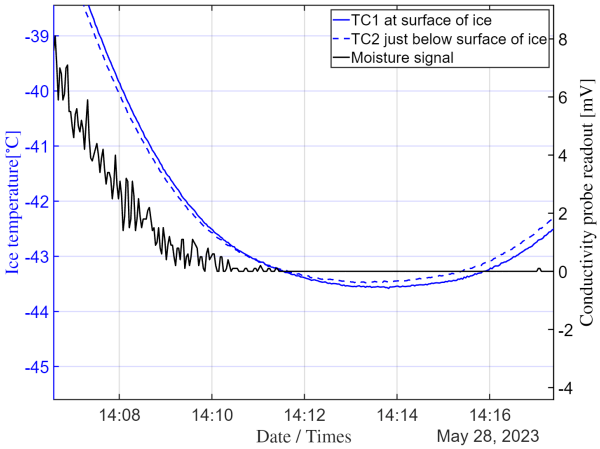

(d) Freezing temperature of first cycle.

Figure B.5: 1% perchlorate concentration first temperature cycle - Trial 2 of 2.

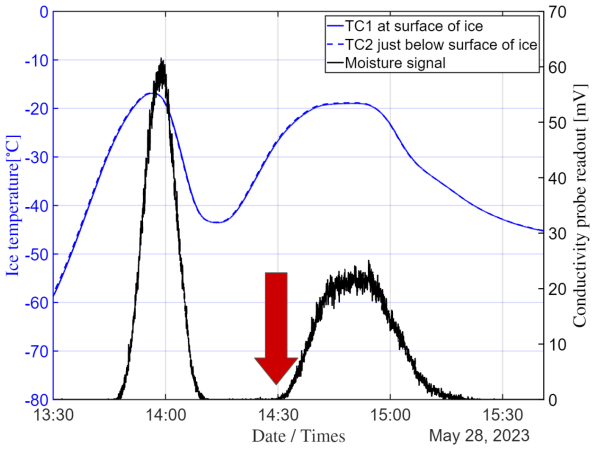

(a) Red arrow locates transition in Figure B.6b.

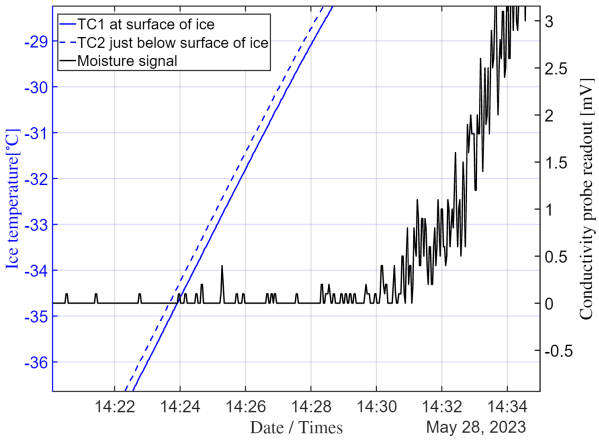

(b) Melting temperature of second cycle.

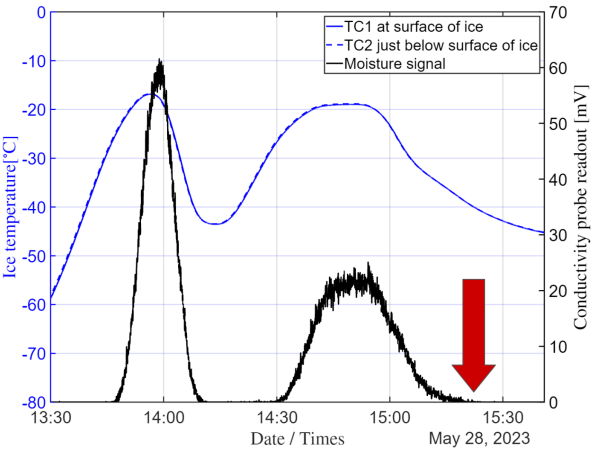

(c) Red arrow locates transition in Figure B.6d.

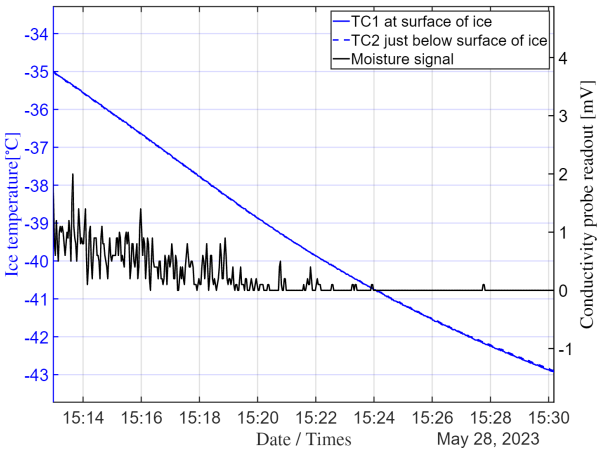

(d) Freezing temperature of second cycle.

Figure B.6: 1% perchlorate concentration second temperature cycle - Trial 2 of 2.

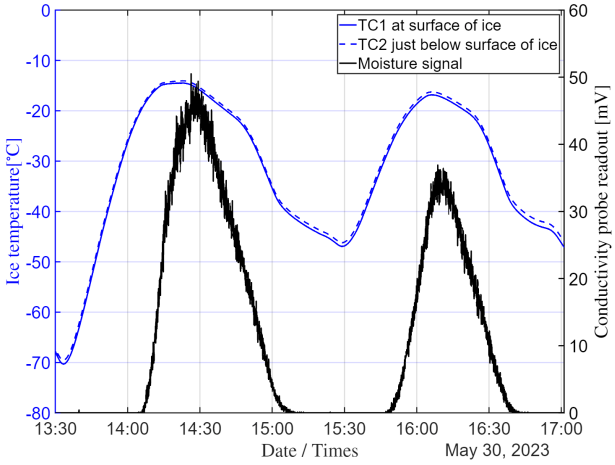

Figure B.7: 0.6% perchlorate concentration full experiment overview - Trial 2 of 2.

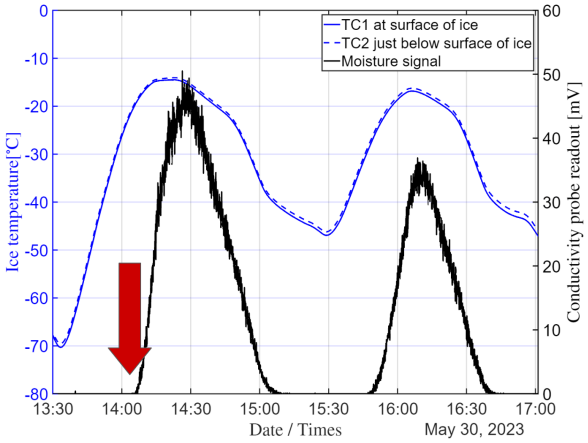

(a) Red arrow locates transition in Figure B.8b.

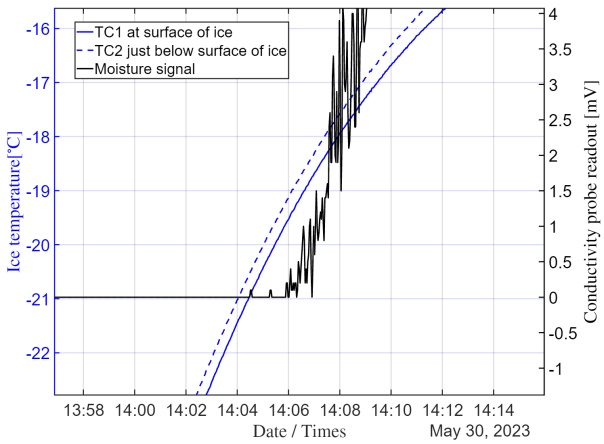

(b) Melting temperature of first cycle.

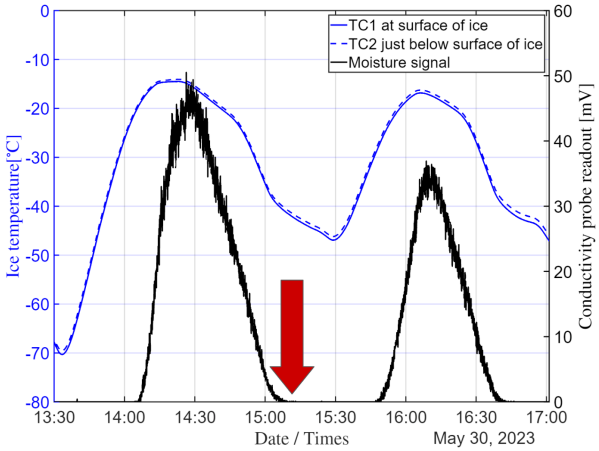

(c) Red arrow locates transition in Figure B.8d.

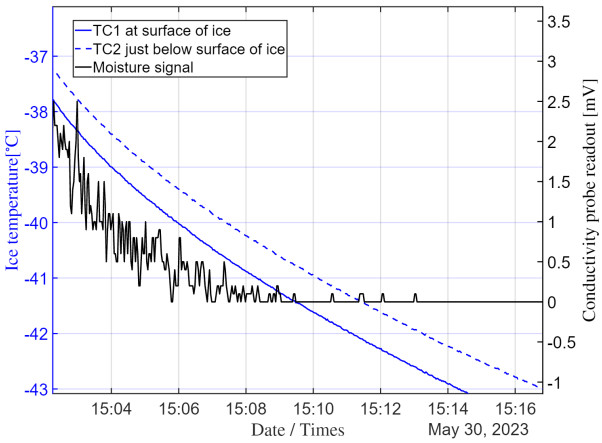

(d) Freezing temperature of first cycle.

Figure B.8: 0.6% perchlorate concentration first temperature cycle - Trial 2 of 2.

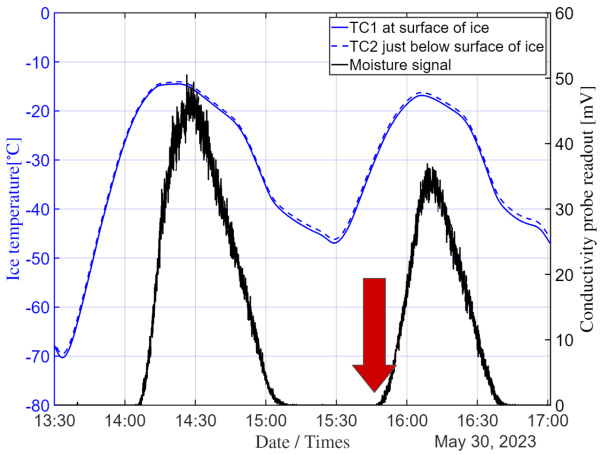

(a) Red arrow locates transition in Figure B.9b.

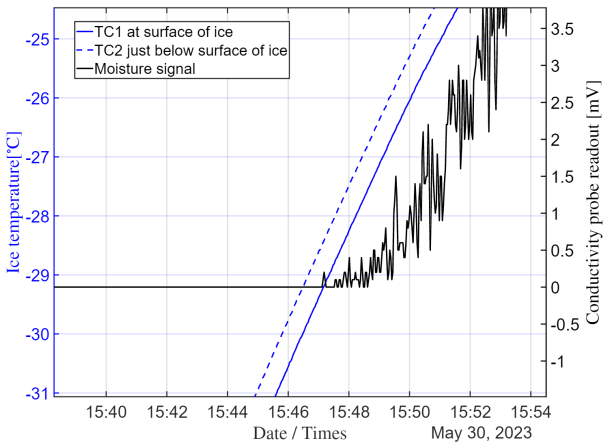

(b) Melting temperature of second cycle.

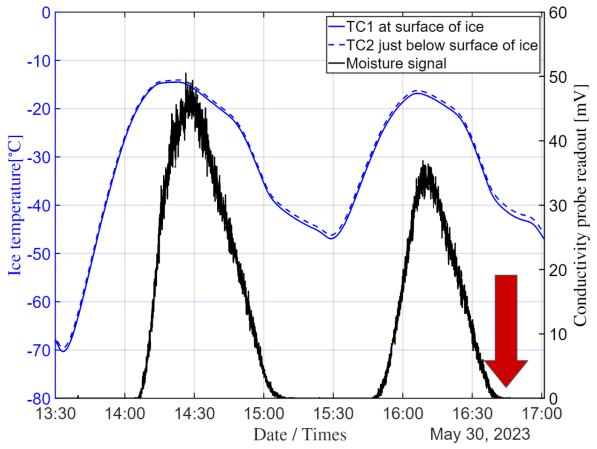

(c) Red arrow locates transition in Figure B.9d.

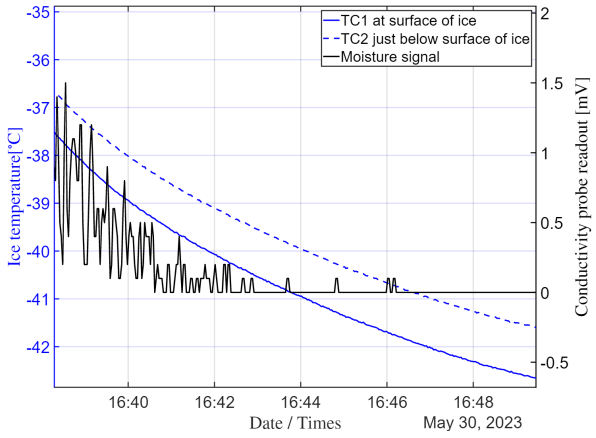

(d) Freezing temperature of second cycle.

Figure B.9: 0.6% perchlorate concentration second temperature cycle - Trial 2 of 2.

References

[1] J. Whiteway, L. Komguem, C. Dickinson, C. Cook, M. Illnicki, J. Seabrook, V. Popovici, T. Duck, R. Davy, P. Taylor, J. Pathak, D. Fisher, A. Carswell, M. Daly, V. Hipkin, A. Zent, M. Hecht, S. Wood, L. Tamppari, and P. Smith, "Mars water-ice clouds and precipitation," *Science (New York, N.Y.)*, vol. 325, pp. 68–70, 08 2009.

[2] P. H. Smith, L. K. Tamppari, R. E. Arvidson, D. Bass, D. Blaney, W. V. Boynton, A. Carswell, D. C. Catling, B. C. Clark, T. Duck, E. DeJong, D. Fisher, W. Goetz, H. P. Gunnlaugsson, M. H. Hecht, V. Hipkin, J. Hoffman, S. F. Hviid, H. U. Keller, S. P. Kounaves, C. F. Lange, M. T. Lemmon, M. B. Madsen, W. J. Markiewicz, J. Marshall, C. P. McKay, M. T. Mellon, D. W. Ming, R. V. Morris, W. T. Pike, N. Renno, U. Staufer, C. Stoker, P. Taylor, J. A. Whiteway, and A. P. Zent, "H_2o at the phoenix landing site," *Science*, vol. 325, no. 5936, pp. 58–61, 2009.

[3] R. M. Haberle and B. M. Jakosky, "Sublimation and transport of water from the north residual polar cap on mars," *Journal of Geophysical Research: Solid Earth*, vol. 95, no. B2, pp. 1423–1437, 1990.

[4] K. A. Farley, K. H. Williford, K. M. Stack, R. Bhartia, A. Chen, M. de la Torre, K. Hand, Y. Goreva, C. D. K. Herd, R. Hueso, Y. Liu, J. N. Maki, G. Martinez, R. C. Moeller, A. Nelessen, C. E. Newman, D. Nunes, A. Ponce, N. Spanovich, P. A. Willis, L. W. Beegle, J. F. Bell, A. J. Brown, S.-E. Hamran, J. A. Hurowitz, S. Maurice, D. A. Paige, J. A. Rodriguez-Manfredi, M. Schulte, and R. C. Wiens, "Mars 2020 Mission Overview," *Space Science Reviews*, vol. 216, no. 8, p. 142, 2020.

[5] M. H. Hecht, S. P. Kounaves, R. C. Quinn, S. J. West, S. M. M. Young, D. W. Ming, D. C. Catling, B. C. Clark, W. V. Boynton, J. Hoffman, L. P. DeFlores, K. Gospodinova, J. Kapit, and P. H. Smith, "Detection of perchlorate and the soluble chemistry of martian soil at the phoenix lander site," *Science*, vol. 325, no. 5936, pp. 64–67, 2009.

[6] G. Nikolakakos and J. A. Whiteway, "Laboratory investigation of perchlorate deliquescence at the surface of mars with a raman scattering lidar," *Geophysical Research Letters*, vol. 42,

no. 19, pp. 7899–7906, 2015.

[7] E. Fischer, G. M. Martínez, H. M. Elliott, and N. O. Rennó, "Experimental evidence for the formation of liquid saline water on Mars.," *Geophysical research letters*, vol. 41, pp. 4456–4462, jul 2014.

[8] A. F. Davila, L. G. Duport, R. Melchiorri, J. Jänchen, S. Valea, A. de los Rios, A. G. Fairén, D. Möhlmann, C. P. McKay, C. Ascaso, and J. Wierzchos, "Hygroscopic salts and the potential for life on mars," *Astrobiology*, vol. 10, no. 6, pp. 617–628, 2010. PMID: 20735252.

[9] G. Nikolakakos and J. A. Whiteway, "Laboratory study of adsorption and deliquescence on the surface of mars," *Icarus*, vol. 308, pp. 221–229, 2018. Mars Polar Science VI.

[10] V. F. Chevrier, J. Hanley, and T. S. Altheide, "Stability of perchlorate hydrates and their liquid solutions at the Phoenix landing site, mars," *Geophysical Research Letters*, vol. 36, no. 10, pp. 1–6, 2009.

[11] B. T. Cardenas and M. P. Lamb, "Paleogeographic reconstructions of an ocean margin on mars based on deltaic sedimentology at aeolis dorsa," *Journal of Geophysical Research: Planets*, vol. 127, no. 10, p. e2022JE007390, 2022. e2022JE007390 2022JE007390.

[12] J. W. Head, H. Hiesinger, M. A. Ivanov, M. A. Kreslavsky, S. Pratt, and B. J. Thomson, "Possible ancient oceans on mars: Evidence from mars orbiter laser altimeter data," *Science*, vol. 286, no. 5447, pp. 2134–2137, 1999.

[13] M. H. Carr, "The martian drainage system and the origin of valley networks and fretted channels," *Journal of Geophysical Research: Planets*, vol. 100, no. E4, pp. 7479–7507, 1995.

[14] T. A. Goudge, J. F. Mustard, J. W. Head, C. I. Fassett, and S. M. Wiseman, "Assessing the mineralogy of the watershed and fan deposits of the jezero crater paleolake system, mars," *Journal of Geophysical Research: Planets*, vol. 120, no. 4, pp. 775–808, 2015.

[15] J. P. Grotzinger, D. Y. Sumner, L. C. Kah, K. Stack, S. Gupta, L. Edgar, D. Rubin, K. Lewis, J. Schieber, and N. Mangold, "A habitable fluvio-lacustrine environment at yellowknife bay, gale crater, mars," *Science*, vol. 343, no. 6169, p. 1242777, 2014.

[16] H. B. Franz, M. G. Trainer, C. A. Malespin, P. R. Mahaffy, S. K. Atreya, R. H. Becker, M. Benna, P. G. Conrad, J. L. Eigenbrode, C. Freissinet, H. L. Manning, B. D. Prats, E. Raaen, and M. H. Wong, "Initial sam calibration gas experiments on mars: Quadrupole mass spectrometer results and implications," *Planetary and Space Science*, vol. 138, pp. 44–54, 2017.

[17] C. McKay, O. Toon, and J. Kasting, "Making mars habitable," *Nature*, vol. 352, no. 6335, pp. 489–496, 1991.

[18] N. O. Rennó, B. J. Bos, D. Catling, B. C. Clark, L. Drube, D. Fisher, W. Goetz, S. F. Hviid, H. U. Keller, J. F. Kok, S. P. Kounaves, K. Leer, M. Lemmon, M. B. Madsen, W. J. Markiewicz, J. Marshall, C. McKay, M. Mehta, M. Smith, M. P. Zorzano, P. H. Smith, C. Stoker, and S. M. M. Young, "Possible physical and thermodynamical evidence for liquid water at the phoenix landing site," *Journal of Geophysical Research: Planets*, vol. 114, no. E1, 2009.

[19] C. R. Stoker, A. Zent, D. C. Catling, S. Douglas, J. R. Marshall, D. Archer Jr., B. Clark, S. P. Kounaves, M. T. Lemmon, R. Quinn, N. Renno, P. H. Smith, and S. M. Young, "Habitability of the phoenix landing site," *Journal of Geophysical Research: Planets*, vol. 115, no. E6, 2010.

[20] A. P. Zent, M. H. Hecht, D. R. Cobos, S. E. Wood, T. L. Hudson, S. M. Milkovich, L. P. DeFlores, and M. T. Mellon, "Initial results from the thermal and electrical conductivity probe (tecp) on phoenix," *Journal of Geophysical Research: Planets*, vol. 115, no. E3, 2010.

[21] T. L. Hudson, O. Aharonson, and N. Schorghofer, "Laboratory experiments and models of diffusive emplacement of ground ice on mars," *Journal of Geophysical Research: Planets*, vol. 114, no. E1, 2009.

[22] S. C. Cull, R. E. Arvidson, J. G. Catalano, D. W. Ming, R. V. Morris, M. T. Mellon, and M. Lemmon, "Concentrated perchlorate at the mars phoenix landing site: Evidence for thin film liquid water on mars," *Geophysical Research Letters*, vol. 37, no. 22, 2010.

[23] D. P. Glavin, C. Freissinet, K. E. Miller, J. L. Eigenbrode, A. E. Brunner, A. Buch, B. Sutter, P. D. Archer, S. K. Atreya, W. B. Brinckerhoff, M. Cabane, P. Coll, P. G. Conrad, D. Coscia, J. P. Dworkin, H. B. Franz, J. P. Grotzinger, L. A. Leshin, M. G. Martin, C. McKay, D. W. Ming, R. Navarro-González, A. Pavlov, A. Steele, R. E. Summons, C. Szopa, S. Teinturier, and

P. R. Mahaffy, "Evidence for perchlorates and the origin of chlorinated hydrocarbons detected by SAM at the Rocknest aeolian deposit in Gale Crater," *Journal of Geophysical Research E: Planets*, vol. 118, no. 10, pp. 1955–1973, 2013.

[24] S. P. Kounaves, N. A. Chaniotakis, V. F. Chevrier, B. L. Carrier, K. E. Folds, V. M. Hansen, K. M. McElhoney, G. D. O'Neil, and A. W. Weber, "Identification of the perchlorate parent salts at the phoenix mars landing site and possible implications," *Icarus*, vol. 232, pp. 226–231, 2014.

[25] J. Toner, D. Catling, and B. Light, "Soluble salts at the phoenix lander site, mars: A reanalysis of the wet chemistry laboratory data," *Geochimica et Cosmochimica Acta*, vol. 136, pp. 142–168, 2014.

[26] G. Nikolakakos, "Laboratory studies of surface-atmosphere water exchange processes on mars." `https://yorkspace.library.yorku.ca/xmlui/bitstream/handle/10315/35808/Nikolakakos_George_2018_PhD.pdf?sequence=2&isAllowed=y`. Ph.D. disseration, Fac. of Graduate Studies, Physics and Astronomy, York Univ., Toronto, 2018. Accessed on: June 25, 2023 [Online].

[27] R. Gough, V. Chevrier, K. Baustian, M. Wise, and M. Tolbert, "Laboratory studies of perchlorate phase transitions: Support for metastable aqueous perchlorate solutions on mars," *Earth and Planetary Science Letters - EARTH PLANET SCI LETT*, vol. 387, 12 2011.

[28] M. I. Nazarious, A. V. Ramachandran, M.-P. Zorzano, and J. Martin-Torres, "Calibration and preliminary tests of the brine observation transition to liquid experiment on habit/exomars 2020 for demonstration of liquid water stability on mars," *Acta Astronautica*, vol. 162, pp. 497–510, 2019.

[29] L. Beegle, G. Peters, G. Mungas, G. Bearman, J. Smith, and R. Anderson, "Mojave martian simulant: A new martian soil simulant," 03 2007.

[30] The Martian Garden, "Mojave mars simulant.." `https://www.themartiangarden.com/mms1/mms1`. Accessed on: June 29, 2023 [Online].

[31] E. Smith and G. Dent, *Modern Raman Spectroscopy: A Practical Approach*. 08 2005.

[32] Meter, "Tdr, fdr, capacitance, resistance: A comparison of common soil moisture sensing methods, their pros and cons, and their unique applications.." `https://www.metergroup.com/en/meter-environment/measurement-insights/tdr-fdr-capacitance-compared`. Accessed on: June 26, 2023 [Online].

[33] L. Yu, W. Gao, R. Shamshiri, S. Tao, Y. Ren, Y. Zhang, and G. Su, "Review of research progress on soil moisture sensor technology," *International Journal of Agricultural and Biological Engineering*, vol. 14, pp. 32–42, 08 2021.